Regulation of the localization and activity of Mps1 kinase at the kinetochore

Lori B Koch

A dissertation
submitted in partial fulfillment of the
requirements for the degree of

Doctor of Philosophy

University of Washington
2018

Reading Committee:
Susan Biggins, Chair
Jihong Bai
Alexander Paredez

Program Authorized to Offer Degree:
Molecular and Cellular Biology

University of Washington

Abstract

Regulation of the localization and activity of Mps1 kinase at the kinetochore

Lori B Koch

Chair of the Supervisory Committee:
Dr. Susan Biggins
Howard Hughes Medical Institute
Division of Basic Sciences, Fred Hutchinson Cancer Research Center

Every time a cell divides, chromosomes must be segregated accurately between daughter cells. Chromosome segregation defects are a hallmark of several major diseases that threaten human health, including cancer and infertility. To be segregated, chromosomes must make and maintain bioriented attachments to dynamic microtubules of a bipolar spindle that forms in dividing cells. The kinetochore is the protein complex that attaches chromosomes to microtubules and it serves as a platform for multiple signaling pathways that promote accurate segregation. The essential protein kinase Mps1 promotes biorientation through multiple mechanisms, however the mechanism by which it associates with kinetochores to carry out these processes is unclear. To address this, I, along with my collaborators, performed reconstitution experiments with kinetochore complexes purified from budding yeast. We found that kinetochore-microtubule attachment did not displace Mps1 bound to kinetochores, as has been proposed. Instead, I showed that autophosphorylation triggers Mps1 release and prevents re-binding to kinetochores. In addition, I

investigated whether Mps1 phosphorylation of kinetochores directly regulates kinetochore-microtubule attachments. I found that Mps1 phosphorylation weakens reconstituted kinetochore-microtubule attachments. I also provide evidence that Mps1 phosphorylation of microtubule-binding components of the kinetochore is required for accurate chromosome segregation in cells. My work elucidates critical mechanisms of Mps1 kinase regulation in budding yeast and future work should address whether such mechanisms are conserved in other organisms.

TABLE OF CONTENTS

ACKNOWLEDGEMENTS 9

CHAPTER 1: INTRODUCTION 12

MICROTUBULE-BINDING COMPONENTS OF THE KINETOCHORE 14

BIORIENTATION 15

ERROR-CORRECTION BY THE KINASE AURORA B^{IPL1} 16

THE KINASE MPS1 PROMOTES BIORIENTATION 17

MPS1 KINASE ACTIVATES THE SPINDLE ASSEMBLY CHECKPOINT 19

SPINDLE ASSEMBLY CHECKPOINT SILENCING AND MPS1 KINETOCHORE LOCALIZATION 21

OVERVIEW OF THESIS 22

CHAPTER 2: REGULATION OF THE KINETOCHORE LOCALIZATION OF THE CHECKPOINT KINASE MPS1 24

2.1 CONTRIBUTIONS OF COLLABORATORS 24

2.2 SUMMARY 24

2.3 INTRODUCTION 25

2.4 RESULTS 27

KINETOCHORES SIMULTANEOUSLY BIND TO MPS1 AND MICROTUBULES *IN VITRO* 27

A SINGLE PARTICLE METHOD TO MEASURE MPS1 LEVELS ON INDIVIDUAL KINETOCHORES 28

INDIVIDUAL KINETOCHORES ASSOCIATE SIMULTANEOUSLY WITH MPS1 AND MICROTUBULES 30

INDIVIDUAL KINETOCHORES TRACKING DISASSEMBLING MICROTUBULE TIPS RETAIN MPS1 31

ACTIVATING MPS1 TRIGGERS ITS RELEASE FROM KINETOCHORES 32

MPS1 AUTOPHOSPHORYLATION REDUCES ITS AFFINITY FOR KINETOCHORES 33

PHOSPHORYLATION OF THE KINETOCHORE-BINDING DOMAIN PROMOTES MPS1 RELEASE FROM KINETOCHORES 35

PHOSPHORYLATION OF MPS1 ALSO PROMOTES ITS ASSOCIATION WITH KINETOCHORES 37

PRELIMINARY EVIDENCE THAT THE *MPS1-R170S* MUTANT IS DEFECTIVE IN KINETOCHORE ASSOCIATION AND SPINDLE ASSEMBLY CHECKPOINT SIGNALING 38

2.5 DISCUSSION 39

2.6 Materials and Methods 43
Yeast Methods 43
Purification of Native Kinetochore Particles and Mps1 44
Immunological techniques 44
Kinase assays 45
Bulk binding assays 45
Analysis of individual fluorescent kinetochore particles 46
2.7 Acknowledgements 46
2.8 Figures 48
Figure 2.1. Isolated kinetochores retain Mps1 when attached laterally to microtubules. 48
Figure 2.2. Kinetochores retain Mps1 when attached to microtubule tips. 50
Figure 2.3. Kinetochores retain Mps1 when tracking with disassembling microtubule tips. 51
Figure 2.4. Mps1 autophosphorylation inhibits its binding to kinetochores. 52
Figure 2.5 - Mps1 N-terminal autophosphorylation regulates its association with kinetochores. 54
Figure 2.6. Characterization of *mps1-16A* and *mps1-D580A*. 56
Figure 2.7. *mps1-16A*, *mps1-D580A*, and *mps1-7* disrupt Mps1 kinetochore function. 58
2.9 Supplementary Figures 60
Supplementary Figure 2.1 - Microtubule attachment to purified kinetochores requires Ndc80. 60
Supplementary Figure 2.2 - Phosphomimetic Dsn1-2D improves retention 61
of Mps1 on isolated kinetochores without disrupting checkpoint silencing in vivo. . 61
Supplementary Figure 2.3 – Preparation of purified kinetochores and Mps1 for binding experiments. 63
Supplementary Figure 2.4 - Purified native Mps1, but not autophosphorylated Mps1, binds de-phosphorylated kinetochores lacking endogenous Mps1. 65
Supplementary Figure 2.5. The N-terminus of Mps1 mediates binding to kinetochores. 66

CHAPTER 3: MPS1 PHOSPHORYLATION OF NDC80 REGULATES KINETOCHORE-MICROTUBULE ATTACHMENTS 68

3.1 CONTRIBUTIONS OF COLLABORATORS 68

3.2 SUMMARY 68

3.3 INTRODUCTION 69

3.4 RESULTS 72

PHOSPHORYLATION OF PURIFIED KINETOCHORES REDUCES KINETOCHORE-MICROTUBULE ATTACHMENT STRENGTH 72

MPS1 ACTIVITY IS RESPONSIBLE FOR THE PHOSPHORYLATION-DEPENDENT DECREASE IN KINETOCHORE-MICROTUBULE ATTACHMENT STRENGTH 74

MPS1 PHOSPHORYLATES NDC80 TO WEAKEN KINETOCHORE-MICROTUBULE ATTACHMENTS 76

MPS1 PHOSPHORYLATION OF NDC80 IS NOT REQUIRED FOR SPINDLE ASSEMBLY CHECKPOINT SIGNALING 78

MIMICKING MPS1 PHOSPHORYLATION OF NDC80 ACTIVATES THE SPINDLE ASSEMBLY CHECKPOINT AND LEADS TO CHROMOSOME MISSEGREGATION 79

PREVENTING MPS1 PHOSPHORYLATION OF NDC80 COMPROMISES CHROMOSOME SEGREGATION 81

MIMICKING MPS1 PHOSPHORYLATION OF NDC80 IS LETHAL DUE TO HYPERACTIVE ERROR-CORRECTION BY AURORA B^{IPL1} 82

3.5 DISCUSSION 85

3.6 MATERIALS AND METHODS 88

YEAST METHODS 88

KINETOCHORE PURIFICATIONS 90

TREATMENT AND PREPARATION OF PURIFIED KINETOCHORES AND DAM1 90

LASER-TRAPPING OF PURIFIED KINETOCHORES 91

IMMUNOLOGICAL TECHNIQUES 91

3.7 ACKNOWLEDGEMENTS 92

3.8 FIGURES 93

FIGURE 3.1. IN VITRO PHOSPHORYLATION OF PURIFIED KINETOCHORES REDUCES MICROTUBULE ATTACHMENT STRENGTH. 93

FIGURE 3.2. MPS1 ACTIVITY IS RESPONSIBLE FOR THE PHOSPHORYLATION-DEPENDENT DECREASE IN KINETOCHORE-MICROTUBULE ATTACHMENT STRENGTH. 95
FIGURE 3.3. MPS1 PHOSPHORYLATION OF NDC80 WEAKENS KINETOCHORE-MICROTUBULE ATTACHMENTS. 97
FIGURE 3.4. MPS1 PHOSPHORYLATION IS NOT REQUIRED FOR SPINDLE ASSEMBLY CHECKPOINT SIGNALING. 99
FIGURE 3.5. MIMICKING CONSTITUTIVE MPS1 PHOSPHORYLATION OF NDC80 ACTIVATES THE SPINDLE ASSEMBLY CHECKPOINT AND CAUSES CHROMOSOME MISSEGREGATION. 101
FIGURE 3.6. MPS1 PHOSPHORYLATION OF NDC80 IS IMPORTANT FOR PROPER CHROMOSOME SEGREGATION. 103
FIGURE 3.7. THE BUB1 KINASE-SGO1-AURORA B^{IPL1} BIORIENTATION PATHWAY IS RESPONSIBLE FOR CELL DEATH CAUSED BY MIMICKING CONSTITUTIVE MPS1 PHOSPHORYLATION OF NDC80. 105
3.9 SUPPLEMENTARY FIGURES 106
SUPPLEMENTARY FIGURE 3.1. DAM1 COMPLEX FUNCTION IS REDUCED IN *MPS1-1* AND *NDC80-14A* CELLS. 107
SUPPLEMENTARY FIGURE 3.2. PREVENTING SPINDLE ASSEMBLY CHECKPOINT SIGNALING DOES NOT RESCUE *NDC80-14D*. 108
SUPPLEMENTARY FIGURE 3.3. PLASMID SHUFFLE ASSAY TO DETERMINE IF ADDITIONAL BIORIENTATION MUTANTS RESCUE *NDC80-14D* 109
SUPPLEMENTARY FIGURE 3.4. *NDC80-14A* AND *IPL1-321* DO NOT ADDITIVELY COMPROMISE GROWTH. 111

CHAPTER 4: CONCLUSIONS AND PERSPECTIVES 112

TABLES 116

TABLE 1. LIST OF RELEVANT PHOSPHO-MUTANT ALLELES 116
TABLE 2: PLASMID LIST 117
TABLE 3: STRAIN LIST 119

REFERENCES 131

Acknowledgements

I have been very fortunate to enjoy the mentorship of so many outstanding people throughout my education. In high school, I was inspired by one of my high school biology teachers, Mrs. Smith, who dared to teach natural selection and evolutionary theory in a conservative religious suburb in Ohio. As I watched this woman field questions from angry students with calm intelligence and grace, I was inspired to become like her—to try and spread the joy and beauty of life—apparent in the molecular and physical world—to other people and to always strive for polite and productive discussion.

Many other teachers, both formal and informal, have aided and abetted my other, sometimes pretty intense, interests in literature, history, and archaeology. Over the years I have come to realize that these other interests have helped me be a much more enthusiastic and dedicated scientist than I would be otherwise—how long can one obsess over molecules without having an active imagination and a passion for truth?

I need to thank the first molecular biology lab that claimed me as one of their own—the Fisk Lab at Ohio State University. I am so grateful to Harold for seeing potential in me—a student frustrated with their lack of laboratory experience—and taking me on and teaching me as one of his students. I learned so much about how scientific research is conducted and planned from my time in the Fisk Lab and I'll always be grateful for that—as well as for how much fun it was doing the research. Specifically, I want to thank Amanda Bliemeister-Manivannan for her amazing mentorship and friendship. She taught me how to do Western blots and how to cope with negative results—a very strong foundation for my graduate work and science in general.

I don't know where to begin thanking my graduate mentor Sue Biggins and honestly I could go on for a long time about it but I'll try to keep it brief. Sue is an incredible manager as well as scientist. She's understanding but she's tough; she's positive but she's critical; she works hard and she plays hard. She makes it seem easy

to make tough decisions and remain positive but I know now that these are some of the most difficult tasks in science. I have learned so much about how to act with confidence and manage difficult situations by observing her and actually discussing these topics with her and other members of the lab—this I think is a rare thing for scientists to promote and actively engage in and I am so grateful for her openness and dedication to overall wellness. She has taught me to plan, to try, and to celebrate every day and I think that's exactly how it should be done.

I want to thank my second mentor, Chip Asbury, for his mentorship over the years. I have learned a lot from observing and working with him—how to ask the critical questions and how to reason through seemingly complicated mechanisms and reduce them to simple concepts. He has also been steadfast in supporting me and my work even when I myself was skeptical of it. I am so grateful for his dedication and for all he has taught me—both scientifically and personally—about being a good scientist.

I need to thank all of the members of the Biggins Lab and Asbury Labs who have made it so fun to come to work. It doesn't feel like work when I get to make inside jokes and learn about new mechanisms with them. I have especially benefitted from the mentorship of Amitabha Gupta and Matt Miller—two postdocs with completely different personalities but who both have always made time to discuss science and life in general with me. I also need to thank my colleagues who have contributed valuable thoughts and experimental results to my projects: Nitobe London, Kwaku Opoku, Yi Deng, Aimee Littleton, Matt Miller, Abraham Gutierrez and Josh Larson.

I want to thank the members of my committee—Jihong Bai, Trisha Davis, Alex Paredez and Susan Parkhurst for their advice, mentorship, and support over the years. Thanks so much for pushing me and for believing in my abilities. I'd also like to thank Trisha Davis and Eric Muller for being great mentors of my first venture into budding yeast genetics and real biochemistry. I got hooked and it's been hard for me to stop.

And last but not least I am grateful to my family. I want to thank my uncle Mark Torlone for teaching me how to read—specifically Alice's Adventures in Wonderland—and to enjoy reading and learning when I was very young. Because of him, I was sent out in the hall in first grade to read chapter books while everyone else read The Ball is

Blue or something like that. Next, I need to thank my parents for always encouraging me not just to pass but to excel. Were it not for their not-so-gentle encouragement, I might be some kind of strange person who reads classic novels for pleasure but can't do fourth grade level mathematics. Thanks to them, I can do both by now. Obviously I need to thank my brothers Scott and Andy as well, for also helping me with the math and for making me fluent in sarcasm. Thank you to my partner Nitobe for being as steadfast of a partner as he is a scientist—this guy really never gives up and never gives in. And finally, thank you to all of my friends who have supported me and kept me laughing.

Chapter 1: Introduction

Every living organism is composed of cells and each cell contains the necessary genetic information to reproduce. The process of cell division is vital for the development and health of organisms. Mitosis is a cell division that results in two daughter cells with identical genetic information. The specialized cell division meiosis results in cells called gametes with half of the genetic complement, enabling sexual reproduction via fusion of gametes from distinct parent organisms.

A chromosome, formed of a double-stranded helix of DNA wound around small protein complexes called nucleosomes, is a basic unit of genetic information. Nucleosomes are composed of four unique histone proteins: H2A, H2B, H3 and H4, which are present in two copies each to form an eight-protein octamer. After a cell commits to begin mitosis, the genetic information is replicated in S ('synthesis') phase, forming two identical strands of DNA wound by nucleosomes. A ring-shaped protein complex called cohesin is then loaded onto the chromosome to hold the two identical sister chromatids together until they can be separated later. Duplication of the centrosome, which nucleates and organizes microtubules that will form the chromosome segregation apparatus known as the mitotic spindle, also begins during S phase. During early M ('mitosis') phase, the chromosomes are dramatically re-structured—untangled by topoisomerases and compacted by the condensin complex. This restructuring ensures that chromosomes can be efficiently and accurately segregated between daughter cells. Also during this time, the two centrosomes

separate and move to opposite ends of the cell, all the while nucleating and anchoring microtubules, to form a bipolar mitotic spindle.

Microtubules are dynamic polymers that grow and shrink through the addition and subtraction of alpha/beta tubulin subunits. This intrinsic property of microtubules to undergo periods of growth and disassembly sporadically has been termed dynamic instability (1). Due to the asymmetry of alpha/beta tubulin subunits, microtubules are polar; an alpha subunit caps the minus end and a beta tubulin tops the more dynamic plus end. Centrosomes associate with microtubules primarily through their minus ends while the plus ends are cytoplasmic.

Chromosomes attach to microtubules of the mitotic spindle through a protein complex called the kinetochore. Even in the simple model organism of budding yeast the kinetochore is composed of greater than 50 unique proteins, many of which are present in multiple copies, making it a very large and intricate structure (2). At one end, the kinetochore binds to a discrete location on each chromosome called the centromere, distinguished cytologically as the major constriction point of the duplicated chromosome. In budding yeast, the centromere is a defined sequence of 125 base pairs of DNA but in most eukaryotic organisms it is marked epigenetically, meaning its recognition does not rely on a specific DNA sequence but instead on the presence of specialized nucleosomes. The specialized nucleosome that forms the centromeric foundation of the kinetochore contains an H3-variant called CENP-A.

At its other end, the kinetochore contacts the dynamic plus-ends of microtubules. Each mammalian kinetochore can interact with 3-30 microtubules (3) but

each kinetochore in budding yeast binds to a single microtubule (4), simplifying the study of kinetochore-microtubule attachments.

Microtubule-binding components of the kinetochore

The portion of the kinetochore that interacts with the microtubule, referred to as the outer kinetochore, consists of the KMN network, which includes the KNL1, Mis12, and Ndc80 subcomplexes. Each of these complexes is present in multiple copies, with approximately 6-7 Mis12 complexes, 7-8 Ndc80 complexes and 16-20 Dam1 complexes in the budding yeast kinetochore counted through quantitative fluorescence imaging (5). The 4-protein Mis12 complex, consisting of the Mtw1, Dsn1, Nnf1, Nsl1 proteins in budding yeast, does not directly contact microtubules but interacts with proteins of the KNL1 and Ndc80 subcomplexes. In budding yeast the KNL1 complex consists of the proteins KNL1^{Spc105} and Kre28; in vertebrates KNL1 and ZWINT (6). KNL1^{Spc105} has been found to form a scaffold for the association of spindle assembly checkpoint proteins with the kinetochore. This will be discussed further below. The Ndc80 complex is the most conserved microtubule-binding component of the kinetochore (7). Structurally, the Ndc80 complex is a rod with globular domains at either end (8, 9). It is a heterotetramer consisting of two heterodimers: a Spc24/Spc25 dimer and an Ndc80/Nuf2 dimer (9). The Spc24/Spc25 heterodimer has a coiled-coil at one end and globular heads that bind to the Mis12 complex at the other. The ends of the coiled-coil domain of Spc24/Spc25 interact with the coiled-coil domain in Ndc80/Nuf2 to tetramerize the complex (10). The globular calponin-homology (CH) head of Ndc80 interacts directly with microtubules. The Ndc80 protein itself also has a

positively charged, unstructured tail of 116 amino acids that is important for proper kinetochore-microtubule attachments (11–14). This tail is essential in higher eukaryotes but non-essential in budding yeast, likely due to redundancy with another microtubule-binding complex, Dam1 (11, 12).

The Dam1 complex is an essential microtubule-binding element in yeast and the recently characterized Ska complex of human cells appears to be a functional ortholog (15–18). Dam1 complex is composed of 10 proteins (Ask1, Dad1, Dad2, Dad3, Dad4, Dam1, Duo1, Hsk3, Spc19, Spc34) and requires the KMN network and microtubules for its localization to the kinetochore (19–21). Dam1 complex interacts directly with the Ndc80 complex and recent work has made great progress in defining the precise binding interface (13, 22, 23). Dam1 complex can oligomerize and form rings containing 16 Dam1 complexes, which suggests a compelling model for tracking with disassembling microtubule tips, which curve outward during disassembly (24, 25). Oligomers with fewer or additional Dam1 complex subunits can be assembled in vitro, and it remains unclear which oligomers are relevant in vivo (26).

Biorientation

The process of biorientation begins with the initial capture of kinetochores by spindle microtubules and terminates with every chromosome equally attached to microtubules from each of the two spindle poles, a configuration known as bioriented. Kinetochores initially make attachments to the lateral sides of microtubules and are then pulled toward the centrosome when the microtubules disassemble past the kinetochore attachment point and kinetochores convert to a tip-attached state (27–30).

In order for chromosomes to be segregated properly so that each daughter cell inherits the correct complement of chromosomes, every chromosome must biorient. However, additional attachment states occur such as: monotelic attachment, where one sister kinetochore fails to attach to microtubules; syntelic attachment, where both sister kinetochores are attached to a single centrosome; and merotelic attachment, where one sister kinetochore is attached to microtubules from both centrosomes. Merotelic attachments do not occur in budding yeast, where each kinetochore binds to a single microtubule (4); however, they are frequently observed in the early stages of mitosis in other organisms (31, 32). There are several different mechanisms to avoid and correct these various incorrect attachment states. These mechanisms include error-correction and the spindle assembly checkpoint, which will be discussed below. Some evidence suggests that the back-to-back geometry or structure of chromosomes promotes biorientation, however this mechanism is more difficult to investigate (33–35).

Error-correction by the kinase Aurora B^{Ipl1}

One major mechanism that promotes biorientation is the selective destabilization of incorrect attachments, which has been called error-correction. Following detachment, the kinetochores then have a chance to make bioriented attachments. The kinase Aurora B, called Ipl1 in budding yeast, is responsible for destabilizing incorrect kinetochore-microtubule attachments (36–40). Aurora B^{Ipl1} phosphorylates microtubule-binding proteins of the kinetochore such as Ndc80 and Dam1 (and Ska, in human cells) (39, 41–45). In vitro work has demonstrated that this

phosphorylation reduces the strength of the attachment between these proteins and the microtubule and it was also shown that phosphorylation of Dam1 reduces its interaction with Ndc80 (26, 46–49). Phosphorylation of Dam1 and Ndc80 by Aurora B^{Ipl1} also promotes microtubule disassembly and reduces the frequency of microtubule rescue (50, 51). Purified kinetochores interact more robustly with assembling microtubule tips, so promoting disassembly is an additional mechanism to detach the kinetochore from the microtubule (50).

A popular model to explain Aurora B^{Ipl1}'s ability to distinguish bioriented kinetochores is the spatial separation model. Aurora B^{Ipl1} localizes to centromeres throughout prometaphase when kinetochore-microtubule attachments are being established. It has been proposed that the tension created by bioriented attachment separates the centromeric Aurora B^{Ipl1} from its microtubule-binding substrates in the outer kinetochore. Experiments in human cells with FRET probes consisting of peptides containing the Aurora B^{Ipl1} consensus motif support this model (52). However, some data suggests that the centromeric localization of Aurora B^{Ipl1} is not required for error-correction, calling into question this model (53). Recently, it has been suggested that the activation of Aurora B^{Ipl1} induced by its clustering, at the inner centromere or elsewhere, is the essential requirement for its error-correction activity rather than a spatial separation model per se (54).

The kinase Mps1 promotes biorientation

The protein kinase Mps1 is another essential regulator of kinetochore-microtubule attachments during the process of biorientation in prometaphase. Mps1

kinase is present in eukaryotic organisms from budding yeast to humans, with the notable exception of the nematode *C. elegans,* where it is thought that the Polo-like kinase 1 (Plk1) takes over its role (55). Mps1 was identified in budding yeast as an essential regulator of centrosome duplication, hence it's name monopolar spindle 1 (56). However, its role in that process is less important in human cells (57). Subsequent research uncovered that Mps1 activity is required to sustain the spindle assembly checkpoint (58), which is a signaling pathway that prevents chromosome segregation until every chromosome is bioriented (59). This will be discussed further below.

Careful studies in budding yeast using an analog-sensitive allele, *mps1-as1*, which can be specifically inhibited using a bulky ATP analog, showed that sister kinetochores do not biorient if Mps1 is inhibited (60, 61). Spindle assembly checkpoint signaling is not required for this phenomenon (60). It was also demonstrated that Mps1 activity is required for proper localization of the Dam1 protein and for kinetochores to properly interact with microtubules, consist with a loss of Dam1 kinetochore function following inhibition of Mps1 (61–64).

There is evidence that Mps1 directs the localization and activation of Aurora B^{Ipl1} to promote biorientation in human cells (65) and, conversely, that Aurora B^{Ipl1} activity is required to promote proper Mps1 kinetochore localization (66, 67). However, other observations indicate that Mps1 can promote biorientation independently of Aurora B^{Ipl1} (60, 68, 69). More recent work in human cells has uncovered that Mps1 phosphorylates the Ska complex and that this phosphorylation destabilizes kinetochore-microtubule attachments, suggesting that Mps1 plays a similar role to

Aurora B^{Ipl1} in the error-correction process (70). This recent work suggests the phosphatase PP2A-B56 reverses phosphorylation of Ska (70).

Mps1 kinase activates the spindle assembly checkpoint

The spindle assembly checkpoint arrests the cell cycle, preventing chromosome segregation in anaphase, in response to incorrect kinetochore-microtubule attachments. It does this by inhibiting the activity of the anaphase promoting complex (APC), an E3 ubiquitin ligase which targets cyclin B, a cofactor of the major mitotic kinase Cdk1, and the protein $Securin^{Pds1}$ for destruction (59). $Securin^{Pds1}$ prevents the protease separase from cleaving open the cohesin ring that holds sister chromatids together. Unattached kinetochores are the scaffold for the generation of a diffusible "wait" signal, the mitotic checkpoint complex (MCC), which inhibits the APC in multiple ways (71).

Most of the spindle assembly checkpoint genes were identified in budding yeast screens for mutants that did not arrest their cell cycle in response to microtubule-depolymerizing drugs (72, 73). The checkpoint proteins Mps1, Bub3, Bub1, Mad1, Mad2, and $BubR1^{Mad3}$ localize to unattached kinetochores (with the exception that $BubR1^{Mad3}$ is not detected at budding yeast kinetochores) (74). Fluorescence recovery after photobleaching (FRAP) experiments showed that the localization of these proteins to kinetochores is highly dynamic (75, 76). Observations from many different studies have created a detailed outline of how the MCC—which consists of the proteins Mad2, $BubR1^{Mad3}$,Bub3 and Cdc20 –is formed and inhibits the APC. In brief, Bub3 and Bub1 form a complex (Bub3/Bub1), as does Mad1 and Mad2 (Mad1/Mad2), and these are

recruited to unattached kinetochores. Mad2 exists in two conformations – named open (O-Mad2) and closed (C-Mad2) (77). C-Mad2 can bind to Mad1 or Cdc20 while O-Mad2 only dimerizes with C-Mad2 (77, 78). Dimerzation of soluble O-Mad2 with kinetochore-bound C-Mad2 (in complex with Mad1) converts it into the C-Mad2 form which can then bind to Cdc20 and form part of the MCC (59).

An elegant genetic analysis determined that Mps1 is the most upstream component of the spindle assembly checkpoint cascade (79). Since then, research has uncovered the underlying mechanism. Mps1 phosphorylates threonines in so-called MELT motifs in KNL1^{Spc105} to recruit the Bub3/Bub1 complex to kinetochores, with Bub3 directly interfacing with KNL1^{Spc105} (80–84). In a second step, Mps1 phosphorylates residues in Bub1 to recruit Mad1/Mad2 to the kinetochore (85, 86). In human cells, the Rod1-Zwilch-Zw10 protein complex (RZZ), which requires KNL1/ZWINT for its kinetochore localization, also appears to contribute to Mad1 kinetochore localization (59). In addition, two KI motifs in human KNL1 directly interact with BubR1^{Mad3}/Bub1 and are important for efficient checkpoint signaling (84, 87). Recently, it was found that Mps1 phosphorylates the threonine in a human-specific SHT motif that lies C-terminal to the MELT motifs in KNL1 and that this enhances recruitment of Bub3/Bub1 to kinetochores (88).

The kinetochore recruitment of Bub1 is also important for proper chromosome segregation outside of checkpoint signaling. Bub1 kinase phosphorylates histone H2A to recruit the centromeric protein Sgo1, which promotes sister kinetochore biorientation and Aurora B^{Ipl1} localization and activity (33, 89–95).

Spindle assembly checkpoint silencing and Mps1 kinetochore localization

While molecular events that generate the MCC and inhibit the APC have been worked out in detail, the events required for spindle assembly checkpoint silencing are less clear. The phosphatase $PP1^{Glc7}$ can reverse Mps1 phosphorylation of $KNL1^{Spc105}$ (80) and is important for proper checkpoint silencing (96, 97). In human cells, the localization of the phosphatase PP2A-B56 to kinetochores, which is antagonized by Aurora B^{Ipl1} phosphorylation of KNL1, promotes the kinetochore localization of PP1 (97). Therefore, downregulating Aurora B^{Ipl1} activity toward KNL1 contributes to checkpoint silencing. These observations may also explain why Aurora B^{Ipl1} activity is required for spindle assembly checkpoint activation in response to tension defects in budding yeast—potentially, $PP1^{Glc7}$ is prematurely localizing to kinetochores when Aurora B^{Ipl1} is inactivated and silencing the checkpoint, making it appear to similar to a checkpoint activation defect.

The position of Mps1 kinase at the top of the checkpoint cascade makes it an obvious target to deactivate and thereby silence the checkpoint. In addition, Mps1 activity accelerates the rate limiting step of MCC formation—the conversion of Mad2—dramatically, making it a central regulator of SAC activity (98). Previous work found that Mps1 is degraded by the APC and that overexpression of Mps1 in anaphase re-activates the spindle assembly checkpoint (99). In addition, both overexpression of Mps1 and tethering Mps1 to kinetochores in prometaphase leads to constitutive checkpoint activation, despite apparently intact bioriented attachments (79, 100).

Mps1 localization at kinetochores correlates with spindle assembly checkpoint activation, with the highest levels of kinetochore Mps1 on unattached or prometaphase

kinetochores and lower levels observed at metaphase (75, 101, 102). Mps1 dimerizes and autophosphorylates in trans and thus localization at kinetochores is thought to provide a platform for the concentration of additional molecules of Mps1 that may be activated further and/or reach Spc105/KNL1 to signal the SAC (100, 103–105). Truncation analyses determined that regions of the extreme N-terminus of human Mps1 are important for kinetochore localization (66, 106–110). Mps1 kinetochore localization depends on the presence of Ndc80 protein and Mps1 binds to Ndc80 in vitro (102, 106, 111).

Interestingly, a mutant of Mps1 lacking the first 100 amino acids that fails to localize to kinetochores was capable of activating a checkpoint arrest in response to nocodazole, suggesting that cytosolic Mps1 is capable of checkpoint activation (69). However, the length of the arrest was reduced compared to cells expressing wild-type Mps1 (69). This suggests that Mps1 kinetochore localization promotes its ability to efficiently signal the spindle assembly checkpoint.

Overview of thesis

Previously, a method for purifying intact kinetochores from budding yeast cells was developed that enables dissection of the molecular requirements for specific kinetochore functions (112, 113). In my thesis work, I aimed to use this method to determine the mechanisms that promote Mps1 dissociation from kinetochores at metaphase, thus shedding light on the requirements for spindle assembly checkpoint silencing. I found that autophosphorylation is sufficient to prevent Mps1 binding to purified kinetochores, indicating that localization is phosphoregulated. Secondly, I

aimed to identify the function of Mps1 phosphorylation of Ndc80, which is a major microtubule-binding protein. I found that Mps1 phosphorylation of Ndc80 weakens kinetochore-microtubule attachments in vitro and promotes proper chromosome segregation in vivo.

Chapter 2: Regulation of the kinetochore localization of the checkpoint kinase Mps1

2.1 Contributions of collaborators

Kwaku N. Opoku, Yi Deng, and Aimee Littleton performed experiments and collected data included in this section. Nitobe London made preliminary observations and contributed to the conceptualization of this project. Kwaku N. Opoku and Yi Deng performed all of the TIRF imaging and analysis. Aimee Littleton purified kinetochores that were analyzed by TIRF and contributed the Pds1 timecourses in Supplementary Figure 2.2. Sue Biggins and Charles L. Asbury jointly directed and supervised the project.

2.2 Summary

Accurate mitosis depends on a surveillance system called the spindle assembly checkpoint. The checkpoint acts at kinetochores, which attach chromosomes to the dynamic tips of spindle microtubules. When a kinetochore is unattached or improperly attached, the kinase Mps1 phosphorylates kinetochore components, catalyzing the generation of a diffusible 'wait' signal that delays anaphase and gives the cell time to correct the error. When a kinetochore becomes properly attached, its checkpoint signal is silenced to allow progression into anaphase. Recently, microtubules were found to compete directly against recombinant Mps1 fragments for binding to truncated forms of the major microtubule-binding kinetochore element, Ndc80c, suggesting a direct

competition model for checkpoint silencing at properly attached kinetochores (102, 106). Here, by developing single-particle fluorescence-based assays, we tested whether such direct competition occurs in the context of native kinetochore particles isolated from yeast. Mps1 levels were not reduced on kinetochore particles bound laterally to the sides of microtubules, nor on particles tracking processively with disassembling tips. Instead, we found that Mps1 kinase activity was sufficient to promote its release from kinetochores in vitro. Mps1 autophosphorylation, rather than phosphorylation of other kinetochore components, was responsible for this dissociation. Our findings suggest that checkpoint silencing does not arise from a direct competition between Mps1 and microtubules, and that phosphoregulation of Mps1 is a critical aspect of the silencing mechanism.

2.3 Introduction

Chromosomes must be accurately segregated into daughter cells for the development and survival of all organisms. However, the process is prone to errors that must be detected and corrected to avoid chromosome missegregation events that generate aneuploidy, a hallmark of cancers and other diseases (114). A surveillance system called the spindle assembly checkpoint helps ensure faithful segregation by preventing cell cycle progression until every chromosome has made proper bioriented attachments to microtubules from opposite poles (59, 115). The checkpoint is initiated by the hierarchical recruitment of proteins to the kinetochore, which subsequently generates a soluble inhibitory signal that halts cell cycle progression. While the activation of this “wait” signal has been extensively characterized, the events that

trigger its deactivation remain unclear. Both premature and abnormally late spindle checkpoint deactivation can lead to genetic abnormalities associated with cancer (116, 117), so understanding this mechanism is relevant to human health.

The conserved protein kinase Mps1 is the most upstream component of the spindle assembly checkpoint and it also regulates sister kinetochore biorientation through an independent mechanism (55). Mps1 expression is cell cycle regulated, with peak protein levels appearing during prometaphase followed by degradation in anaphase (99, 107). It localizes to kinetochores through binding to the microtubule-binding protein Ndc80 (79, 111, 118), perfectly positioning it to sense and respond to the attachment state of the kinetochore. Mps1 kinetochore localization is highly dynamic, cycling on and off the kinetochore with a half-life of several seconds in mammalian cells (75, 100). Tethering Mps1 to the central kinetochore leads to constitutive activation of the spindle assembly checkpoint, suggesting that regulating Mps1 kinetochore localization is critical for proper checkpoint signaling (70, 100, 101). In addition, the level of Mps1 on kinetochores peaks in prometaphase when attachments are being established and declines as bioriented attachments are achieved at metaphase (75, 101, 119). Thus, it seems likely that the dissociation of Mps1 protein from kinetochores is a key aspect of spindle assembly checkpoint silencing.

A simple and elegant model for spindle checkpoint silencing posits that Mps1 and microtubules compete directly for binding to Ndc80, thus linking microtubule attachment to checkpoint deactivation (102, 106). Although this model was supported by biochemical data collected using recombinant proteins, it does not account for a

residual pool of Mps1 that remains on bioriented metaphase kinetochores in cells (75, 101, 102). Other mechanisms have been proposed to explain the loss of Mps1 checkpoint activity upon biorientation, which invoke spatial or enzymatic regulation of Mps1 (100, 101, 108, 120–124). Despite the evidence for multiple mechanisms that control Mps1 localization and checkpoint activity, it has been difficult to discern their relative importance or sequential order given the intertwined nature of events within cells. Thus, the mechanism that causes Mps1 dissociation from microtubule-attached kinetochores remains incompletely understood, despite its relevance to checkpoint silencing.

To elucidate the mechanisms that control Mps1 dissociation from kinetochores, we developed a unique *in vitro* reconstitution system with kinetochores purified from budding yeast. Using single particle microscopy assays, we found that microtubules and Mps1 do not compete directly for association with isolated native kinetochores. Instead, our biochemical assays show that Mps1 kinase activity is sufficient for its release from kinetochores. The key substrate appears to be Mps1 itself rather than core kinetochore proteins. Together, these data lead us to propose that biorientation promotes Mps1 autophosphorylation, which decreases the affinity of Mps1 for kinetochores and contributes to checkpoint silencing.

2.4 Results

Kinetochores simultaneously bind to Mps1 and microtubules *in vitro*

We began by testing whether microtubule binding excludes Mps1 from isolated kinetochores. We purified kinetochores by immunoprecipitation (IP) of the Dsn1

kinetochore component from budding yeast cells expressing epitope-tagged Mps1, which co-immunoprecipitates with kinetochore complexes (112). The kinetochores were retained on the antibody-conjugated magnetic beads and then incubated with fluorescently labeled taxol-stabilized microtubules or with unpolymerized tubulin (Figure 2.1A). As negative controls, we also incubated beads lacking kinetochores with tubulin or with microtubules. After the incubation, the beads were washed and the relative levels of tubulin and Mps1 that remained associated with the bead-bound kinetochores were analyzed by SDS-PAGE followed by fluorescence imaging and immunoblotting (Figure 2.1A). As expected, the kinetochores bound to more tubulin in the taxol-stabilized microtubules than unpolymerized tubulin, and this microtubule binding required the Ndc80 protein (Supplementary Figure 2.1). However, there was no change in the amount of Mps1 that remained associated with kinetochores in the presence or absence of microtubule attachments (Figure 2.1A). These data suggest that kinetochores can simultaneously bind Mps1 and microtubules, in apparent contradiction to a competitive binding model.

A single particle method to measure Mps1 levels on individual kinetochores

Because subpopulations of microtubule-bound and unbound kinetochores could not be distinguished in our initial experiments, we developed a single-particle method to visualize and quantify Mps1 levels on individual kinetochores. To control for heterogeneity in the composition of purified kinetochores as well as the fact that kinetochores contain multiple molecules of Ndc80 and Mps1 (41, 42, 125), we

quantified the levels of the core kinetochore protein Mtw1 as well as Mps1. A previous study counted roughly equal numbers of Mtw1 and Ndc80 molecules in the budding yeast kinetochore (5). We created strains in which endogenous Mps1 and Mtw1 were fused at their C-termini to SNAP and CLIP epitope tags (126, 127), respectively, for labeling with bright, photostable organic fluorophores. Cells expressing Mtw1-CLIP and Mps1-SNAP activated the spindle assembly checkpoint in response to the microtubule-destabilizing drug nocodazole, confirming the functionality of the fusion proteins (Supplementary Figure 2.2B). Kinetochores isolated from these cells were dyed with SNAP-Surface-549 and CLIP-Surface-647, and then tethered sparsely to coverslips for imaging by multi-color TIRF (total internal reflection fluorescence) microscopy. Most of the particles were single-color, carrying Mtw1 but lacking Mps1, with only a small fraction of particles, 20 ± 5 %, carrying both Mps1 and Mtw1 (Supplementary Figure 2.2D).

Given the relatively poor colocalization, we sought to improve the recovery of kinetochore-bound Mps1 to allow a better dynamic range for single particle experiments. We found that kinetochore particles purified from a mutant *dsn1-2D* strain, with the phosphomimetic mutations S240D and S250D that have previously been shown to improve retention of outer kinetochore proteins (128, 129), contained Mps1 more frequently. The fraction of phosphomimetic Dsn1-2D particles carrying both Mps1 and Mtw1 was 47 ± 6 % (Supplementary Figure 2.2D), more than double the retention of wild-type. Particles with just one detectable Mps1 or Mtw1, identifiable by their single-step photobleaching behavior, served as internal controls, allowing normalization of particle brightness and estimation of the ratios of Mps1 to Mtw1

molecules. On average, Dsn1-2D kinetochore particles carried 0.51 ± 0.02 Mps1 molecules per Mtw1, a ratio 5-fold higher than wild-type particles, which carried only 0.11 ± 0.02 Mps1 molecules per Mtw1 (Supplementary Figure 2.2E). We confirmed that *dsn1-2D* cells have normal checkpoint function (Supplementary Figure 2.2A-B) and used them for subsequent single particle experiments.

Individual kinetochores associate simultaneously with Mps1 and microtubules

If Mps1 and microtubules compete directly for binding to the kinetochores, then high-occupancy particles, carrying one or more Mps1 molecules per Mtw1, should be inhibited from binding to microtubules. Conversely, the population of particles that do bind microtubules should be enriched for low-occupancy particles. To test this, we anchored taxol-stabilized microtubules to coverslips, introduced the labeled kinetochores, and then allowed them to bind the sides of the filaments (Figure 2.1B) (50, 112). Contrary to our expectation, microtubule-bound kinetochores had an even higher Mps1 occupancy than unbound particles. The fraction of microtubule-bound kinetochores that retained Mps1 was 96 ± 3 % (Figure 2.1C), roughly double that of the control unbound population (50 ± 3 %). The microtubule lattice-bound kinetochores also carried a higher number Mps1 molecules per Mtw1 molecule, 1.33 ± 0.01 on average, which was 3-fold higher than the ratio measured for the control unbound population, 0.45 ± 0.01 (Figure 2.1D). Thus, microtubule attachment appears to select for, rather than against the high-occupancy particles. We speculate that this higher retention of Mps1 might occur because binding to microtubules selects for more complete

kinetochore particles. Regardless, our observations indicate that isolated yeast kinetochores can associate simultaneously with Mps1 and with the microtubule lattice in a non-competitive manner.

While kinetochores initially associate with the lateral sides of microtubules, they convert to end-on attachments during biorientation. Because the checkpoint is only silenced when chromosomes have established bioriented end-on attachments (130), we developed a single particle technique to analyze Mps1 association with tip-attached kinetochores. Purified, labeled kinetochores were tethered to coverslips and fluorescent taxol-stabilized microtubules were introduced into the chamber. Through thermal diffusion, the ends of the microtubules tended to interact with the kinetochores (Figure 2.2A). Surface-tethered kinetochores in the same fields of view that failed to capture a microtubule served as internal controls. Nearly all of the kinetochores that captured microtubule ends retained Mps1, 93 ± 21 % (Figure 2.2B). A smaller fraction of the control, unattached particles retained Mps1, 35 ± 14 %, which was similar to the retention observed in experiments without microtubules (Figure 2.1C, 2.2B). Together, these data suggest that kinetochore attachment to the lateral surfaces or tips of microtubules does not displace Mps1 from the kinetochore.

Individual kinetochores tracking disassembling microtubule tips retain Mps1

Bioriented kinetochores in vivo attach persistently to dynamic microtubule tips, an arrangement that allows them to harness tip disassembly to drive chromosome movement (131, 132) and might also be important for silencing their checkpoint

signals. To examine whether dynamic tip attachments are required to exclude Mps1 from kinetochores, we grew microtubules from coverslip-anchored seeds and allowed purified, labeled kinetochores to attach laterally to the growing filaments. We then induced microtubule disassembly by rapid buffer exchange to remove the free tubulin (Figure 2.3A). When disassembling tips encountered individual kinetochore particles, the particles began tracking with the tips and were usually carried all the way to the coverslip-anchored seed (Figure 2.3B), as previously observed (112). Nearly all the tip-tracking particles, 95 ± 22 %, retained Mps1 throughout their movement (Figure 2.3C). A similarly high level of Mps1 retention, 93 ± 11 %, was seen for laterally attached particles in the same fields of view (Figure 2.3C), consistent with the results using taxol-stabilized filaments. These data show that kinetochore attachment to dynamic microtubule tips does not dissociate Mps1 and suggests that spindle checkpoint silencing is carried out through a different mechanism.

Activating Mps1 triggers its release from kinetochores

Microtubule binding did not release Mps1 from kinetochores in our reconstitution experiments, yet Mps1 levels are clearly reduced on bioriented versus unattached kinetochores in cells (75, 101, 107). Previous research in human cells found that abrogating Mps1 activity with inhibitors increases the level of kinetochore-associated Mps1 and also reduces Mps1 turnover at kinetochores, suggesting that Mps1 release from kinetochores is phosphoregulated (100, 121–123). Additionally, mutational analyses found that Mps1 autophosphorylation regulates its localization to kinetochores, but there were conflicting observations on whether it aids or inhibits its

kinetochore association (102, 108, 109). We hypothesized that Mps1 activity might be sufficient to promote its release from isolated kinetochores and were able to test this because Mps1 is the primary kinase activity that co-purifies with the isolated yeast kinetochores (80). I therefore purified kinetochores carrying Mps1-SNAP and Mtw1-CLIP, dyed them, and then treated them with or without ATP. I analyzed Mps1 levels that remained associated with kinetochores as well as those that were released into the supernatants via fluorescent gel imaging. ATP treatment was sufficient to release Mps1 from the purified kinetochores and the electrophoretic mobility of the released Mps1 was clearly reduced (Figure 2.4A), suggesting it had become phosphorylated. To confirm that the mobility shift was due to phosphorylation, I purified Mps1 itself, treated it with ATP, and then added λ-phosphatase. Indeed, an ATP-dependent mobility shift occurred and was eliminated by phosphatase treatment (Figure 2.4B). These results show that activating kinetochore-associated Mps1 triggers its autophosphorylation as well as its release from kinetochores.

Mps1 autophosphorylation reduces its affinity for kinetochores

Mps1 phosphorylates several major kinetochore proteins *in vitro* (80, 111), including Ndc80, making it unclear whether Mps1 release is due to phosphorylation of sites on kinetochore proteins, on Mps1 itself, or both. To distinguish among these possibilities, I independently manipulated the phosphorylation states of isolated kinetochores and Mps1 and then tested whether they would associate *in vitro*.

First, I tested whether Mps1-mediated phosphorylation of kinetochores alters their affinity for Mps1. I created phosphorylated kinetochores lacking endogenous

Mps1 by incubating purified kinetochores with ATP (Figure 2.4C). Immunoblotting confirmed the release of endogenous Mps1 (Supplementary Figure 2.3A) and an electrophoretic mobility shift of Spc105, a known Mps1 substrate (80), served as a readout for kinetochore phosphorylation by Mps1 (Figure 2.4D). To create de-phosphorylated kinetochores for use as controls, I divided the ATP-treated kinetochores and treated half with λ-phosphatase. The phosphorylated and de-phosphorylated kinetochores were then incubated with exogenous Mps1-V5 (~97kD) that had been purified separately under high stringency conditions from asynchronously growing yeast cells (Supplementary Figure 2.3B). I found that similar amounts of exogenous Mps1-V5 bound to the kinetochores regardless of their phosphorylation state (Lanes i and ii, Figure 2.4D), indicating that kinetochore phosphorylation by Mps1 does not inhibit Mps1 from associating with kinetochores.

To test whether the affinity of Mps1 for kinetochores is reduced specifically by autophosphorylation, I generated autophosphorylated Mps1-V5 by incubating the purified kinase with ATP (Supplementary Figure 2.3B). De-phosphorylated kinetochores lacking endogenous Mps1 were also prepared by sequential treatment with ATP and λ-phosphatase (Figure 2.4C, Supplementary Figure 2.4), and then incubated with either native Mps1-V5 or in vitro autophosphorylated P-Mps1-V5. Strikingly, while native Mps1-V5 bound well to the kinetochores, the autophosphorylated P-Mps1-V5 bound poorly (Lanes iii and iv, Figure 2.4E, Supplementary Figure 2.4). Taken together, these results demonstrate that autophosphorylated forms of Mps1 have lower affinity for kinetochores.

Phosphorylation of the kinetochore-binding domain promotes Mps1 release from kinetochores

We hypothesized that the phosphorylation sites required for Mps1 release resided in its kinetochore localization domain. Although the regions of human Mps1 that mediate kinetochore localization have been determined (66, 107, 110), yeast Mps1 bears almost no homology to human Mps1 in the non-catalytic region. I therefore ectopically expressed Mps1 truncations in cells to identify the yeast kinetochore localization domain. The truncations lacked the Mps1 dimerization region to avoid association with the endogenous full-length Mps1 (Figure 2.5A, (133)). I found that ectopically overexpressed Mps1 N-terminus (1-400) did not associate with full-length endogenous Mps1 (Figure 2.5B), as expected, but did co-purify with kinetochores (Figure 2.5C), albeit weakly. This suggests that the N-terminus of yeast Mps1 contains the kinetochore localization domain, similar to human Mps1 (66, 107, 110). In contrast to the N-terminus, the Mps1 C-terminus (440-765) did not significantly co-purify with kinetochores, despite its high protein level in the lysate (Figure 2.5D). Taken together, these results suggest that the N-terminus of yeast Mps1 contains its major kinetochore localization domain.

We reasoned that mutating Mps1 autophosphorylation sites in the N-terminus to prevent their phosphorylation should increase the affinity of Mps1 for kinetochores and prevent its release from them. Previous genetic analyses demonstrated that the N-terminus of budding yeast Mps1 mediates two essential functions, centrosome duplication and biorientation (133). To avoid pleiotropic effects, I focused on a region previously identified to be specifically required for biorientation, amino acids 151-200

(133). Mass-spectrometry data indicated that four residues within this region are phosphorylated *in vivo* (134). To test whether phosphorylation of this region releases Mps1 from kinetochores, I mutated all 8 serines and threonines within it to alanine to prevent their phosphorylation, generating the *mps1-8A* allele (Figure 2.5A). I found that *mps1-8A* cells grew comparably to wild-type on rich media and media containing the microtubule destabilizing drug benomyl (Supplemental Figure 2.5A). The latter suggests that Mps1-8A is capable of activating the checkpoint and supporting faithful chromosome segregation under conditions in which prolonged checkpoint activation is required for full viability. *Mps1-8A* cells were also able to release from a spindle assembly checkpoint arrest induced by nocodazole (Supplementary Figure 2.5B), indicating that phosphorylation of these sites is not strictly required for checkpoint silencing *in vivo.* However, I found that preventing phosphorylation of these sites deaccelerated the kinetics of Mps1 release from kinetochores in vitro. To measure Mps1 release kinetics, I isolated kinetochores from strains expressing wild-type Mps1 or Mps1-8A, incubated them with ATP for varying time periods, and then analyzed the amount of Mps1 that remained bound to the kinetochores. While most of the wild-type Mps1 was released from kinetochores by 4 minutes, a significant fraction of Mps1-8A was retained on kinetochores at 4 and 20 minutes following the addition of ATP (Figure 2.5E, Supplementary Figure 2.5C). These observations demonstrate that phosphorylation of the kinetochore localization domain in the N-terminus of Mps1 accelerate its release from kinetochores.

Phosphorylation of Mps1 also promotes its association with kinetochores

To identify all of the phosphorylation sites that mediate release from kinetochores, I mutated 8 additional potential phosphorylation sites in the extreme N-terminus of Mps1, generating an *mps1-16A* allele (Table 1). Of the newly mutated sites, 5 (S22, T28, S50, T71, S203) were detected as phosphorylated in our unpublished mass spectrometry data and 3 (T47, S129, T145) were selected because they resemble an Mps1 consensus sequence (135). Using a plasmid shuffle assay, I found that cells were viable with *mps1-16A* as the sole copy of *MPS1* (136) (Figure 2.6A). However, I found that *mps1-16A* behaved as a dominant negative in meiosis, causing nearly complete spore inviability despite the normal appearance of tetrads (2/176 living spores, Figure 2.6B). In analyzing the association of Mps1-16A with kinetochores through co-immunoprecipitation, I found that less Mps1-16A associated with kinetochores compared to wild-type, suggesting that the phosphorylation promotes Mps1 kinetochore association (Figure 2.6C-D). Through growth assays, I observed that *mps1-16A* cells grew poorly on media containing benomyl, consistent with a possible spindle assembly checkpoint defect (Figure 2.7A). Next, I performed a spindle assembly checkpoint silencing assay in *mps1-16A* versus wild-type cells and found that *mps1-16A* cells silenced the checkpoint activated in response to nocodazole with wild-type-like kinetics (Preliminary result: Figure 2.7C). This suggests that Mps1-16A does not delay spindle assembly checkpoint silencing as might be expected if the mutations only delayed Mps1 autophosphorylation-induced release from kinetochores. Since Mps1-16A was hypomorphic for binding to kinetochores, the lack of a delay in checkpoint silencing could possibly be due to a hypomorphic checkpoint activation not

reflected by the levels of Securin^{Pds1} in the lysates from the nocodazole-treated cells. Alternatively or in addition to this, it is possible that Mps1-16A is a less active kinase, also weakening checkpoint activation and lowering the threshold needed for silencing.

I hypothesized that a constitutively catalytically inactive mutant, Mps1-D580A (137), might have a stronger association with kinetochores than wild-type, in line with observations following kinase inhibition in human cells (100, 121–123). Surprisingly however, I found that Mps1-D580A did not associate with kinetochores as strongly as wild-type (Figure 2.6C-D). This observation suggests that Mps1 kinase activity promotes its association with kinetochores. Similar to my findings with *mps1-16A*, I found that *mps1-D580A* caused a growth defect (Figure 2.7B) and spore inviability in a dominant negative manner (5/176 living spores, Figure 2.6B). I performed a spindle assembly checkpoint silencing assay with *MPS1/mps1-D580A* and *MPS1/MPS1* diploids and found that while wild-type cells silenced the checkpoint efficiently following nocodazole washout, *MPS1/mps1-D580A* cells continued to signal the checkpoint throughout the duration of the timecourse (Preliminary result: Figure 2.7D). I speculate that the constitutively inactive Mps1-D580A may induce significant defects in spindle pole body duplication or function that cause continuous activation of the checkpoint despite its lowered levels on kinetochores.

Preliminary evidence that the *mps1-R170S* mutant is defective in kinetochore association and spindle assembly checkpoint signaling

Mps1-7 was isolated as a separation-of-function allele that appears to be competent for the spindle pole body functions of Mps1 based on genetic data but it

renders cells sensitive to the microtubule destabilizing drug benomyl, similar to spindle assembly checkpoint mutants (62, 138). The single point mutation R170S was found to cause the *mps1-7* phenotype (138). Mps1-R170S is defective in meiotic chromosome alignment and segregation (62) but has wild-type-like kinase activity in vitro (138). In a preliminary experiment, I found that Mps1-R170S renders cells unable to activate the spindle assembly checkpoint in response to nocodazole (Figure 2.7E). Because R170 lies within the kinetochore-binding domain of Mps1 I was characterizing, I tested whether this mutation affects the association of Mps1 with kinetochores by purifying kinetochores from *mps1-R170S* cells and analyzing the associated Mps1 by immunoblotting. I found that Mps1-R170S failed to co-immunoprecipitate with kinetochores (Figure 2.7F). It is possible that Mps1-R170S disrupts an essential electrostatic interaction between the Mps1 N-terminus and kinetochores. Alternatively, the mutation may reduce kinase activity in cells and this is not reflected by the in vitro kinase assays, as has been recently demonstrated for a human Mps1 N-terminal mutant (139).

2.5 Discussion

Mps1 initiates and sustains the spindle assembly checkpoint, so understanding the regulation of its activity is paramount to understanding spindle checkpoint function. The release of Mps1 from bioriented kinetochores in vivo (75, 101, 119), and evidence that the duration of checkpoint signaling is modulated by Mps1 kinetochore localization (70, 100, 101), together strongly suggest that regulating Mps1 kinetochore localization is a key aspect of spindle assembly checkpoint function. Here, by

developing in vitro assays to monitor spindle assembly checkpoint protein colocalization with isolated yeast kinetochore particles, we show that native, kinetochore-bound Mps1 does not interfere with the attachment of the kinetochores to microtubules in several different configurations, arguing against the direct competition model for checkpoint silencing.

How is it that competition between Mps1 and microtubules for binding to Ndc80 was observed previously (102, 106) but not in our kinetochore reconstitution system? A simple explanation (102, 106) is that previous studies used recombinant proteins and fragments of the Mps1 N-terminus, which may not reconstitute the native binding configuration or may lack regulatory elements present in the full-length Mps1. For example, full-length, semi-phosphorylated Mps1 may have a higher affinity for kinetochores, consistent with our observation that an N-terminal Mps1 fragment was poorly associated with native kinetochores. Alternatively, the mechanism of Mps1 interaction with Ndc80 may vary across species. The N-termini of yeast and human Mps1 are quite divergent but both human and yeast Mps1 bind to a relatively short and highly conserved region of the N-terminus of Ndc80/Nuf2 (66, 111), suggesting that the variation would likely be found in Mps1 itself. In addition, multiple Mps1-Ndc80 interaction surfaces that are regulated differently by microtubule binding to Ndc80 might exist in full-length Mps1. Indeed, within the N-terminus of human Mps1, three distinct Ndc80c interaction domains have been described—the “N-terminal extension” (aa 1-62), the TPR domain (aa 63-192), and a region of the middle domain of the N-terminus residues 261-300 (66, 102, 103, 106). However, recent biochemical analyses on the interaction between full-length human Mps1 and the Ndc80 complex uncovered

no evidence for cooperative binding, suggesting that Mps1 binds to Ndc80 preferentially through one major interaction site (102). Finally, multiple distinct pools of Mps1 may exist in cells, perhaps distinguished by structural differences or post-translational modifications, and certain pools might interact with kinetochores in different ways. However, this hypothesis is not supported by FRAP data that showed there is only a single, highly dynamic pool of Mps1 at mammalian kinetochores (75).

Our results show that Mps1 autophosphorylation promotes its release from isolated yeast kinetochore particles. This observation is consistent with prior work in human cells, where chemical inhibition of Mps1 causes its accumulation at kinetochores (100, 103, 108, 121–123), and where phosphomimetic mutations in Mps1 reduce its levels at kinetochores (108). Therefore, autophosphorylation of Mps1 kinase could be a conserved mechanism for promoting its release from kinetochores. However, other evidence suggests that autophosphorylation of Mps1 might promote its interaction with, rather than its release from the core kinetochore component Ndc80 (Figure 2.6) (102, 109). Given that Mps1 is heavily phosphorylated in mitotic cells, we hypothesize that autophosphorylation of some sites might promote kinetochore localization while phosphorylation of others might promote release (66, 99, 100, 102, 106, 107, 109, 140).

Our results lead us to speculate that molecular or physical events occurring when sister kinetochores make end-on bioriented attachments might stimulate Mps1 autophosphorylation and release. Consistent with this possibility, a previous study found that microtubules stimulate Mps1 kinase activity *in vitro* (110). It seems possible that as a kinetochore interacts with a microtubule, a transient interaction between

Mps1 and the microtubule might enable Mps1 autophosphorylation, lowering its affinity for Ndc80. Alternatively, a conformational change in the kinetochore (101) that occurs when it attaches to a microtubule might promote Mps1 autophosphorylation. In addition, such a conformational change might distance Mps1 from its checkpoint substrate KNL1/Spc105 (101). In this way, a conformational change in the kinetochore caused by microtubule binding or tension could silence Mps1 checkpoint activity in multiple ways—it might simultaneously block Mps1 activity toward checkpoint substrates and redirect its activity toward itself, triggering its release from the kinetochore.

Because autophosphorylation inhibits Mps1 kinetochore localization, re-localization of Mps1 to kinetochores to continue checkpoint signaling while incorrect attachments persist must require either dephosphorylation or the localization of new molecules of Mps1. Recent evidence in *Drosophila* suggests that Mps1 is dephosphorylated by PP1, however the PP1 recognition motif identified is not found in yeast or human Mps1 (120). Mps1 protein levels on kinetochores are higher in metaphase-arrested cells versus untreated metaphase cells, lending some support to the idea that there is some degradation of Mps1 following auto-release from bioriented kinetochores (101). Thus, it is possible that phosphorylated forms of Mps1 are degraded in the time leading up to anaphase.

Consistent with our model of heightened Mps1 auto-activity during checkpoint silencing, FRAP data suggests that Mps1 is more dynamic on metaphase versus prometaphase kinetochores in mammalian cells (75). Additionally, prior studies have reported that both yeast and human Mps1 remain hyperphosphorylated throughout a

metaphase arrest where chromosomes biorient but are not segregated, suggesting that Mps1 hyperphosphorylation is correlated with spindle assembly checkpoint silencing (99, 107). Such a model in which overall checkpoint activity is tuned by the phosphorylation state of Mps1 would fit well with kinetic evidence demonstrating that spindle checkpoint signaling is graded rather than switch-like (59). In addition, a more nuanced regulation of Mps1 kinetochore localization, which favors a decrease in Mps1 affinity rather than its complete loss from kinetochores, would better allow for rapid checkpoint re-activation should an attachment be lost. In the future, the single molecule assays we established here should be useful for further understanding how microtubule attachment affects the activity and kinetochore localization of Mps1 and other checkpoint proteins.

2.6 Materials and Methods

Yeast Methods

Standard media, microbial, and genetic techniques were used (141). Yeast strains are isogenic with the W303 background and are listed in Table 3. Galactose induction was performed by culturing cells in 2% lactic acid media until cells reached at OD600 ~1.0, then cells were washed into 2% galactose media to induce *pGAL-Myc-MPS1* or *pGAL-Myc-Mps1(1-400)* expression for 2 hours prior to harvest. Spindle assembly checkpoint silencing assays were performed by arresting cells with 10 μg/ml nocodazole for 2 hours, washing cells 3 times in fresh media lacking nocodazole, then resupending cells in YPDA (YEP + 2% glucose + 0.02% adenine) and taking samples

at the indicated times. 1 μg/ml alpha factor was added to the cultures 40-50 minutes after the beginning of the timecourse to prevent cells from entering a second cell cycle. All experiments were repeated at least 2-3 times, except those indicated as preliminary.

Purification of Native Kinetochore Particles and Mps1

Kinetochores were purified by IP from asynchronously growing yeast as described in (112) with modifications to the lysis as described in (142). Mps1 was purified by the same method except that the lysis buffer contained 0.75 M KCl and the first wash buffer following the IP contained 1 M KCl.

Immunological techniques

Immunoblotting and detection using chemiluminescence was performed as described in (142). Commercial antibodies used for immunoblotting were: 9E10 (Covance) at a 1:10,000 dilution for the Myc tag, anti-Flag M2 antibodies (Sigma-Aldrich) at 1:3,000, anti-Pgk1 antibodies (Invitrogen) at 1:10,000, and anti-V5 (Invitrogen) at 1:5,000. Anti-Spc105 antibodies were used at 1:10,000 (Akiyoshi et al 2010). The anti-Ndc80 antibodies (OD4) were a kind gift from Arshad Desai and were used at a 1:10,000 dilution. Silver-staining was performed using 4-12 % NuPAGE Novex Bis-Tris gels (Invitrogen) and a SilverQuest silver-staining kit (Invitrogen).

Kinase assays

Mps1 or kinetochores were purified and maintained on magnetic beads. Next, they were washed once in buffer H/0.15 (112) without inhibitors and then incubated in kinase buffer (28 mM HEPES pH 8.0, 2.8 mM $MgCl_2$, 143 mM KCl, 14% glycerol, 0.1 mM EDTA, 0.5 mM EGTA, 0.1% NP-40, with or without 200 μM ATP) for the indicated period of time in a 30 °C water bath. Following the kinase reaction, the beads were washed once in buffer H/0.15 with protease and phosphatase inhibitors and then proteins were eluted by boiling in SDS sample buffer.

Bulk binding assays

Kinetochores were purified and maintained on beads. As a control for the binding assays, mock-treated beads were generated by performing an anti-Flag IP from a wild-type yeast strain lacking a Flag-tagged protein. Phosphatase reactions were performed with 1 mM MnCl2 and 200 units of lambda phosphatase (NEB) in BH0.15 buffer at 30 ℃ for 20 minutes. Mock phosphatase reactions also included phosphatase inhibitors (0.1 mM Na-orthovanadate, 0.2 μM microcystin, 2 mM β-glycerophosphate, 1 mM Na pyrophosphate, 5 mM NaF). To perform the Mps1 binding assays, kinetochores or mock-treated beads were incubated with purified Mps1-V5 protein (either 1 or 5 ng) in buffer H/0.15 at 23 °C for 25 minutes. The concentration of purified kinetochores in each reaction was 1-3 ng/μl of the central kinetochore protein Dsn1. Following the binding reaction, Dynabead-associated proteins were washed once in buffer H/0.15 and the proteins were then eluted by boiling in SDS sample buffer.

Analysis of individual fluorescent kinetochore particles

Native kinetochores were purified from asynchronously growing yeast, essentially as described in (112), and labeled with fluorescent dyes as in (127). For examining the levels of Mps1 on unattached kinetochorse, purified kinetochores were tethered sparsely to coverslips with antibodies that bound specifically to a 6xHis tag on the Dsn1 protein. For examining Mps1 levels on laterally attached kinetochores, the kinetochores were incubated with taxol-stabilized microtubules that had been anchored to coverslips via anti-tubulin antibodies. To examine tip-attached kinetochores, kinetochore particles tethered sparsely to coverslips with anti-His antibodies were incubated with short, taxol-stabilized microtubules, which tended to attach to the coverslip-tethered kinetochores by their ends. To examine tip-tracking particles, dynamic microtubule extensions were grown from coverslip-anchored seeds in the presence free kinetochores and then tubulin was removed by buffer exchange to trigger microtubule disassembly. For all single-particle experiments, images were recorded using an automated, multicolor total internal reflection fluorescence (TIRF) microscope (143) and analyzed using custom routines written in LabView (National Instruments) and IGOR Pro (Wavemetrics).

2.7 Acknowledgements

We are grateful to Geert Kops for communicating results and useful discussions. We are grateful to Arshad Desai, Aaron Hoskins, Leon Chan, and Mark Winey for providing reagents. We thank members of the Seattle Mitosis Group and the Asbury

and Biggins labs for helpful discussions and comments. L.B.K. was supported by a National Science Foundation Graduate Research Fellowship (DGE-1256082) and K.N.O. was supported by a grant from the NIH. Y.D. was supported by NIH grant RO1GM079373 (to C.L.A.) and PO1GM105537 (to Mark Winey). N.L. was supported by an NIH inter-disciplinary training grant (T32 CA080416). This work was supported by a Packard Fellowship 2006-30521 (to C.L.A.), NIH grants R01GM079373, P01GM105537 (to C.L.A) and R01GM064386 (to S.B.), and by the Genomics and Scientific Imaging Shared Resources of the Fred Hutch/University of Washington Cancer Consortium (P30 CA015704). S.B. is an investigator of the Howard Hughes Medical Institute.

2.8 Figures

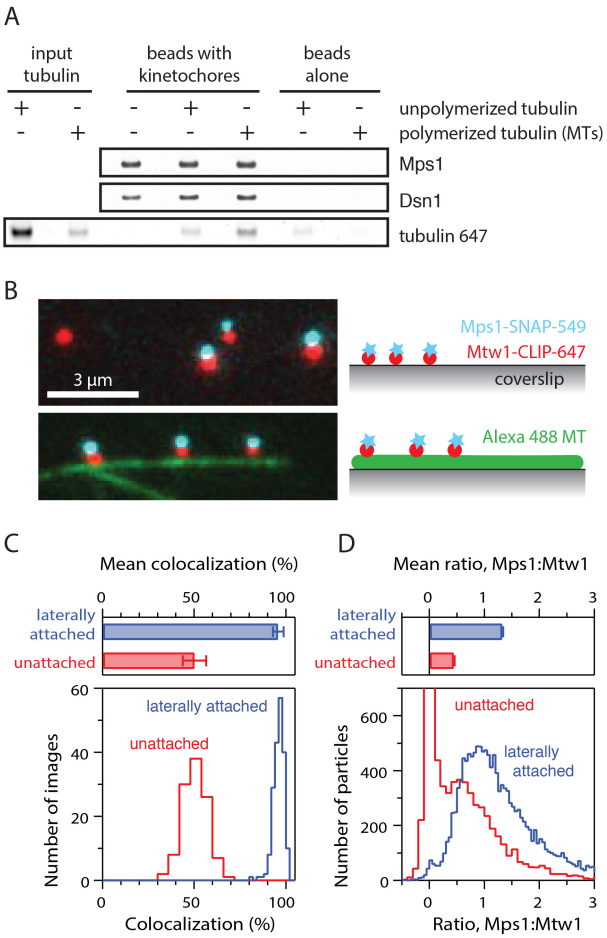

Figure 2.1. Isolated kinetochores retain Mps1 when attached laterally to microtubules.

(A) Kinetochores isolated (from SBY9190) bound to magnetic beads were either mock-treated, incubated with unpolymerized fluorescent tubulin, or incubated with fluorescent taxol-stabilized microtubules. The amount of tubulin retained after washing the beads was assessed by fluorescence. Kinetochores (represented by Dsn1) and kinetochore-associated Mps1 were detected by immunoblotting. (B) Fluorescence images of individual kinetochore particles (from SBY15285) carrying Mps1-SNAP-549 (cyan) and Mtw1-CLIP-647 (red), tethered to a coverslip (top) or attached laterally to a microtubule (green, bottom). Colors are offset vertically; cyan-red pairs are colocalized, dual-color particles. (C) Percentages of kinetochore particles retaining Mps1. Bars show means (± SD) from N = 192 and 112 images of microtubule-attached and coverslip-tethered particles, respectively. Histograms show corresponding

distributions. (D) Approximate ratios of Mps1 to Mtw1 molecules, estimated from particle brightness relative to the brightness of single Mps1-SNAP-549 and Mtw1-CLIP-647 molecules. Bars show mean ratios (± SEM) from N = 14,189 and 7,830 laterally attached and coverslip-tethered particles, respectively. Histograms show corresponding distributions.

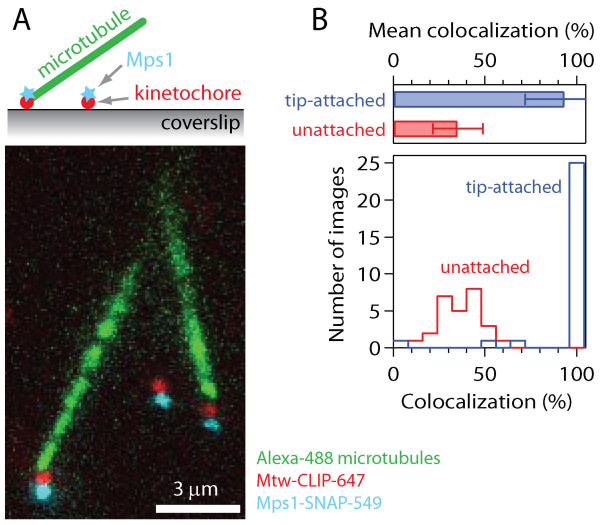

Figure 2.2. Kinetochores retain Mps1 when attached to microtubule tips.

(A) Fluorescence image of kinetochore particles (from SBY15285) carrying Mps1-SNAP-549 (cyan) and Mtw1-CLIP-647 (red) tethered to a coverslip and exposed to free, taxol-stabilized Alexa-488 microtubules (green). By thermal diffusion, the filaments attached via their tips to the coverslip-tethered kinetochores. Colors are offset vertically; cyan-red pairs are colocalized, dual-color kinetochore particles. (B) Percentages of kinetochore particles retaining Mps1. Bars show means (± SD) from N = 28 images of 40 tip-attached and 366 coverslip-tethered particles. Histograms show corresponding distributions.

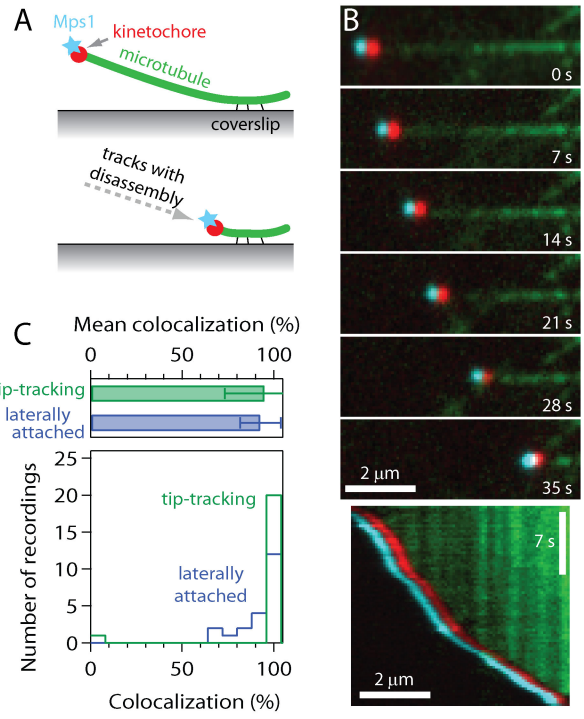

Figure 2.3. Kinetochores retain Mps1 when tracking with disassembling microtubule tips.

(A) Schematic of the experiment. Dynamic microtubules were grown from coverslip-anchored seeds and decorated with kinetochore particles. Then, disassembly was induced by buffer exchange to remove free tubulin. (B) Selected frames (top) and kymograph (bottom) showing a kinetochore particle (from SBY15285) tracking with the disassembling tip of a microtubule (green) and carrying Mps1-SNAP-549 (cyan) and Mtw1-CLIP-647 (red). Colors are offset horizontally. (C) Percentages of kinetochore particles retaining Mps1. Bars show means (± SD) from N = 21 recordings of 32 tip-tracking and 213 laterally attached particles. Histograms show corresponding distributions.

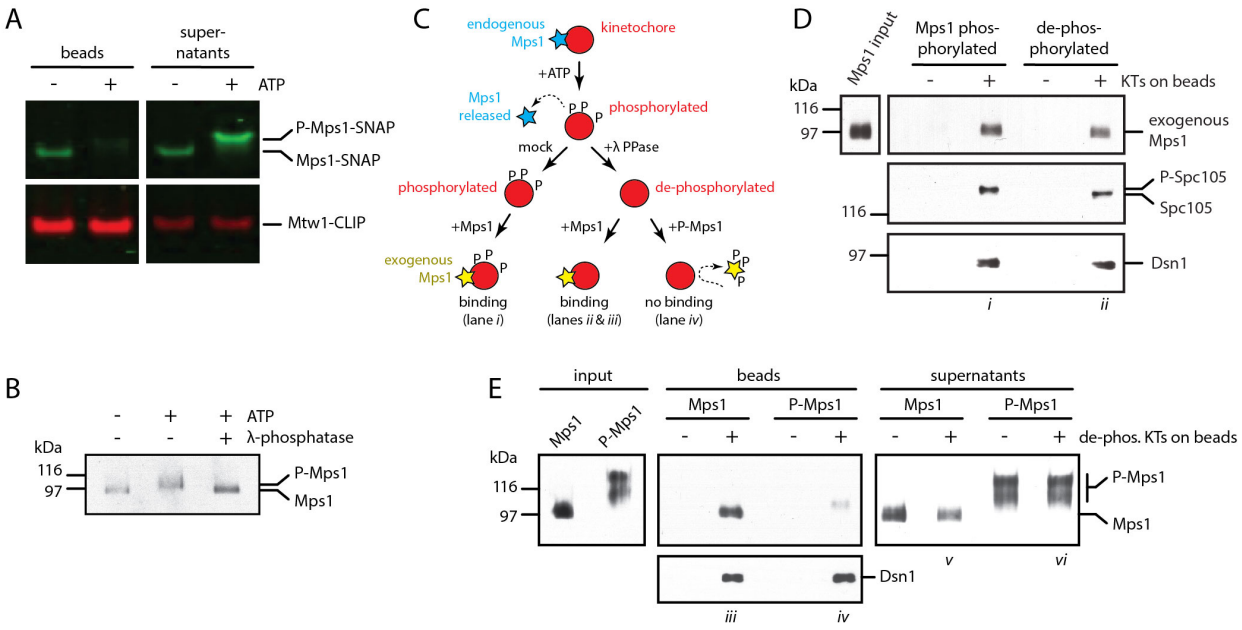

Figure 2.4. Mps1 autophosphorylation inhibits its binding to kinetochores. (A) An *in vitro* kinase reaction releases Mps1 from isolated kinetochores. Kinetochores carrying Mps1-SNAP-549 (green) and Mtw1-CLIP-647 (red) (from SBY15285) were immunoprecipitated on magnetic beads and incubated with or without ATP. Proteins retained on beads and released into the supernatants were analyzed by SDS-PAGE and fluorescent imaging. (B) The electrophoretic mobility shift caused by incubation of Mps1 with ATP is due to phosphorylation. Exogenous Mps1 was purified (from SBY12412) via immunoprecipitation under stringent conditions to remove co-purifying proteins and then incubated with or without ATP. An aliquot of the ATP-treated sample was subsequently treated with λ-phosphatase. Resulting samples were analyzed by immunoblotting. (C) Schematic illustrating preparation of Mps1-phosphorylated and de-phosphorylated kinetochores for binding to exogenous Mps1. (D) Mps1 binds

equivalently to Mps1-phosphorylated or de-phosphorylated kinetochores. Kinetochores (from SBY9190) and control beads lacking kinetochores were prepared, incubated with purified exogenous Mps1 (as diagrammed in C), washed, and then analyzed by immunoblotting. (E) Autophosphorylated Mps1 fails to bind kinetochores. Immobilized kinetochores (from SBY9190) and beads lacking kinetochores were treated sequentially with ATP and then λ-phosphatase, to release endogenous Mps1 and remove phosphates. Subsequently they were washed and incubated with native Mps1, or with autophosphorylated P-Mps1 (as diagrammed in C). Native Mps1 that had not been autophosphorylated *in vitro* bound well to the kinetochores (lane *iii*) with some excess remaining in the supernatant (lane *v*). Autophosphorylated P-Mps1 bound poorly (lane *iv*).

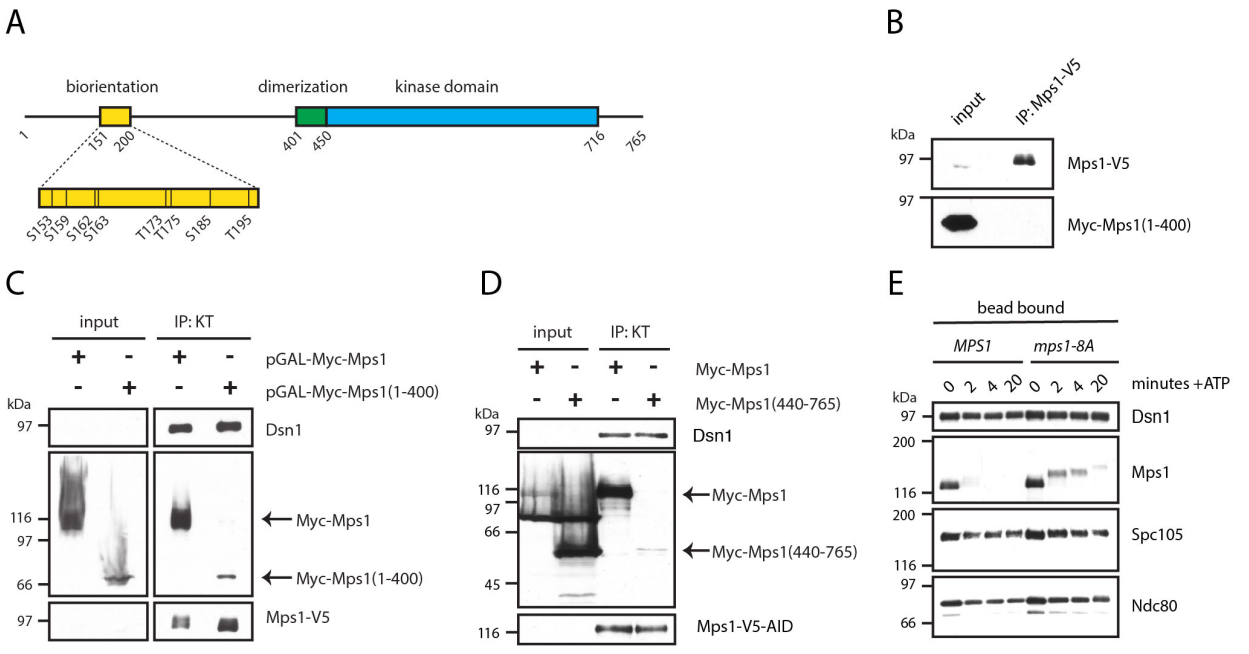

Figure 2.5 - Mps1 N-terminal autophosphorylation regulates its association with kinetochores.

(A) Domain diagram of budding yeast Mps1. The N-terminus includes a domain implicated in biorientation but not spindle pole body function (133). There are 8 potential S/T Mps1 autophosphorylation sites in this putative kinetochore localization domain. (B) Mps1(1-400) does not associate with full length endogenous Mps1. Endogenous full-length Mps1-V5 was immunoprecipitated from a yeast strain grown in galactose to induce expression of Myc-Mps1(1-400) from an ectopic locus (SBY16862). Co-immunoprecipitation was determined by immunoblotting. (C) The N-terminus of Mps1 is sufficient for kinetochore binding. Yeast strains containing an ectopic copy of full-length Myc-Mps1 (SBY17018) or Myc-Mps1(1-400) (SBY16862) under the control of a galactose-inducible promoter were grown in galactose for 2 hours. Kinetochores were purified and analyzed for the association of Myc-Mps1 or Myc-Mps1(1-400) by immunoblotting. (D) The C-terminus of Mps1 does not bind to kinetochores. Kinetochores were purified from a yeast strain expressing Myc-Mps1 (SBY14108) or Myc-Mps1(440-765) (SBY13704) from an ectopic locus and analyzed for the co-immunoprecipitation with kinetochores by immunoblotting. (E) Preventing

phosphorylation of residues in the Mps1 N-terminus slows Mps1 auto-release from kinetochores. Kinetochores were purified from yeast expressing either Myc-Mps1 (SBY17931) or Myc-Mps1-8A (SBY17274), retained on magnetic dynabeads, and treated with ATP for the indicated period of time. Next, the supernatants and bead-bound kinetochores were separated and the kinetochores were washed before analysis of Dsn1 and kinetochore-associated Mps1 by immunoblotting.

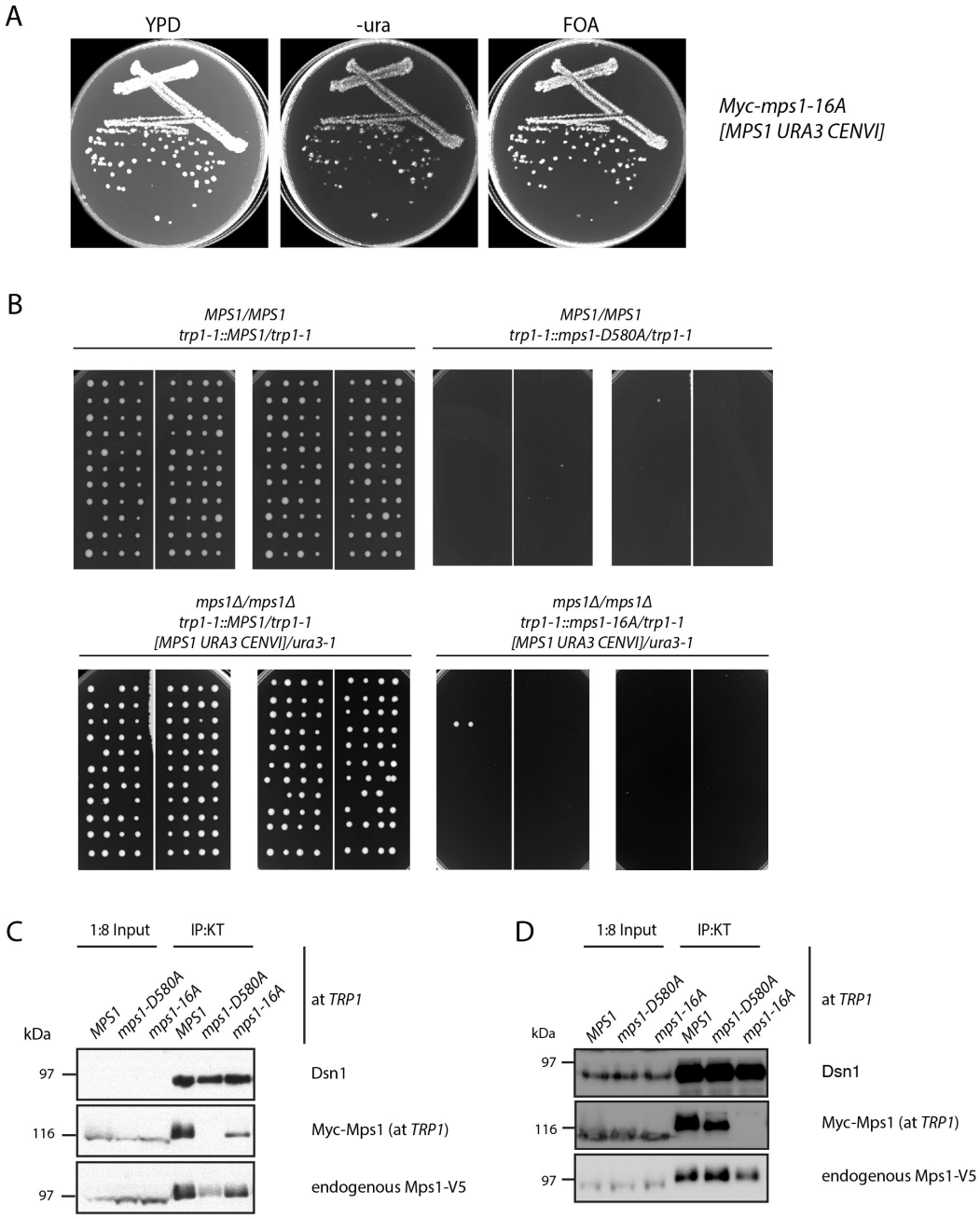

Figure 2.6. Characterization of *mps1-16A* and *mps1-D580A*.

(A) *mps1-16A* is viable. A strain containing *mps1-16A* and WT *MPS1* on a centromeric URA3 plasmid (SBY17571) was struck for single colonies on a YPD plate. When single colonies were grown, the plate was replica plated to -ura dropout media and media containing 5'FOA which is toxic to *URA3+* cells to assess whether cells with only *mps1-*

16A were viable. (B) Catalytically dead *mps1-D580A* and *mps1-16A*, an N-term mutant, disrupt meiosis in a dominant negative manner. Strains with two copies of WT *MPS1* (cross 281 SBY17182 x SBY8476 and cross 296 SBY17475 x SBY15099) form viable spores (175/176 spores viable for cross 281, 169/176 spores viable for cross 296). When a single parent strain has either catalytically dead *mps1-D580A* (cross 282 SBY17183 x SBY8476) or *mps1-16A* (cross 297 SBY17571 x SBY15099) in addition to WT *MPS1*, there is dramatic spore inviability despite normal appearance of dissected tetrads. (C) Preventing kinase activity or mutating phosphoreceptive residues in the N-terminus of Mps1 abrogates kinetochore localization. Kinetochores were purified from asynchronous yeast expressing WT Mps1 (SBY17383), Mps1-D580A (catalytically inactive) (SBY17628), or Mps1-16A (SBY17629) in addition to WT Mps1 and analyzed for the association of Mps1 with kinetochores by immunoblotting. The immunoblot against the endogenous full length Mps1 in each strain is included here. (D) Replicate of (C), with PDS1-Myc in the strain background. Strains used: SBY18316, SBY18317, SBY18318.

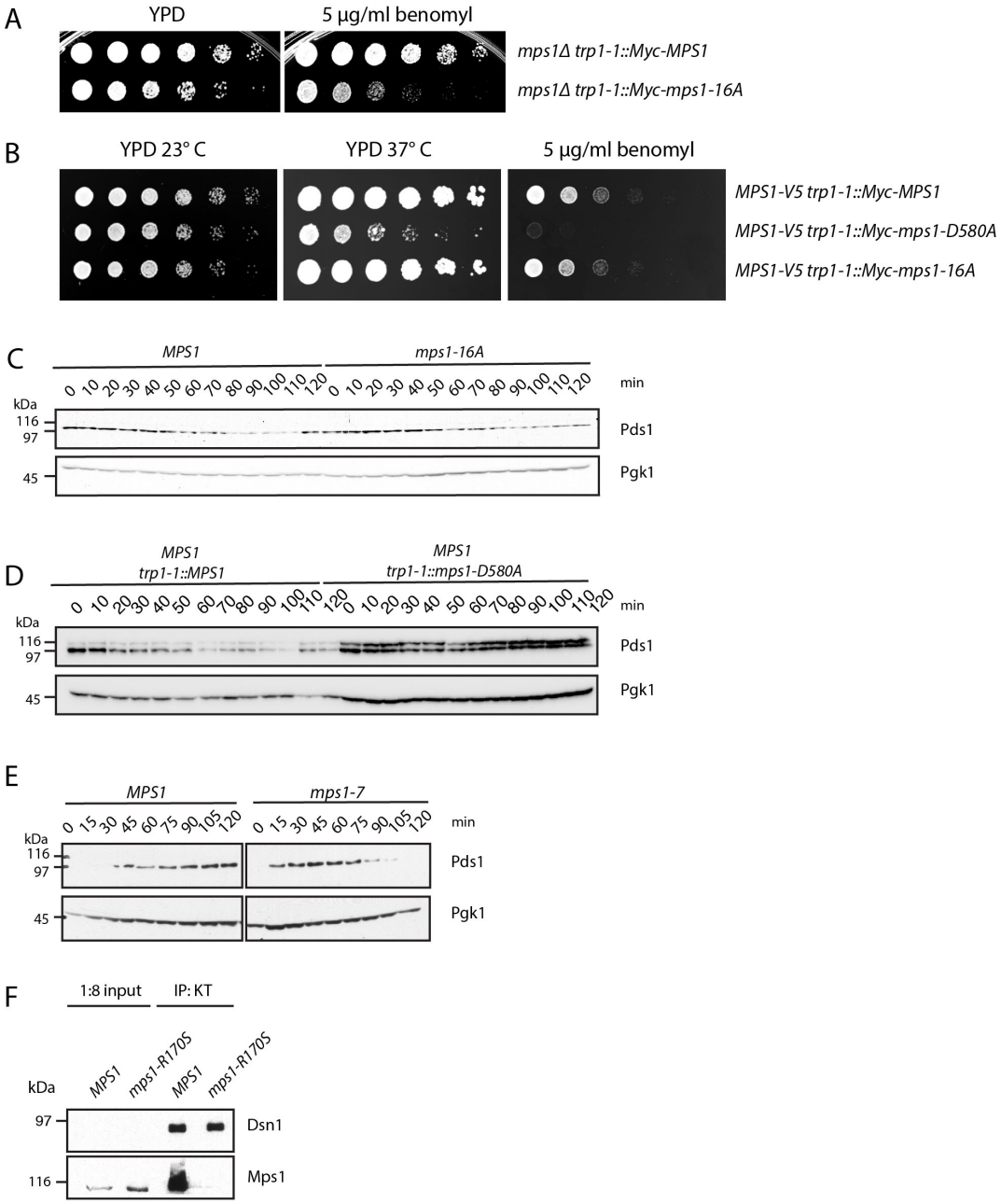

Figure 2.7. *mps1-16A*, *mps1-D580A*, and *mps1-7* disrupt Mps1 kinetochore function.

(A) *mps1-16A* cells grow poorly on media containing the microtubule-destabilizing drug benomyl. Strains used: SBY18307, SBY18308. (B) Catalytically dead *mps1-D580A* acts as a dominant negative to prevent cell growth at higher temperatures and in the presence of benomyl. *mps1-16A* is recessive in mitotically dividing yeast. Strains used: SBY17383, SBY17628, SBY17629. (C) Preliminary result: *mps1-16A* silences the

spindle assembly checkpoint activated by nocodazole similarly to wild-type cells. Strains used: SBY18319, SBY18320. (D) Preliminary result: Haploid yeast heterozygous for catalytically dead *mps1-D580A* silence the spindle assembly checkpoint activated by nocodazole more slowly than wild-type. Strains used: SBY18316, SBY18317. (E) Preliminary result: *mps1-7* cells have defects in activating the spindle assembly checkpoint in response to nocodazole. Strains used: SBY1960, SBY12374. (F) Preliminary result: Mps1-R170S weakly associates with purified kinetochores from asynchronously growing yeast. Strains used: SBY9190, SBY13196.

2.9 Supplementary Figures

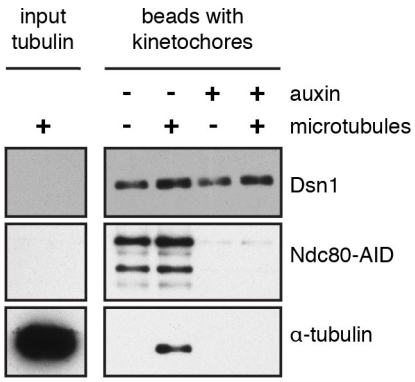

Supplementary Figure 2.1 - Microtubule attachment to purified kinetochores requires Ndc80.

Yeast expressing Ndc80-V5-AID (SBY12352) were grown to mid-log phase and then 500 mM of auxin or vehicle alone (DMSO) was added. Cells were harvested 2 hours later. Kinetochores isolated from the lysates were bound to beads and either mock-treated or incubated with taxol-stabilized microtubules. The levels of kinetochore proteins and the amount of a-tubulin retained after washing the beads were assessed by SDS-PAGE followed by immunoblotting.

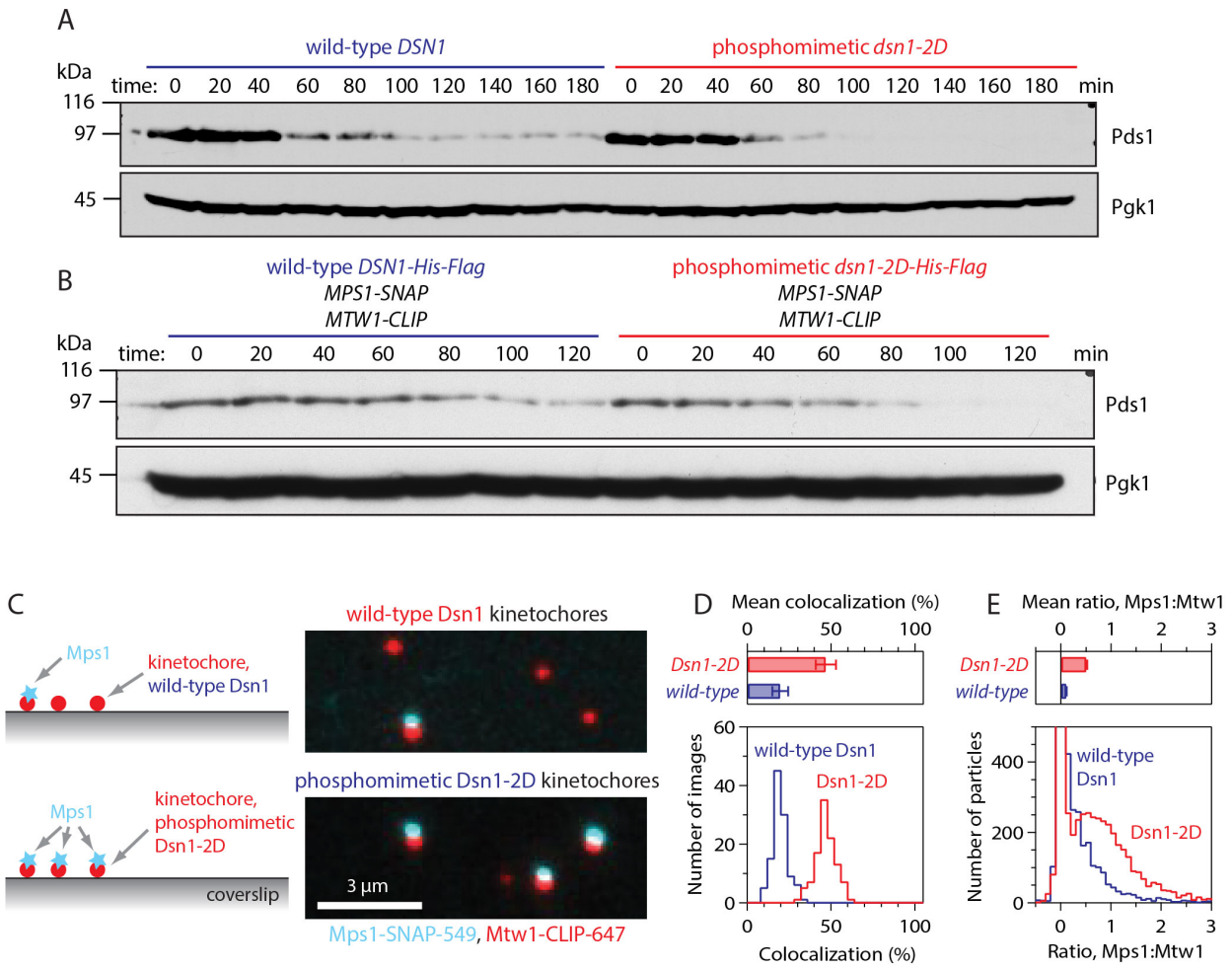

Supplementary Figure 2.2 - Phosphomimetic Dsn1-2D improves retention of Mps1 on isolated kinetochores without disrupting checkpoint silencing in vivo.

(A and B) *dsn1-2D* cells silence the spindle assembly checkpoint with wild-type-like kinetics. Yeast strains expressing wild-type Dsn1 or with phosphomimetic Dsn1-2D were arrested in prometaphase by exposure for 3 hours to nocodazole. After nocodazole was washed out of the media, samples were collected at indicated timepoints and analyzed for the levels of Pds1 and Pgk1 by SDS-PAGE and immunoblotting. (A) Wild-type strain with *DSN1-His-Flag*, *MPS1-SNAP*, and *MTW1-CLIP* (SBY16381), versus phosphomimetic strain with *dsn1-2D-His-Flag*, *MPS1-SNAP*, and *MTW1-CLIP* (SBY16417). (B) Wild-type strain with *DSN1* (SBY4880), versus

phosphomimetic strain with *dsn1-2D* (SBY8066). (C) Schematic diagram (left) and fluorescence images (right) of kinetochore particles carrying wild-type Dsn1 (top, from SBY12571) or phosphomimetic Dsn1-2D (bottom, from SBY15285). Both were labeled with Mps1-SNAP-549 (cyan) and Mtw1-CLIP-647 (red) and tethered to coverslips. Colors are offset vertically; cyan-red pairs are colocalized particles. (D) Percentages of kinetochore particles retaining Mps1. Bars show means (± SD) from N = 111 and 108 images of wild-type and Dsn1-2D particles, respectively. Histograms show corresponding distributions. (E) Approximate ratios of Mps1 to Mtw1 molecules, estimated from particle brightness relative to the brightness of single Mps1-SNAP-549 and Mtw1-CLIP-647 molecules. Bars show mean ratios (± SEM) from N = 8,863 and 6,891 wild-type and Dsn1-2D particles, respectively. Histograms show corresponding distributions.

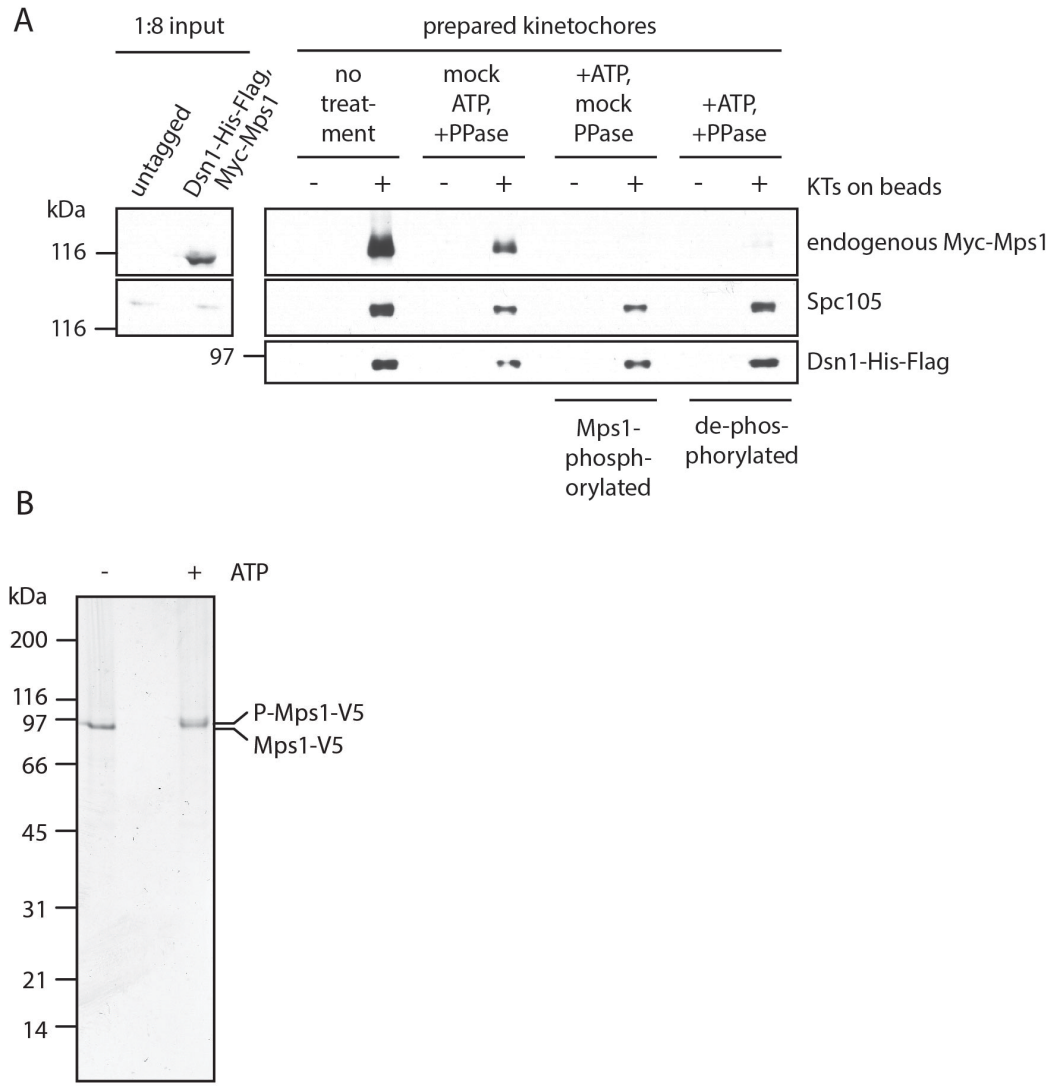

Supplementary Figure 2.3 – Preparation of purified kinetochores and Mps1 for binding experiments.

(A) Preparation of kinetochores phosphorylated by Mps1 or de-phosphorylated and lacking endogenous Mps1. Kinetochores were purified (from SBY9190) via immunoprecipitation of Dsn1-His-Flag and maintained on beads. Control beads lacking kinetochores were also generated by immunoprecipitation from a wild-type strain lacking any tagged proteins (SBY3). Beads with or without kinetochores were incubated in kinase buffer with or without ATP. The ATP-treated samples were then divided and treated either with λ-phosphatase or with λ-phosphatase plus phosphatase inhibitors. All samples were analyzed by SDS-PAGE and

immunoblotting. (B) Full length Mps1 purified from budding yeast and induced to autophosphorylate by treatment with ATP. Mps1-V5 was purified (from SBY12412) via immunoprecipitation under stringent conditions to remove co-purifying proteins, incubated with or without ATP, and analyzed by silver-stained SDS-PAGE.

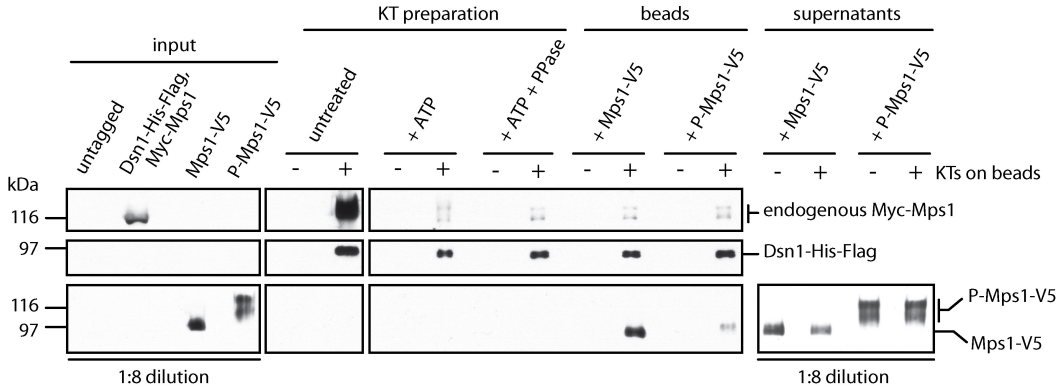

Supplementary Figure 2.4 - Purified native Mps1, but not autophosphorylated Mps1, binds de-phosphorylated kinetochores lacking endogenous Mps1.

Kinetochores (KTs) were purified (from SBY9190) via immunoprecipitation of Dsn1-His-Flag and maintained on beads. Immunoprecipitation from a wild-type strain lacking any tagged proteins (SBY3) generated control beads lacking kinetochores. Immobilized kinetochores and control beads were incubated in kinase buffer with ATP to release endogenous Myc-Mps1 (+ATP), washed, and then dephosphorylated with l-phosphatase (+ATP +PPase). Following phosphatase treatment, kinetochores or control beads were washed and incubated with either purified Mps1-V5 or autophosphorylated P-Mps1-V5 (prepared as in Supplementary Figure 2.3B). All samples were analyzed by SDS-PAGE and immunoblotting.

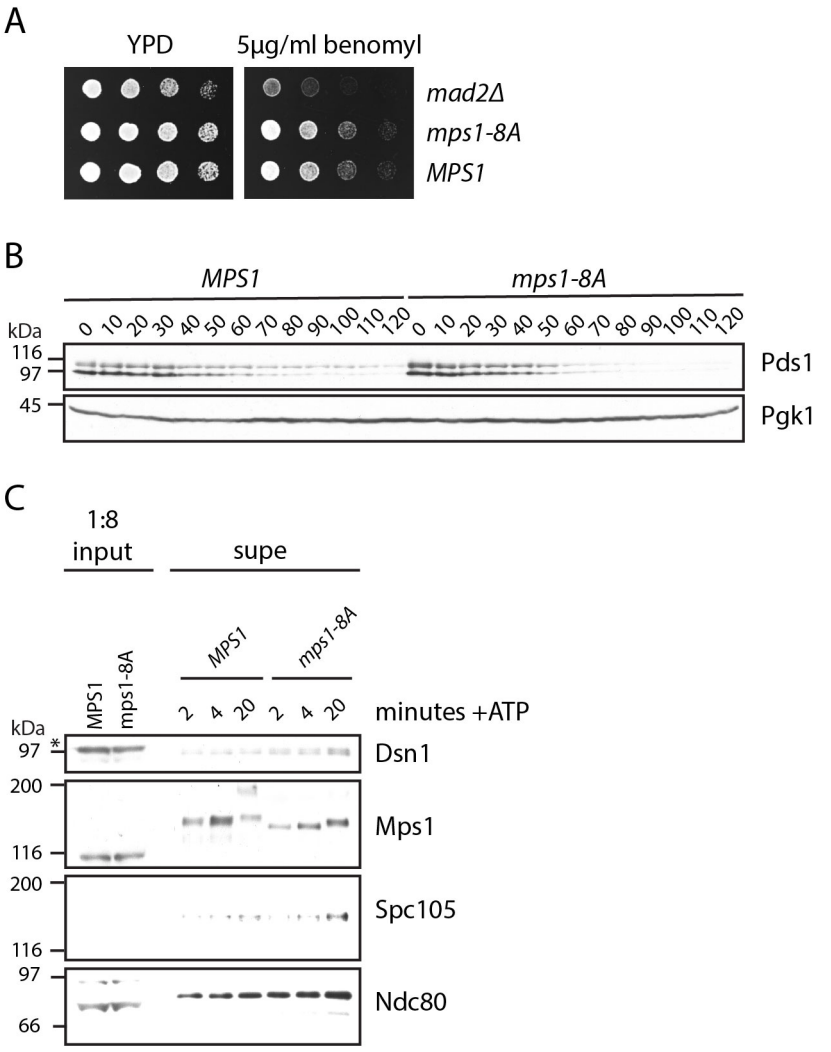

Supplementary Figure 2.5. The N-terminus of Mps1 mediates binding to kinetochores.

(A) *mps1-8A* does not render cells sensitive to the microtubule destabilizing drug benomyl. *mad2Δ* (SBY15062) cells are sensitive to benomyl while strains with *mps1-8A* (SBY17184) or WT *MPS1* (SBY17366) are not. (B) *Mps1-8A* does not alter the kinetics of spindle assembly checkpoint silencing. Strains expressing wild-type Mps1 (SBY17906) or Mps1-8A (SBY17909) were arrested in prometaphase with nocodazole. Nocodazole was washed out and samples were collected at the indicated timepoints following release into fresh media. Samples were analyzed for the levels of Securin (Pds1) or a loading control (Pgk1) by SDS-PAGE and immunoblotting. (C) Input and supernatant samples from the kinetochore kinase reaction in Figure 2.5E. Kinetochores

were purified by IP of Dsn1 from strains expressing wild-type Myc-Mps1 (SBY17931) or Myc-Mps1-8A (SBY17274) and incubated in kinase buffer with ATP for the indicated period of time. Samples were analyzed by SDS-PAGE and immunoblotting. Shown here are the input samples from the IPs and the supernatants from the kinase reactions. The star indicates a background band in the lysate recognized by the Flag antibody used to visualize Dsn1-His-Flag.

Chapter 3: Mps1 phosphorylation of Ndc80 regulates kinetochore-microtubule attachments

3.1 Contributions of collaborators

Krishna K. Sarangapani, Matthew P. Miller, and Abraham Gutierrez performed experiments relevant to this project and collected data included in this section. Krishna K. Sarangapani performed all laser trapping experiments and analysis and contributed to project design. Matthew P Miller contributed data on the association of Dam1 complex with *mps1-1* and *ndc80-14A* kinetochores in Figure 3.2C and Supplementary Figure 3.1 Abraham Gutierrez purified native yeast Dam1 complex that was used in selected laser trapping experiments, as noted. Sue Biggins and Charles L. Asbury directed and supervised the project.

3.2 Summary

Mps1 activity ensures proper kinetochore-microtubule attachments but the underlying mechanism is poorly understood. Mps1 phosphorylates many kinetochore proteins, including those that directly interact with microtubules, such as Dam1 and Ndc80. Since Aurora B^{Ipl1} phosphorylation of these proteins has been shown to destabilize kinetochore-microtubule attachments, we hypothesized that Mps1 phosphorylation might also weaken attachments. We tested this by purifying kinetochores from yeast, phosphorylating them with the co-purifying Mps1, and then testing for their ability to maintain attachments to dynamic microtubules using laser

trapping. We found that Mps1 phosphorylation of purified kinetochores weakens their attachments to microtubules and that Ndc80 is an important substrate for this activity. We characterized cell cycle progression and chromosome segregation in strains of yeast with Mps1 phosphorylation sites in Ndc80 mutated to mimic or prevent phosphorylation. We found that both types of mutations delayed cell cycle progression in a spindle assembly checkpoint-dependent manner and resulted in chromosome segregation defects. Our work suggests that dynamic Mps1 phosphorylation of Ndc80 is important for proper chromosome segregation.

3.3 Introduction

Duplicated chromosomes need to properly attach to microtubules so that they are equally distributed into daughter cells. Only a bioriented attachment configuration, where a chromosome is attached to microtubules emanating from each of the two spindle poles, results in equal partitioning during segregation. Initially, kinetochores are captured by the nearest microtubule and usually interact with its lateral surface before attaching to the dynamic tip (30). Because this initial capture process occurs somewhat randomly, chromosomes often make attachments to microtubules from only one spindle pole or to more microtubules from one pole versus the other. Thus, proper segregation of chromosomes depends on kinetochores making attachments that can withstand microtubule dynamics and also on error correction systems that destabilize incorrect kinetochore-microtubule attachments to give cells another chance to make bioriented attachments.

Inactivation of the kinase Aurora B^{Ipl1} causes a biorientation defect where many chromosomes remain attached to only the mother centrosome and this results in gross chromosome segregation errors (36–38). Previous work has demonstrated that Aurora B^{Ipl1} promotes biorientation by destabilizing attachments through phosphorylation of kinetochore proteins, reducing their affinity for microtubules (39, 40, 42, 44, 48, 49, 51). In addition, Aurora B^{Ipl1} phosphorylation of kinetochore proteins promotes depolymerization of kinetochore microtubules and reduces the frequency of microtubule rescue, further weakening attachments (50, 51). Finally, Aurora B^{Ipl1} phosphorylation may also inhibit interactions between key microtubule-binding elements of the kinetochore, compromising attachment strength further (46, 47, 144).

The key Aurora B^{Ipl1} substrate appears to be the major microtubule binding protein Ndc80/Hec1 because preventing its phosphorylation causes significant errors in chromosome segregation in human cells (42). Although Aurora B^{Ipl1} phosphorylation of Ndc80 is conserved across eukaryotic organisms from yeast to human cells, preventing Aurora B^{Ipl1} phosphorylation of Ndc80 in budding yeast only causes a mild phenotype in cells (43), despite decreasing the strength of kinetochore-microtubule interactions in vitro (50). Genetic evidence suggests that this is due to redundancy with the other microtubule-binding complex in budding yeast, Dam1 (11). Interestingly, Dam1 is also a substrate of Aurora B^{Ipl1} and this phosphorylation inhibits Dam1 complex function in promoting attachments in cells and in vitro (26, 39, 41, 45, 46, 48, 50). More recent work has uncovered that Aurora B^{Ipl1} phosphorylation of the Ska complex, an apparent functional ortholog of the Dam1 complex in higher eukaryotes, also destabilizes attachments by inhibiting Ska complex binding to kinetochores (145).

The conserved protein kinase Mps1 is also required for accurate biorientation in both budding yeast and human cells, independently of its role in the spindle assembly checkpoint (60, 61, 146). In mammalian cells, Mps1 phosphorylation of the plus-end directed motor CENP-E aids chromosome alignment (147) and recent work has uncovered that Mps1 phosphorylation of the Ska complex destabilizes kinetochore-microtubule attachments (70). Mps1 phosphorylation of Dam1 in budding yeast appears to promote proper kinetochore-microtubule interactions (64) and inhibition of Mps1 kinase activity during meiosis decreases the co-localization of Dam1 with kinetochores, suggesting that Mps1 activity is required for proper Dam1 function (62, 63). Finally, while it has been suggested that Mps1 activates Aurora B^{Ipl1} (65, 146), other evidence indicates that their activities in promoting biorientation are separable (68, 69).

To determine the effect of Mps1 phosphorylation of kinetochores on kinetochore-microtubule attachment independently of Aurora B^{Ipl1}, we employed a reconstitution system. We previously demonstrated that Mps1 is the primary kinase that co-purifies with budding yeast kinetochores and that this co-purifying Mps1 phosphorylates purified kinetochores in vitro (80). Mps1 phosphorylates several kinetochore proteins, including Ndc80 and Dam1, and the effects are not well understood. We hypothesized that Mps1 phosphorylation of kinetochores weakens attachments and in this work we present evidence to support this. We identify Ndc80 as the key substrate for this effect. Consistent with this, cells that carry mutations in Mps1 phosphorylation sites in Ndc80 exhibit defects in mitotic progression and

chromosome segregation. Together, our work suggests that Mps1 phosphorylation of Ndc80 is important for proper mitosis and contributes to the error correction process.

3.4 Results

Phosphorylation of purified kinetochores reduces kinetochore-microtubule attachment strength

We hypothesized that Mps1 phosphorylation of kinetochores may destabilize kinetochore-microtubule attachments, given the similarity between the Mps1 and Aurora B^{Ipl1} biorientation defect. To test this directly, I purified kinetochores, treated them with ATP to induce Mps1 phosphorylation, and we tested their ability to attach to microtubules in vitro using laser trapping. I isolated the kinetochores from budding yeast as previously described, via affinity purification of a Flag epitope tag on Dsn1, which is part of the $Mis12^{MIND}$ complex (112). Dsn1 was also tagged with 6His (Dsn1-6His-3Flag) to enable linking to polystyrene beads in the laser trapping. Following the initial purification, I retained the kinetochores on beads and divided them into three. I eluted one sample from the beads immediately by incubation with excess Flag peptide, creating an untreated sample of kinetochores as a control (Figure 3.1A-B, Lane i). For the remaining samples, I either stimulated Mps1 to phosphorylate kinetochores by treatment with ATP in a kinase buffer or withheld the ATP in the kinase buffer in a mock treatment (Figure 3.1A). After the kinase treatment, I either removed phosphorylation by incubating with lambda phosphatase or maintained phosphorylation by treating the kinetochores with lambda phosphatase plus phosphatase inhibitors (Figure 3.1A-B, Lanes ii-iv). I then eluted the kinetochores from the beads by incubating with Flag

peptide. I determined that there were no major alterations in the composition of the purified kinetochores by PAGE and silver-staining (Figure 3.1B).

My colleague Krishna linked the purified kinetochore particles to polystyrene beads (0.44-0.56 μm diameter) to manipulate them using a laser trap (Figure 3.1C) (50, 112, 127). The density of kinetochore particles decorating the beads was adjusted by mixing 6 pM beads with different amounts of purified kinetochore material, corresponding to Dsn1 concentrations of 5-10 nM (Dsn1:bead ratios of 800:1 to 1600:1) so as to ensure single particle interactions (50, 112, 127). The kinetochore-decorated beads were introduced into a chamber containing dynamic microtubules grown from stable, coverslip-anchored seeds. Beads were captured with the laser and brought to the tip of a dynamic microtubule. A computer-controlled laser trap was used to apply precise tensile forces to the kinetochore-microtubule interaction in the direction of microtubule growth. Bead-trap separation was initially kept constant (pre-load regime) and then automatically increased at a constant rate until the kinetochore-microtubule attachment ruptured (ramp regime). This process was repeated to generate rupture force distributions for each type of kinetochores.

Consistent with our previous work, we found that untreated wild-type kinetochores ruptured from microtubules at an average force of 9.52 ± 0.46 pN (Figure 3.1D Lane i). Similarly, kinetochores that went through a mock kinase and then mock phosphatase treatment ruptured from microtubules at an average of 9.69 ± 1.01 pN (Figure 3.1D Lane ii, Figure 3.1E). In support of our initial hypothesis, we found that it required markedly less force to rupture phosphorylated kinetochores from microtubules, at an average of 4.65 ± 0.27 pN (Figure 3.1D Lane iii, Figure 3.1E). We

also found that removing phosphorylation through a subsequent incubation with lambda phosphatase increased the average rupture force to nearly wild-type levels, 8.85 ± 0.61 pN (Figure 3.1D Lane iv, Figure 3.1E). This latter observation suggests that the reduction in rupture force caused by ATP treatment is due to phosphorylation itself and not to other changes that might occur, such as in kinetochore composition.

Mps1 activity is responsible for the phosphorylation-dependent decrease in kinetochore-microtubule attachment strength

Although our previous work strongly suggests that Mps1 is the primary kinase responsible for in vitro phosphorylation of purified kinetochores, we tested whether Mps1 activity was responsible for the phosphorylation that reduced the ability of ATP-treated kinetochores to maintain attachments to dynamic microtubules. To this end, I isolated kinetochores from *mps1-1* cells grown at the restrictive temperature to inactivate the kinase and also from wild-type cells grown in the same way as a control. Following the initial purification, I divided each type of kinetochores and treated half with a kinase buffer with ATP or a kinase buffer lacking ATP. I then eluted the kinetochores with Flag peptide. These kinetochores appear to maintain wild-type composition when analyzed by PAGE and silver-staining (Figure 3.2A).

We tested the ability of these kinetochores to maintain attachments to microtubules using the rupture force assay. Again, we found that treatment with ATP reduced the strength required to rupture the wild-type kinetochore-microtubule attachment, this time to an average rupture force of 7.27 ± 0.68 pN (Figure 3.2B) while wild-type mock treated kinetochores ruptured at an average of 9.59 ± 1.34 pN (Figure

3.2B). Interestingly, we found that both mock and ATP treated Mps1-1 kinetochores ruptured at similar average forces, 5.10 ± 0.62 pN and 5.12 ± 0.42 pN respectively (Figure 3.2B).

Notably, the rupture force of mock treated Mps1-1 kinetochores was significantly lower than wild-type. This is consistent with our observations that a reduced amount of the Dam1 complex proteins Dam1 and Ask1 co-purify with Mps1-1 kinetochores (Figure 3.2C, Supplementary Figure 3.1A). Previous work demonstrated that purified kinetochores lacking functional Dam1c have reduced average rupture forces (112). Because of this, we reasoned it might be possible that the reduced rupture forces due to the lack of Dam1 complex might mask any differences in attachment strength due to ATP treatment of kinetochores. To rule out this possibility, we added 2nM separately purified native yeast Dam1 complex into the laser trap chamber containing kinetochore-coated beads and dynamic microtubules (i.e. after the kinetochores had been mock or ATP-treated) and repeated the laser trapping experiments with Mps1-1 kinetochores. We found that the average rupture force of mock treated and ATP treated Mps1-1 kinetochores increased to 10.67 ± 0.90 pN and 10.68 ± 0.72 pN respectively, consistent with the addition of Dam1 improving the strength of kinetochores that have less Dam1 (Figure 3.2D). The results also suggest that Mps1 activity is required for the reduction in attachment strength observed when purified kinetochores are treated with ATP. Overall, our results thus far suggest that Mps1 phosphorylation of purified kinetochores reduces their ability to stay bound to microtubules under tension.

Mps1 phosphorylates Ndc80 to weaken kinetochore-microtubule attachments

Mps1 phosphorylates the microtubule-binding kinetochore proteins Dam1 and Ndc80 (64, 111). However, evidence from several studies suggests that Mps1 activity promotes Dam1 kinetochore function rather than disrupts it (62–64). Given this, we hypothesized that Ndc80 may be the substrate which Mps1 phosphorylates to weaken attachment strength of purified kinetochores (111).

Although some evidence suggested that the ability of kinetochores to bind to microtubules was not abolished by mutations in Ndc80 that mimic Mps1 phosphorylation (111), we reasoned that Mps1 phosphorylation of Ndc80 might still weaken attachments and that such a weakening may not be detectable by the previous assays or may be masked by compensatory pathways in vivo. To test this hypothesis directly, I purified kinetochores from *ndc80-14A* cells, which have the Mps1 phosphorylation sites in Ndc80 mutated to alanine to prevent their phosphorylation (Figure 3.3A) (111), and tested whether treatment with ATP would still reduce kinetochore-microtubule attachment strength using the rupture force assay. Our hypothesis was that the attachment strength of Ndc80-14A kinetochores phosphorylated by Mps1 should be higher than that of wild-type kinetochores phosphorylated by Mps1 if Mps1 phosphorylation of Ndc80 weakens kinetochore-microtubule attachments. Thus, we purified kinetochores with wild-type Ndc80-HA or Ndc80-14A-HA and incubated them in a kinase buffer with or without ATP. First, I analyzed their composition by PAGE and silver staining and found that they appear similar to the wild-type kinetochores analyzed previously (Figure 3.3B). However, I

found that Ndc80-14A-HA kinetochores co-purify with a reduced amount of the Dam1 complex protein Ask1 (Figure 3.3C), similar to Mps1-1 kinetochores.

Because my colleague found that very few Ndc80-14A-HA kinetochores were able to bind to microtubules in the early steps of the rupture force assay, we added separately purified native yeast Dam1 complex to kinetochores in the laser trap. After the addition of Dam1 complex, we found that the mock treated wild-type Ndc80-HA kinetochores ruptured at an average of 11.51 ± 0.82 pN but that wild-type Ndc80-HA kinetochores treated with ATP had a lower average rupture force of 6.98 ± 0.58 pN (Figure 3.3D). Thus, the addition of Dam1 complex in the laser trap does not appear to mask the ability of Mps1 phosphorylation to weaken the kinetochore-microtubule attachment but does appear to increase the overall ability of kinetochores to attach to microtubules. When we analyzed Ndc80-14A-HA kinetochores with additional Dam1 complex, we found that mock treated Ndc80-14A-HA kinetochores ruptured at an average of 9.98 ± 0.67 pN and that Ndc80-14A-HA treated with ATP ruptured at an average of 9.19 ± 0.53 pN (Figure 3.3D). These results suggest that Ndc80 is a primary target that Mps1 phosphorylates to weaken kinetochore-microtubule attachments.

To address the possibility that Mps1 kinase is not active on Ndc80-14A-HA kinetochores, I analyzed the electrophoretic mobility of the Mps1 substrate Spc105 following ATP treatment of the kinetochores (Figure 3.3E). I found that Spc105 migrated slightly slower, consistent with it being phosphorylated, when kinetochores were treated with ATP than it did when they were mock treated, on wild-type as well as Ndc80-14A kinetochores (Figure 3.3E). These results indicate that Mps1 appears comparably active on wild-type and Ndc80-14A kinetochores.

Mps1 phosphorylation of Ndc80 is not required for spindle assembly checkpoint signaling

Given our results thus far, we hypothesized that Mps1 phosphorylation of Ndc80 might promote chromosome segregation in vivo, playing a role in error-correction alongside Aurora B^{Ipl1}. A previous study reported that *ndc80-14A* cells were defective in sustaining a spindle assembly checkpoint arrest in response to nocodazole (111), complicating the interpretation of the phenotype of the Ndc80 phospho-mutant. However, when I tested the ability of *ndc80-14A* cells to activate the spindle assembly checkpoint in response to nocodazole, I found that *ndc80-14A* cells could sustain a checkpoint arrest comparably to wild-type, as determined by the stability of the anaphase inhibitor Securin^{Pds1} (Figure 3.4A). In addition, *ndc80-14A mad2Δ* double mutants grew poorly compared to each of the *ndc80-14A* and *mad2Δ* single mutants, suggesting that *ndc80-14A* cells have a defect that is not due to loss of spindle assembly checkpoint function (Figure 3.4B). I note that *ndc80-14A* cells grew poorly in the presence of the microtubule-destabilizing drug benomyl, as previously observed (Figure 3.4B) (111). I also found that *ndc80-14A* cells grew poorly at higher temperatures compared to wild-type (Figure 3.4B).

I performed timecourses to assess whether *ndc80-14A* cells transited through the cell cycle at a rate similar to wild-type. Interestingly, I found that *ndc80-14A* cells entered anaphase at a significantly delayed rate compared to wild-type (Figure 3.4C). This delay appears at least partially caused by a spindle assembly checkpoint arrest,

as the cell cycle profile of *ndc80-14A mad2Δ* double mutants appeared similar to that of *mad2Δ* cells (Figure 3.4C).

A previous publication found that mimicking phosphorylation of the 14 mapped Mps1 sites in Ndc80 (the *ndc80-14D* allele) was lethal and rescued by deleting spindle assembly checkpoint signaling, leading the authors to conclude that the phosphorylation functioned in spindle assembly checkpoint signaling (111). However, using a plasmid shuffle assay, I did not find that preventing spindle assembly checkpoint signaling allowed *ndc80-14D* cells to grow without a wild-type copy of *NDC80* (Figure 3.5A). Colonies did appear after several days in the *ndc80-14D bub1Δ* and *ndc80-14D mad3Δ* double mutants, however these likely contain suppressor mutations (Supplementary Figure 3.2). Therefore, I conclude that *ndc80-14D* cells are not inviable solely due to spindle assembly checkpoint signaling.

Mimicking Mps1 phosphorylation of Ndc80 activates the spindle assembly checkpoint and leads to chromosome missegregation

I tested whether mimicking constitutive Mps1 phosphorylation of Ndc80 led to a spindle assembly checkpoint arrest by conditionally expressing *ndc80-14D* as the sole source of *NDC80* and performing a timecourse of a synchronized cell cycle. To do this I tagged the wild-type copy of *NDC80* needed for viability of *ndc80-14D* cells with an auxin-inducible degron (AID) (148). I arrested control and *ndc80-14D* cells in G1 and then released into media containing auxin to degrade the wild-type Ndc80-AID protein. I found that cells expressing Ndc80-14D were arrested in metaphase throughout the 2-hour timecourse while wild-type cells entered anaphase around 75 minutes (Figure

3.5B). These data are consistent with *ndc80-14D* cells experiencing a prolonged spindle assembly checkpoint arrest.

To determine whether *ndc80-14D* cells were activating the spindle assembly checkpoint due to a kinetochore-microtubule attachment defect, I measured the fidelity of the segregation GFP-labeled chromosome 8 in *ndc80-14D NDC80-AID mad2Δ* cells (149). I synchronized control and *ndc80-14D* cells in G1 and then released into media with or without auxin. I collected samples throughout the timecourse and fixed them with formaldehyde for microscopy. I found that *ndc80-14D NDC80-AID mad2Δ* cells missegregated chromosome 8 at a rate higher than the wild-type strain even when auxin was not added to the media (Figure 3.5C). Additionally, when auxin was added and the wild-type Ndc80 protein was degraded (data not shown), *ndc80-14D* caused a notable chromosome segregation defect (Figure 3.5C).

To determine whether the Ndc80-14A and Ndc80-14D phosphomutant proteins are incorporated into kinetochores similarly to wild-type, I constructed diploid strains that expressed wild-type Ndc80, Ndc80-14A, or Ndc80-14D in addition to Ndc80-AID. I arrested these cells in mitosis by treating them with benomyl and then degraded the wild-type Ndc80-AID allele by adding auxin to the media. I purified kinetochores from these cultures and found that the incorporation of Ndc80-14D protein into kinetochores is severely reduced compared to wild-type, regardless of whether the wild-type Ndc80-AID protein is degraded or not (Figure 3.5D). This result suggests that phosphorylation of Ndc80 by Mps1 might destabilize the interaction of Ndc80 with kinetochores. It also suggests that the chromosome segregation defect observed in the earlier experiments is likely caused by the lack of Ndc80-14D protein in

kinetochores. Interestingly, the incorporation of Ndc80-14A protein into kinetochores appears comparable to wild-type, suggesting that preventing Ndc80 phosphorylation does not compromise the association of Ndc80 with kinetochores (Figure 3.5D).

Preventing Mps1 phosphorylation of Ndc80 compromises chromosome segregation

Given our observation that Mps1 phosphorylation of Ndc80 regulates kinetochore-microtubule attachments in vitro, we hypothesized that it may also regulate attachments in cells. We tested this by measuring the fidelity of chromosome segregation in *ndc80-14A* cells. To do this, I analyzed the segregation of GFP-labeled chromosome VIII in *ndc80-14A* versus wild-type cells in a *mad2Δ* background, to ensure that the strains were in anaphase at the same time during a synchronized cell cycle. I arrested the cells in G1 using alpha factor, then washed out the alpha factor and released them into rich media and collected samples throughout the cell cycle, fixing them with formaldehyde. I found that by 150 minutes following release from G1, almost all cells were in anaphase as judged by the segregation of DAPI-stained DNA between the daughter cells. In the samples from this time, I counted the number of cells in which GFP-labeled chromosome VIII was segregated correctly into daughter cells or which had both copies in only one daughter (either appearing as a single focus or 2 foci) (Figure 3.6A). By this time, 15 percent of ndc80-14A cells had missegregated chromosome VIII (one daughter cell was missing a GFP focus), while this was only observed in 2 percent of wild-type cells (Figure 3.6B). I measured an even higher rate

of chromosome missegregation in *ndc80-14A* cells at 37 °C, consistent with the growth defect observed at that temperature (Figure 3.6C).

Treatment of yeast cells with nocodazole depolymerizes microtubules but most kinetochores maintain attachments to short, intact microtubules from the centrosomes of the collapsed spindle. Previous studies used the time it takes cells to segregate chromosomes following nocodazole treatment and washout as a readout for the ability of cells to biorient chromosomes and correct errors (33, 93). I repeated this experimental strategy to assay the ability of *ndc80-14A* cells to correct attachment errors, biorient, and segregate chromosomes. I analyzed the segregation of DAPI-stained chromosomes and found that while 63 percent of wild-type cells had segregated all of their chromosomes by 80 minutes after nocodazole was washed out, only 23 percent of ndc80-14A cells had done so by that time (Preliminary result: Figure 3.6D). Together, our chromosome segregation data suggests that preventing Mps1 phosphorylation of Ndc80 causes minor defects in chromosome segregation that are exacerbated when cells are challenged.

Mimicking Mps1 phosphorylation of Ndc80 is lethal due to hyperactive error-correction by Aurora B^{Ipl1}

Mimicking constitutive Mps1 phosphorylation of Ndc80 with the *ndc80-14D* mutant led to hyperactivation of the spindle assembly checkpoint, likely due to improper kinetochore-microtubule attachments. Therefore, I reasoned that the additional Mps1 present on Ndc80-14D kinetochores, observed in my kinetochore purifications (Figure 3.5D), continues to recruit Bub1 to kinetochores to signal the

checkpoint. This additional Bub1 kinase might then recruit additional Sgo1, which has been shown to be important for Aurora B^{Ipl1} activation (33, 92). Therefore, I speculated that extended error-correction by activated Aurora B^{Ipl1} might be responsible for the severe chromosome missegregation phenotype and lethality of *ndc80-14D* cells.

To test this, I constructed double mutant strains with *ndc80-14D* and mutants of the Bub1-Sgo1-Aurora B^{Ipl1} biorientation pathway and tested for their growth in the absence of a wild-type copy of *NDC80* using a plasmid shuffle assay. To our surprise, I found that a few different *SGO1* mutant alleles, including *sgo1-100* and *sgo1-3A*, rescued the growth of *ndc80-14D* cells (Figure 3.7A). *Sgo1-100* was isolated as a mutant defective in activating the spindle assembly checkpoint in response to tension defects (93). Sgo1-3A (Y47A, Q50A, S52A) is defective in binding to the catalytic subunit of the phosphatase PP2A, which is also involved in biorientation (150, 151). I backcrossed the initial *sgo1-100 ndc80-14D* double mutant and confirmed that *sgo1-100* alone was responsible for the rescue of *ndc80-14D* (data not shown). Additionally, I found that large tags on Sgo1, including 3GFP and 6HA, also suppressed the *ndc80-14D* lethality, suggesting that generally compromising Sgo1 function is sufficient for the rescue (Supplementary Figure 3.3B). Sgo1-700-6HA, which is defective in localizing the condensin complex to centromeres, also suppressed *ndc80-14D* but it is unclear whether this is due to the mutation in *SGO1* or the 6HA tags (33) (Supplementary Figure 3.3A). The *bub1Δkinase* mutant, which lacks the C-terminal kinase domain, also suppressed the inviability of *ndc80-14D* (Supplementary Figure 3.3A). Bub1 kinase activity is required to recruit Sgo1 so this is consistent with that pathway being involved in the death of *ndc80-14D* cells (89). Next, I found that a *ndc80-14D BUB3-*

3GFP double mutant strain was viable (Supplementary Figure 3.3B). Because Bub3 forms a complex with Bub1, it is possible that the bulky 3GFP tag on Bub3 might reduce Bub1 kinase localization at kinetochores. This might in turn reduce the ability of Bub1 kinase to recruit Sgo1, again implicating this pathway in the death of *ndc80-14D* cells. I constructed various other *ndc80-14D* double mutants but did not see that they rescued the lethality of *ndc80-14D* (Supplementary Figure 3.3C-D).

Since I had observed high levels of chromosome missegregation in *ndc80-14D* cells earlier, I tested whether chromosome segregation defects persisted in *sgo1-100 ndc80-14D* double mutants. I synchronized cells in G1 using alpha factor, then released into fresh media and collected samples throughout the cell cycle. In anaphase cells, I analyzed the segregation of GFP-labeled chromosome VIII into daughter cells. By 150 minutes from G1 release, I found that *sgo1-100* and *sgo1-100 ndc80-14D* cells had missegregated chromosome VIII at a similar rate, which was much lower than the missegregation rate observed for *ndc80-14D NDC80-AID* cells (Figure 3.7B).

I had previously observed that Ndc80-14D did not associate with kinetochores as well as wild-type or Ndc80-14A. Therefore, I tested whether kinetochore association was restored in the viable *ndc80-14D bub1Δkinase* cells by purifying kinetochores and analyzing the levels of Ndc80 by immunoblotting. I found that the levels of Ndc80-14D in kinetochores appeared similar to wild-type in the *bub1Δkinase* background (Figure 3.7C). This suggests that whatever defect was causing lack of incorporation of Ndc80-14D in cells that require wild-type Ndc80 for viability is remedied by reducing the activity of the Bub1-Sgo1-Aurora B^{Ipl1} biorientation pathway.

I hypothesized that extended or hyperactive Aurora B^{Ipl1} activity may be responsible for the death of *ndc80-14D* cells. I constructed a *ndc80-14D ipl1-321* double mutant strain and found that it could grow in the absence of wild-type *NDC80* at the permissive temperature, confirming this hypothesis (Figure 3.7D). Even at the permissive temperature, Ipl1-321 has lower kinase activity than wild-type. As before, I backcrossed the *ndc80-14D ipl1-321* strain and confirmed that *ipl1-321* alone was responsible for the rescue of *ndc80-14D* (data not shown). Together, my data suggests that *ndc80-14D* causes cell death due to elevated activity of the Bub1-Sgo1-Aurora B^{Ipl1} biorientation axis, which is triggered by kinetochore-microtubule attachment defects.

3.5 Discussion

While it has been known that Mps1 activity is required for sister kinetochore biorientation for over a decade (60, 61), the underlying mechanism has remained elusive. In our work, we found that Mps1 phosphorylation of kinetochores, and specifically of Ndc80, reduces the strength of kinetochore-microtubule attachments in vitro. In addition, I showed that both mimicking and preventing Mps1 phosphorylation of Ndc80 causes a chromosome segregation defect in cells. My genetic data suggests that mimicking Mps1 phosphorylation of Ndc80 activates Aurora B^{Ipl1}, which also suggests that the phosphorylation causes kinetochore-microtubule attachment errors. Taken together, our data suggest that Mps1 plays a role in destabilizing kinetochore-microtubule attachments through phosphorylating Ndc80, in a manner reminiscent of the error-correction activity of Aurora B^{Ipl1}.

One obvious and potential issue with this model is the fact that both Mps1 and Aurora B^{Ipl1} single mutants have strong biorientation defects (36, 38, 60, 61). Inactivation of either kinase causes dramatic chromosome segregation defects and cell death (36, 38, 60, 61). In human cells, there is evidence that Mps1 and Aurora B^{Ipl1} activity are interdependent, providing a possible explanation for the lack of compensation in single mutants (65–67, 146). However, there is also evidence that they are independent (60, 68, 69). One possible explanation for lack of Aurora B^{Ipl1} compensation in *mps1-1* mutants could be due to the low Dam1 protein levels on *mps1-1* kinetochores. It seems possible that Aurora B^{Ipl1} may not be able to correct biorientation errors as efficiently when one of its substrates in that process is compromised. Conversely, in Aurora B^{Ipl1} mutants, additional $PP1^{Glc7}$ is recruited to kinetochores and this may remove Mps1 phosphorylation (152, 153).

Irrespective of whether Mps1 and Aurora B^{Ipl1} activity are changed in single mutants of either kinase, it is clear that preventing Mps1 phosphorylation of Ndc80 causes a defect in cell cycle progression that is ameliorated by preventing spindle assembly checkpoint signaling. Additionally, preventing this phosphorylation also induces chromosome segregation errors. This missegregation might be caused by a defect in Dam1 complex function, as we observed that Dam1 complex proteins were less strongly associated with kinetochores isolated from *mps1-1* as well as *ndc80-14A* cells. It might also be caused by a direct weakening of Ndc80-microtubule interactions, as suggested by our laser trapping data with Ndc80-14A kinetochores in the presence of additional Dam1 protein. Regardless of the precise mechanism, our results that Mps1 phosphorylation of Ndc80 disrupts kinetochore-microtubule interactions are

consistent with recent findings in human cells that Mps1 phosphorylation of the Ska complex destabilizes attachments (70).

Previous studies have suggested that Mps1 promotes biorientation through localizing Bub1 kinase and Sgo1 (154–156) and we provide additional evidence of this in our study. We found that the cell death caused by mimicking constitutive Mps1 phosphorylation of Ndc80 could be rescued by mutations in Bub1 kinase, Sgo1 and Aurora B^{Ipl1}. Thus, in addition to directly regulating the strength of kinetochore-microtubule attachments, Mps1 phosphorylation of Ndc80 might also indirectly promote Aurora B^{Ipl1}-mediated error correction. One study found that overexpression of *SGO1* was sufficient to rescue cell death caused by inactivation of Mps1 following centrosome duplication in budding yeast, where the spindle assembly checkpoint is non-essential (154). This might suggest that enabling Sgo1 localization is the primary role of Mps1 in promoting biorientation. However, inactivation of Mps1 results in a biorientation defect far worse than that seen in *SGO1* mutants, suggesting that the rescue enabled by *SGO1* overexpression is likely due to a compensatory mechanism that is not up-regulated wild-type cells.

Because 3 of the 14 Mps1 phosphorylation sites were previously found to be phosphorylated by Aurora B^{Ipl1} kinase (specifically, T21, S37, and T74), it remains to be rigorously tested whether both kinases contribute to the phosphorylation of these sites in vivo and what proportion of the phenotype of the *ndc80-14A* mutant is due to the lack of phosphorylation of the Aurora B^{Ipl1} sites. A previous study found that mutating S37 specifically is important for the benomyl sensitivity phenotype the *ndc80-7A* mutant, which prevents Aurora B^{Ipl1} phosphorylation of Ndc80 (43). However,

preventing phosphorylation of S37 alone did not render cells sensitive to benomyl, making it unclear whether the identify or number of available phosphorylation sites is important for specific phenotypes (43). Other studies have suggested that the number of phosphorylation sites, rather than their specific position in the tail of Ndc80, determines the ability of Ndc80 to interact with microtubules, at least in vitro (49). However, it has recently been shown that different phosphorylation sites in the Ndc80 tail are regulated differently in cells, with some becoming dephosphorylated at metaphase and others remaining phosphorylated throughout the cell cycle (157, 158). This implies that specific sites need to be phosphorylated or dephosphorylated at specific times in the cell cycle for proper chromosome alignment and segregation to occur. Future dissection of the dynamics of phosphorylation of specific Mps1 and Aurora B^{Ipl1} sites in Ndc80 within cells should reveal the precise requirements for proper chromosome segregation. By uncovering that Mps1 phosphorylation of Ndc80 regulates attachment strength, our study sets the stage for these investigations.

3.6 Materials and Methods

Yeast Methods

Standard media, microbial, and genetic techniques were used (141). Yeast strains are listed in Table 3. Spindle assembly checkpoint activation (Pds1 stability) assays were performed by arresting haploid *MAT*a cells in G1 with 1 µg/ml alpha factor for 3-4 hours then releasing into fresh media with 10 µg/ml nocodazole. Samples of the culture were taken at the indicated times and whole cell extracts were prepared by bead-beating lysis and boiling in SDS sample buffer. For synchronous cell cycle

experiments (for Pds1 stability and chromosome segregation assays), cells were arrested in G1 with 1 μg/ml alpha factor for 3-4 hours and then washed into fresh media. 1 μg/ml alpha factor was added to the cultures 40-50 minutes after the beginning of the timecourse to prevent cells from entering a second cell cycle. All cells were grown at room temperature, 23 °C, unless otherwise indicated. For the chromosome segregation assay at 37 °C, cells were shifted to 37 °C starting at time zero following alpha factor washout. For the nocodazole washout experiment, cells were incubated in media with 10 μg/ml nocodazole for 2 hours, then washed into media lacking nocodazole and samples were taken at the indicated times. For the chromosome segregation analysis of n*dc80-14D* cells, haploid strains were synchronized in G1 with 1 μg/ml alpha factor for 3 hours and 500μM indoleacetic acid (IAA, auxin) was added 1 hour before the alpha factor was washed out. Following this 3 hour alpha factor/1 hour IAA arrest, cells were washed into fresh media containing 500μM IAA to continue degrading Ndc80-AID throughout the timecourse. Chromosome segregation analysis of GFP-labeled chromosomes and DAPI staining were performed as described in (142). For the kinetochore IPs from Ndc80 heterozygous diploids, the indicated yeast strains were arrested for 2 hours in 30 μg/ml benomyl, then the culture was divided and 500μM IAA was added to half for 1 hour before harvesting (3 hours in benomyl, 1 hour in IAA total). The other half was harvested immediately after 2 hours in benomyl. All experiments were repeated a minimum of twice, with the exception of those that are indicated as preliminary.

Kinetochore purifications

Kinetochores were purified by IP from asynchronously growing yeast as described in (112) with modifications to the lysis as described in (142). The concentration of purified kinetochores was estimated by comparing the intensity of the Dsn1 or Dsn1/Ndc80-HA band in samples of the kinetochores with that of BSA standards in silver-stained PAGE gels. The concentration of Dsn1, or Dsn1 and Ndc80-HA, from each preparation of kinetochores ranged from 1-3 ng/µl.

Treatment and preparation of purified kinetochores and Dam1

Kinetochores were purified as normal and then maintained on magnetic beads. Next, they were washed once in buffer H/0.15 (112) without any inhibitors and then incubated in kinase buffer (28 mM HEPES pH 8.0, 2.8 mM $MgCl_2$, 143 mM KCl, 14% glycerol, 0.1 mM EDTA, 0.5 mM EGTA, 0.1% NP-40, with or without 200 µM ATP) for 30 minutes in a 30 °C water bath. Following the kinase reaction, the beads with kinetochores were washed once in buffer H/0.15 with protease inhibitors (20 µg/mL final concentration for each of leupeptin, pepstatin A, chymostatin and 200 µM phenylmethylsulfonyl fluoride) and phosphatase inhibitors (0.1 mM Na-orthovanadate, 0.2 µM microcystin, 2 mM β-glycerophosphate, 1 mM Na pyrophosphate,5 mM NaF). For the phosphatase treatment of kinetochores, bead-bound kinetochores were then incubated in buffer H/0.15 with 1 mM MnCl2 buffer (NEB) and 200 units of lambda phosphatase (NEB) at 30℃ for 20 minutes. Mock phosphatase reactions also included phosphatase inhibitors (concentrations as above). Following treatments, kinetochores

were eluted from beads with 0.5mg/ml 3x Flag peptide in bufferH/0.15 with protease and phosphatase inhibitors.

Dam1 complex was purified by immunoprecipitation of Dad1-3Fflag from SBY12464321 using the same protocol as that used to purify kinetochores, except with bufferH/0.4 (0.4M KCl) used in the first set of washes following the IP instead of bufferH/0.15. The concentration of purified Dam1 complex was estimated by comparing the intensity of Dad1-3Flag to a series of BSA standards on a silver-stained gel.

Laser-trapping of purified kinetochores

Laser trapping was performed essentially as described in (50). In brief, streptavidin-coated polystyrene beads were conjugated with anti-His antibodies and incubated with His-tagged purified kinetochores. Kinetochore-decorated beads were tested for binding to dynamic microtubules grown from GMPCPP seeds using a laser trap using custom control software. Records of bead position were recorded using customized LabView software and analyzed with IGOR Pro. For the experiments with additional Dam1 complex protein added into the trap chamber, Dam1 complex was added to a final concentration of 2nM.

Immunological techniques

Immunoblotting and detection using chemiluminescence was performed as described in (142). Commercial antibodies used for immunoblotting were: 9E10 (Covance) at a 1:10,000 dilution for the Myc tag, anti-Flag M2 antibodies (Sigma-

Aldrich) at 1:3,000, anti-Pgk1 antibodies (Invitrogen) at 1:10,000, anti-HA (12CA5, Roche) antibodies at 1:10,000, and anti-V5 (Invitrogen) at 1:5,000. Anti-Spc105 antibodies were used at 1:10,000 (Akiyoshi et al 2010). The anti-Ndc80 antibodies (OD4) were a kind gift from Arshad Desai and were used at a 1:10,000 dilution. Silver-staining was performed using 4-12 % NuPAGE Novex Bis-Tris gels (Invitrogen) and a SilverQuest silver-staining kit (Invitrogen).

3.7 Acknowledgements

We are grateful for feedback from members of the Biggins and Asbury Labs, as well as the Seattle Mitosis Group. We are grateful to Leon Chan, the Lechner Lab, Winey Lab, and Marston Lab for contributing reagents. L.B.K. was supported by a National Science Foundation Graduate Research Fellowship (DGE-1256082). M.P.M is an HHMI fellow of the Damon Runyon Cancer Research Foundation. A.G. was supported by a Ford Foundation Fellowship. This work was supported by a Packard Fellowship 2006-30521 (to C.L.A.), NIH grants R01GM079373, P01GM105537 (to C.L.A) and R01GM064386 (to S.B.), and by the Genomics and Scientific Imaging Shared Resources of the Fred Hutch/University of Washington Cancer Consortium (P30 CA015704). S.B. is an investigator of the Howard Hughes Medical Institute.

3.8 Figures

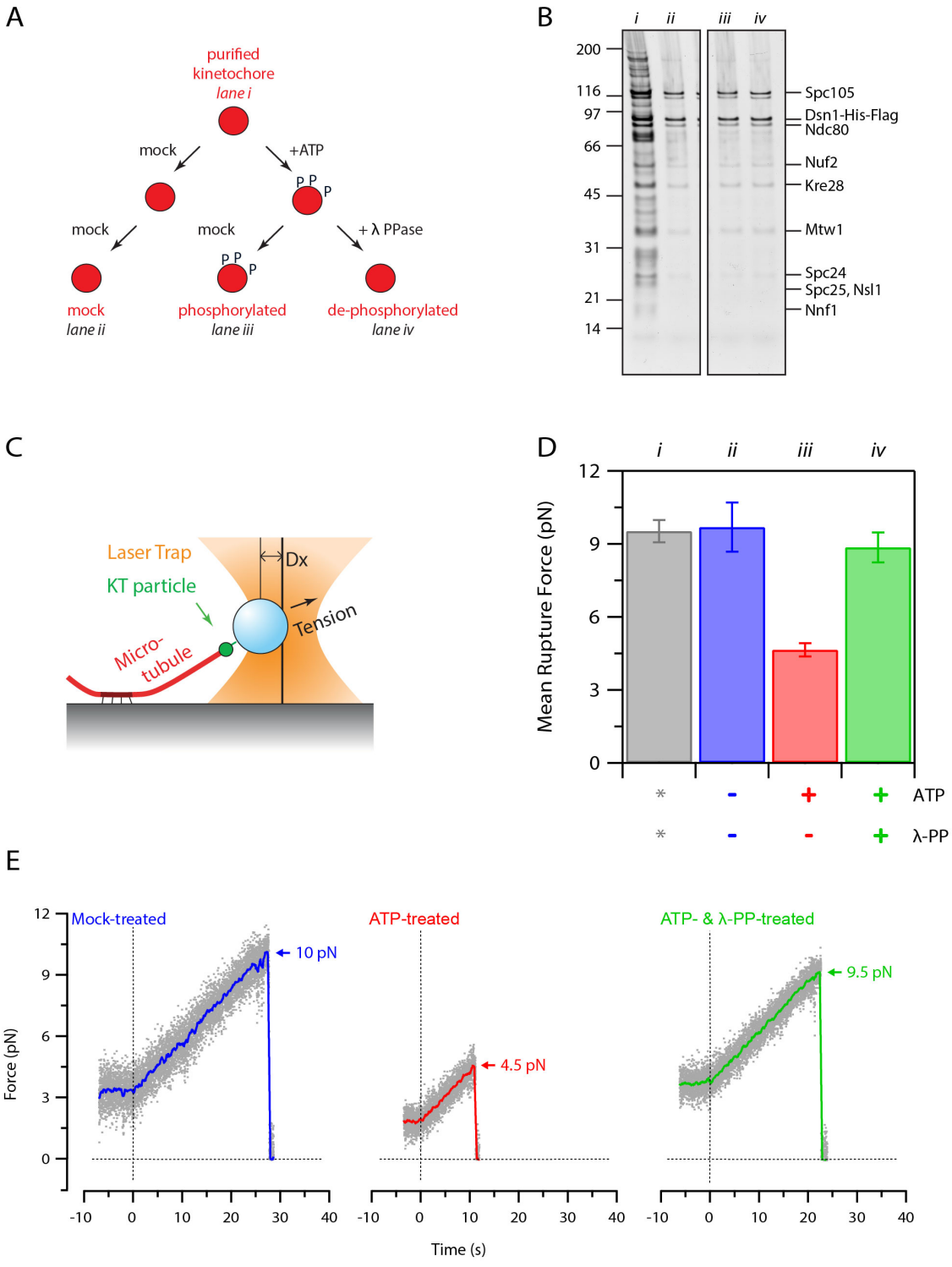

Figure 3.1. In vitro phosphorylation of purified kinetochores reduces microtubule attachment strength.

(A) Schematic of preparation of in vitro phosphorylated and de-phosphorylated kinetochores for characterization by laser trapping. (B) Silver-stained PAGE of kinetochores (purified from SBY8253) following treatments as indicated in A. (C) Diagram of laser trapping of purified kinetochores and microtubules. (D) ATP treatment reduces the average rupture force of the kinetochore-microtubule attachment while treatment with λ phosphatase following ATP treatment returns the average rupture force to a nearly wild-type level. Mean rupture forces for purified kinetochores prepared as in A. Asterisks indicate untreated kinetochores while the minus sign indicates that a mock treatment (either in ATP or PPase buffer) was performed. N=3. (E) Example traces from the laser trapping experiments summarized in D.

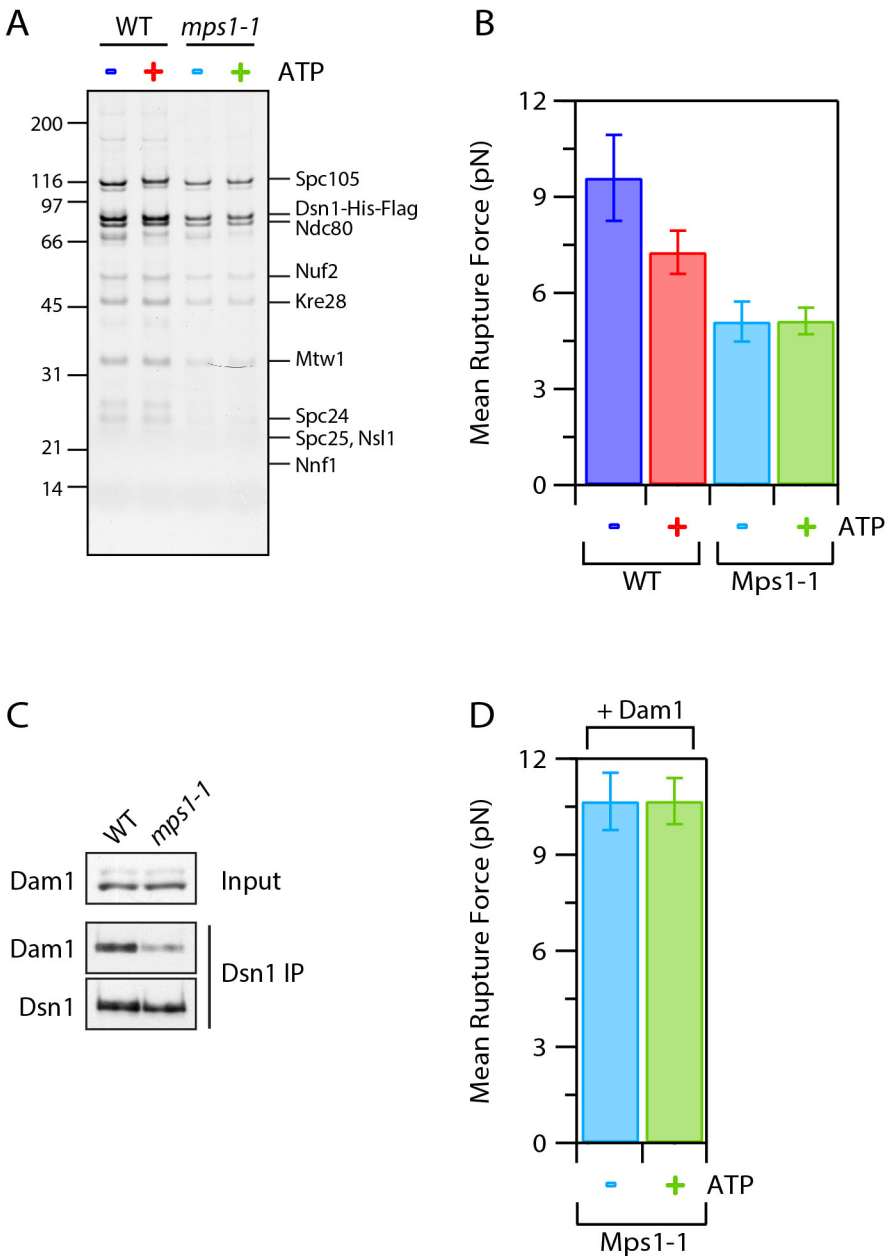

Figure 3.2. Mps1 activity is responsible for the phosphorylation-dependent decrease in kinetochore-microtubule attachment strength.

(A) Silver-stained PAGE of kinetochores purified from wild-type (SBY8253) and *mps1-1* (SBY8726) cells shifted to the restrictive temperature for 2 hours prior to harvest. (B) Mps1 activity is required for the reduction in rupture force following treatment of purified kinetochores with ATP. Mean rupture forces for the kinetochores prepared as

in A. N=3. (C) Kinetochores purified from *mps1-1* cells (SBY8938) have less Dam1 protein than wild-type cells (SBY10274). (D) Addition of separately purified native yeast Dam1 complex (from SBY12464) to kinetochores post-purification increases the rupture forces of kinetochores overall but does not affect *mps1-1* kinetochores treated with ATP differently than those which were not treated with ATP.

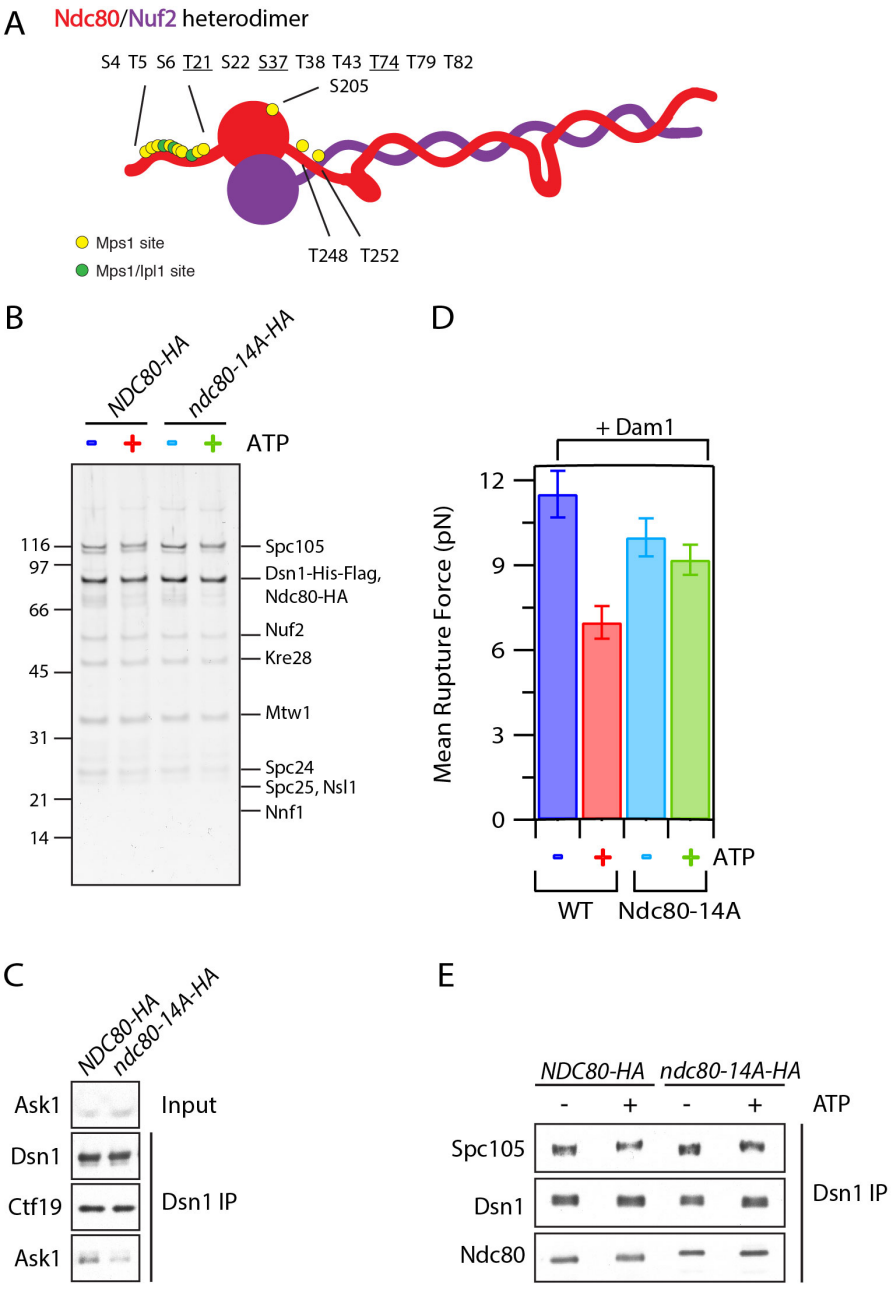

Figure 3.3. Mps1 phosphorylation of Ndc80 weakens kinetochore-microtubule attachments.

(A) Diagram of the Ndc80/Nuf2 heterodimer with 14 Mps1 phosphorylation sites indicated. Sites were identified by a combination of in vitro and in vivo mass spectrometry in Kemmler et al 2009. Underlines indicate sites that are phosphorylated by Aurora B^{Ipl1}. (B) Silver-stained PAGE of kinetochores purified from NDC80-HA (WT

NDC80) (SBY11808) or ndc80-14A-HA cells (SBY13086) and treated with ATP post-purification as indicated. Note that Dsn1 and Ndc80 run at the same MW when Ndc80 is HA tagged. (C) Ndc80-14A kinetochores have a reduced level of the Dam1 complex protein Ask1. Immunoblot of kinetochores purified from WT NDC80-HA (SBY12076) and ndc80-14A-HA cells (SBY12039) expressing tagged Ask1. (D) Mps1 phosphorylation of Ndc80 mediates the ATP-dependent weakening of attachments. Mean rupture forces required to rupture kinetochore-microtubule bonds for the kinetochores prepared as in B. Additional separately purified yeast Dam1 complex (from SBY12464) was added since Ndc80-14A kinetochores have limited Dam1 following purification. (E) Mps1 remains active on Ndc80-14A kinetochores. Immunoblot of purified kinetochores from cells expressing WT NDC80-HA (SBY11808) and Ndc80-14A-HA (SBY13086) and treated as in B. Treatment of both WT and Ndc80-14A kinetochores with ATP causes a mobility shift upward of Spc105, a known target of Mps1.

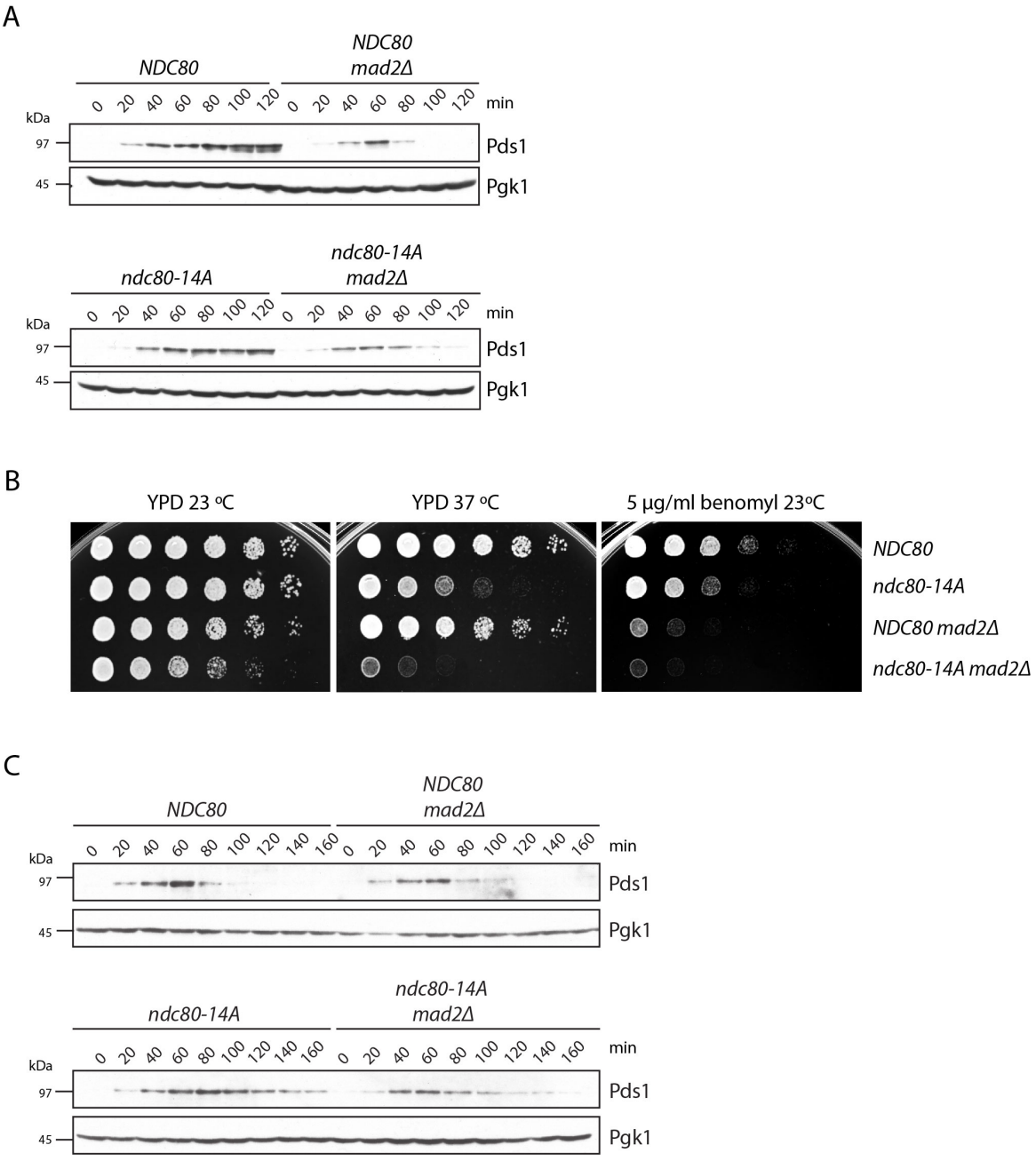

Figure 3.4. Mps1 phosphorylation is not required for spindle assembly checkpoint signaling.

(A) *Ndc80-14A* cells maintain a spindle assembly checkpoint arrest in response to nocodazole. The indicated yeast strains were arrested in G1 for 3 hours using alpha factor, then the alpha factor was washed out and the cells were resuspended in media containing 10 µg/ml nocodazole. Samples were taken at the indicated timepoints and

analyzed for Pds1 and Pgk1 by immunoblotting. Strains used: SBY17648, SBY17624, SBY17807, SBY17895. (B) *Ndc80-14A* shows synthetic sickness with *mad2Δ* and grows poorly at 37 °C and in media containing benomyl. 5-fold serial dilutions of cultures of the indicated strains of yeast were plated on YPD plates without or with 5 μg/ml benomyl and grown at the indicated temperatures. Strains used: SBY17901, SBY17898, SBY18141, SBY18208. (C) *Ndc80-14A* causes a spindle assembly checkpoint-dependent delay in cell cycle progression. The indicated yeast strains were arrested in G1 for 3 hours using alpha factor, then the alpha factor was washed out and the cells were resuspended in rich media. Samples were taken at the indicated timepoints and analyzed for Pds1 and Pgk1 by immunoblotting. Strains used: SBY17648, SBY17624, SBY17807, SBY17895.

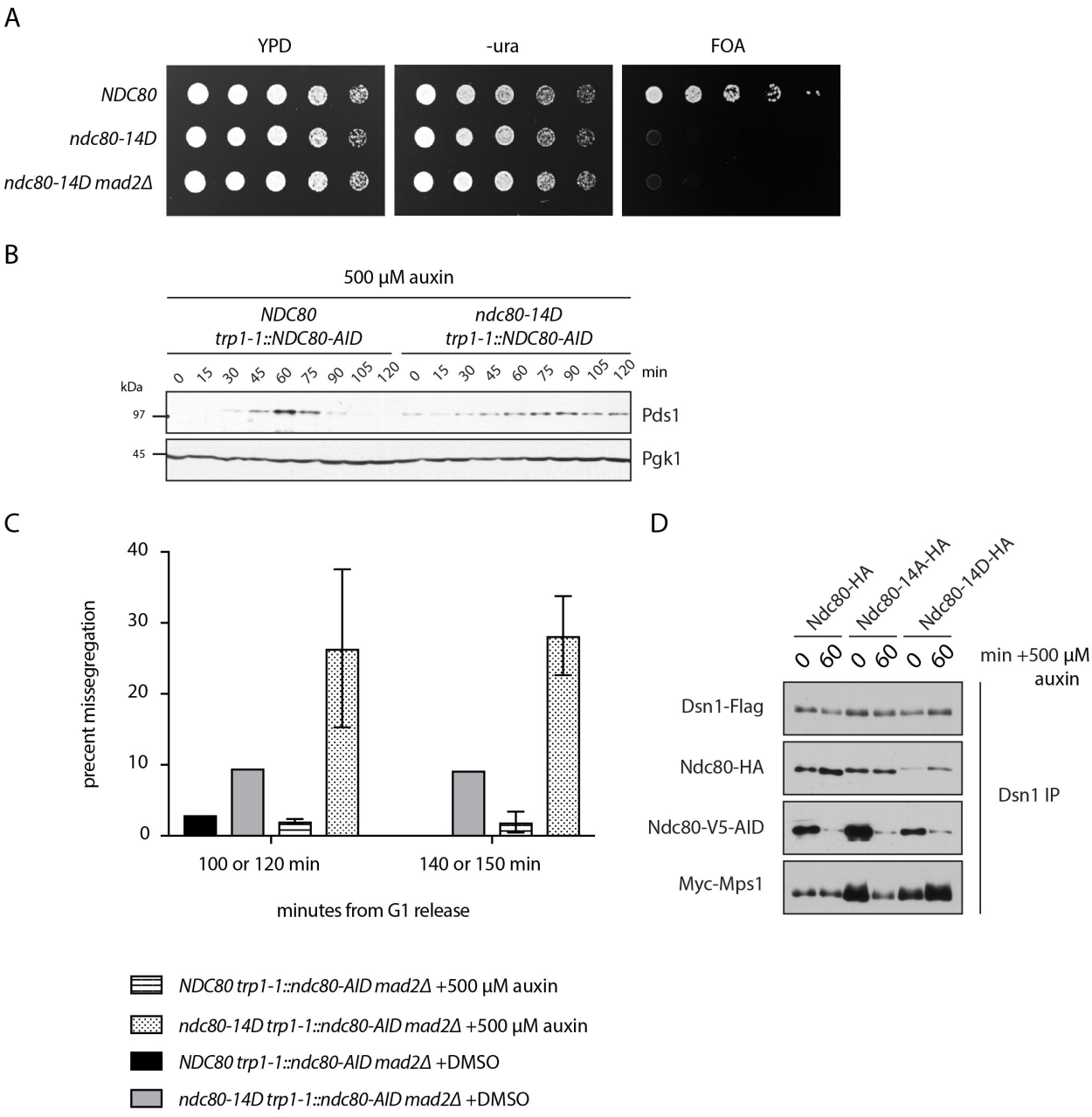

Figure 3.5. Mimicking constitutive Mps1 phosphorylation of Ndc80 activates the spindle assembly checkpoint and causes chromosome missegregation.

(A) *Ndc80-14D* cells are not inviable due to constitutive spindle assembly checkpoint signaling. 5-fold serial dilutions of the indicated strains were plated onto YPD, -ura, or FOA plates and grown at 23 °C. Strains used: SBY15149, SBY9453, SBY15087. (B)

Ndc80-14D cells activate the spindle assembly checkpoint. Cultures of the indicated strains were arrested in G1 with alpha factor for 4 hours, then released into fresh media. Samples were taken at the indicated timepoints and analyzed for Pds1 and Pgk1 by immunoblotting. Strains used: SBY15096, SBY15206. (C) Mimicking constitutive Mps1 phosphorylation of Ndc80 causes chromosome missegregation. The indicated yeast strains were arrested in G1 using alpha factor for 4 hours and then washed into fresh media. Samples were collected and fixed with formaldehyde for analysis of the segregation of GFP chromosome VIII in large budded cells at the indicated timepoints. Error bars show SD from 2 biological replicates. Segregation was analyzed in a minimum of n=100 cells for each strain and condition. Strains used: SBY15829, SBY15830. (D) Ndc80-14D does not incorporate into kinetochores properly. Diploid yeast expressing Ndc80-V5-AID as well as WT, Ndc80-14A, or Ndc80-14A were arrested as large budded cells using benomyl for 180 minutes. In the last 60 minutes, 500 μM auxin was added to the media to degrade Ndc80-V5-AID. Cells were harvested and kinetochores were purified and analyzed for the indicated proteins by immunoblotting. Representative of 2 biological replicates. Strains used: SBY12549, SBY12550, SBY12570.

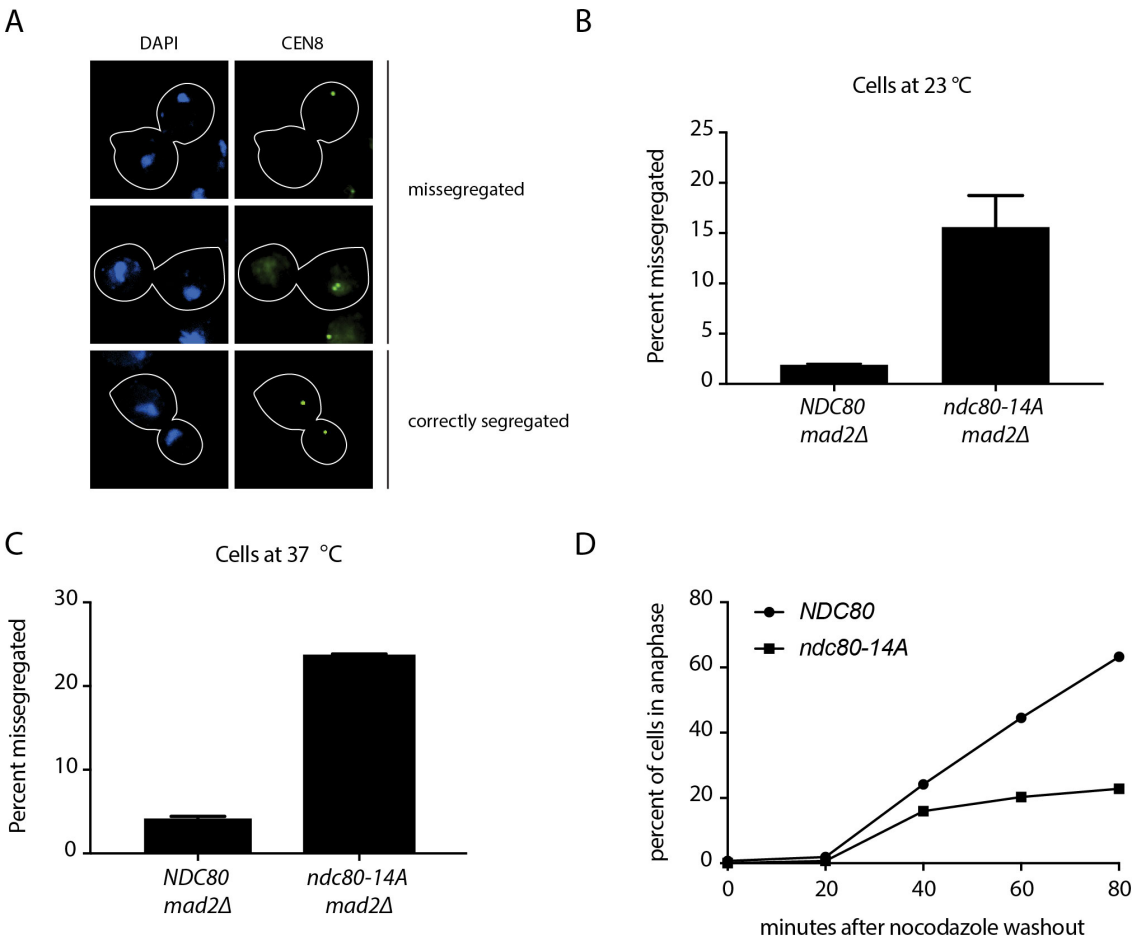

Figure 3.6. Mps1 phosphorylation of Ndc80 is important for proper chromosome segregation.

(A-C) *Ndc80-14A* causes chromosome segregation defects. Cultures with the indicated genotypes were synchronized in G1 with alpha factor for 3 hours, then released into rich media at the indicated temperature. Timepoints were collected, fixed with formaldehyde, and total DNA was DAPI stained. By 150 minutes, the majority of cells had segregated their DNA between the daughter cells. A minimum of 200 cells of each genotype and growth condition were analyzed for segregation of GFP-labeled chromosome 8 by fluorescent microscopy in the sample from the 150 timepoint. Strains used: SBY18141, SBY18208. (A) Representative images of correctly segregated and missegregated chromosome categories. (B) Anaphase segregation of GFP-labeled chromosome 8 in *mad2Δ* and *mad2Δ ndc80-14A* cells grown at 23 °C. (C)

Anaphase segregation of GFP-labeled chromosome 8 in *mad2Δ* and *mad2Δ ndc80-14A* cells grown at 37 °C. (D) Preliminary result: *Ndc80-14A* cells recover poorly after treatment with nocodazole. Cultures of yeast with the indicated genotypes were treated with 10 μg/ml nocodazole for 2 hours and then washed into fresh media and samples were taken at the indicated timepoints and fixed with formaldehyde. Total DNA was DAPI stained. DAPI segregation was analyzed at each timepoint and the percent of cells with 2 DAPI masses, 1 in each daughter cell, is plotted. A minimum of 100 cells were analyzed for each timepoint. Strains used: SBY17564, SBY17565.

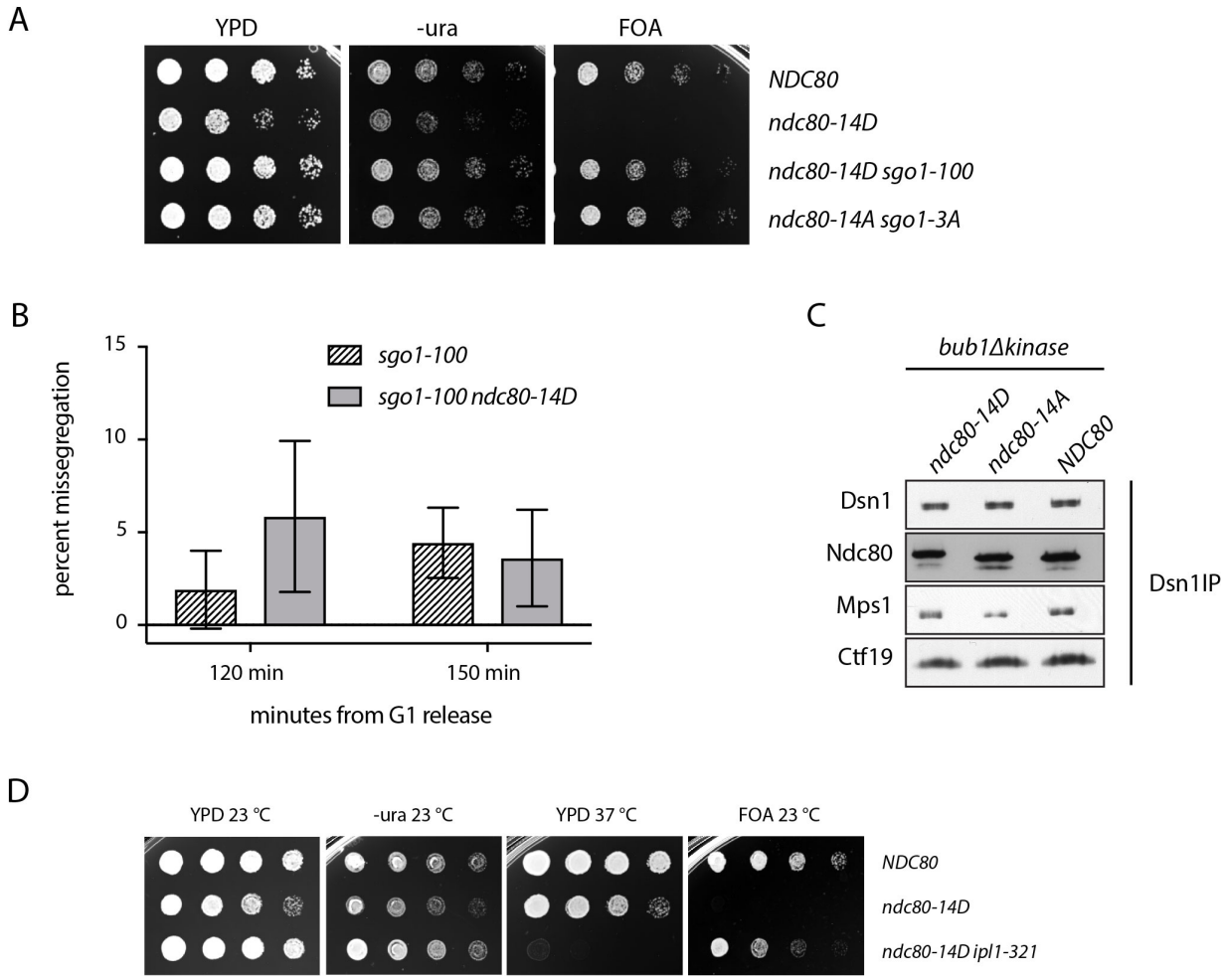

Figure 3.7. The Bub1 kinase-Sgo1-Aurora B^{Ipl1} biorientation pathway is responsible for cell death caused by mimicking constitutive Mps1 phosphorylation of Ndc80.

(A) The *sgo1-100* and *sgo1-3A* alleles suppress the lethality of *ndc80-14D*. 5-fold serial dilutions of the indicated strains were plated onto YPD, -ura, and FOA media. Strains used: SBY18446, SBY9453, SBY14429, SBY15524. (B) *sgo1-100* rescues the chromosome segregation defect of *ndc80-14D*. Cells were synchronized in G1 with alpha factor and washed into fresh media. Samples were collected during a synchronous cell cycle. Alpha factor was added back at budding to prevent a subsequent cell cycle. Segregation of GFP-labeled chromosome 8 was analyzed by flourescent microscopy and DAPI staining for selected timepoints. Chromosome

missegregation was defined as 1 or 2 visible GFP foci in only 1 daughter cell. Strains used: SBY15246, SBY16224. N=2. (C) Ndc80-14D incorporates into kinetochores comparably to WT in the *bub1Δkinase* background. Kinetochores were purified through IP of Dsn1 and association of the indicated proteins was analyzed by immunoblotting. Strains used: SBY15333, SBY15442, SBY15444. (D) *ipl1-321* suppresses the inviability of *ndc80-14D*. 5-fold serial dilutions of the indicated strains were plated onto YPD, -ura, and FOA media. Strains used: SBY18446, SBY9453, SBY18561.

3.9 Supplementary Figures

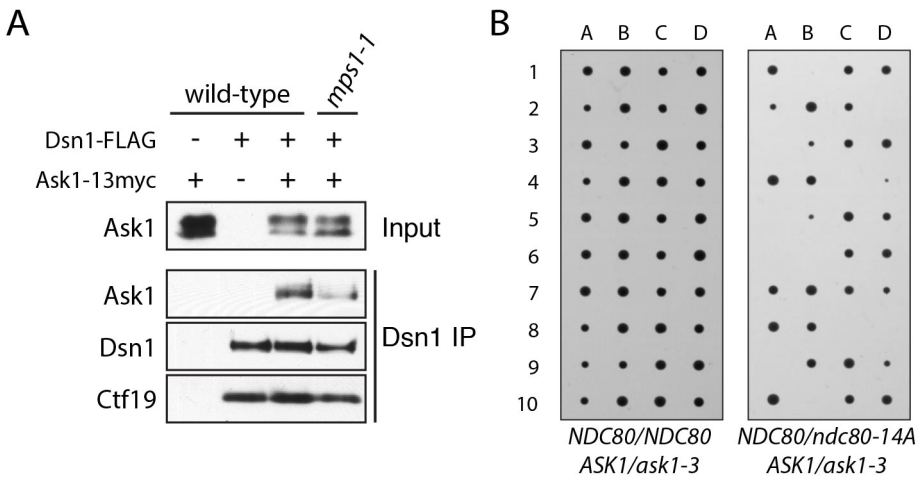

Supplementary Figure 3.1. Dam1 complex function is reduced in *mps1-1* and *ndc80-14A* cells.

(A) *mps1-1* kinetochores (from SBY12090) have less Ask1 protein than wild-type (SBY12088) kinetochores. Strains with only Ask1 tagged (SBY1772) or Dsn1 tagged (SBY8253) are shown on the left. (B) *ndc80-14A* is synthetic lethal with *ask1-3*. Haploid yeast were mated, sporulated and dissected. Tetrads are arrayed in rows. (left) Tetrads dissected from an *ask1-3* heterozygote. (crossed SBY8366 x SBY11809) (right) Tetrads dissected from a diploid heterozygous for *ndc80-14A* and *ask1-3* (crossed SBY8366 x SBY10572). The inviable cells inherited both *ndc80-14A* and *ask1-3*.

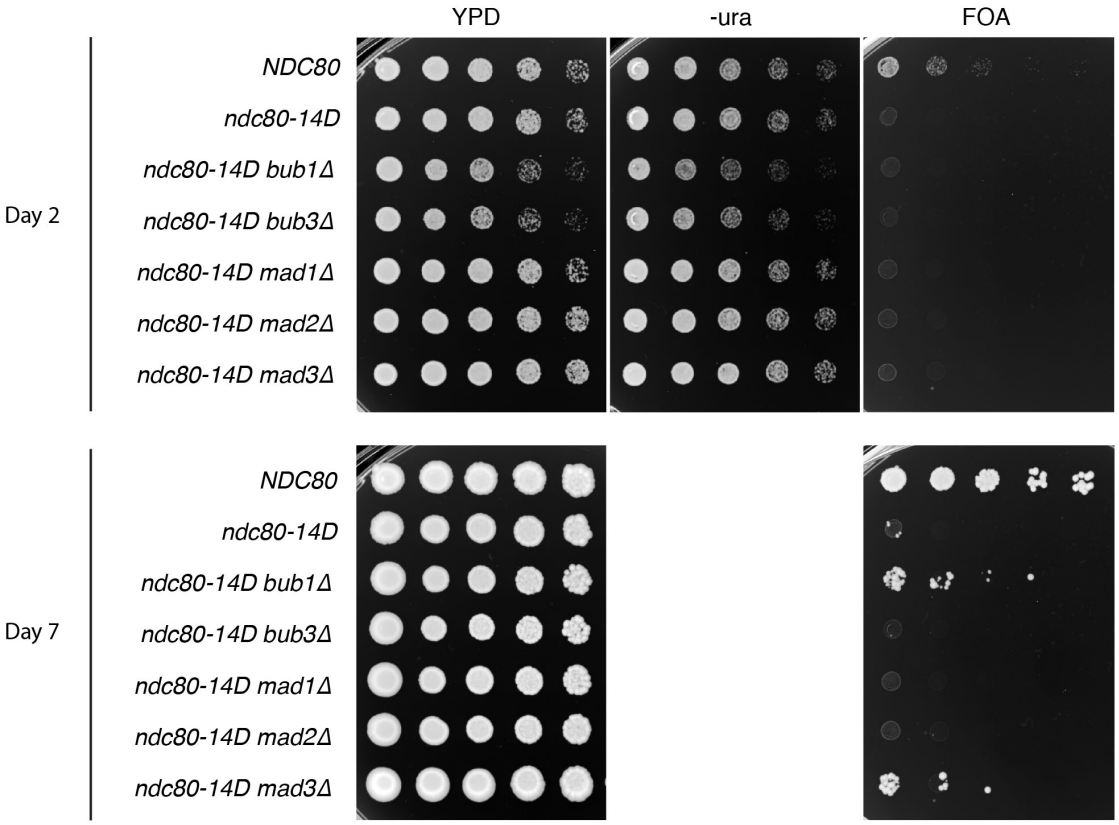

Supplementary Figure 3.2. Preventing spindle assembly checkpoint signaling does not rescue *ndc80-14D*.

Plasmid shuffle assay. 5-fold serial dilutions of cultures of the indicated strains of yeast were plated on YPD , -ura, and FOA plates. All strains contained a CEN/URA plasmid with wild-type *NDC80*. *ndc80-14D* colonies growing at Day 7 likely contain suppressor mutations. Strains used from top to bottom: SBY15149, SBY9453, SBY15139, SBY17991, SBY17993, SBY15087, SBY11334.

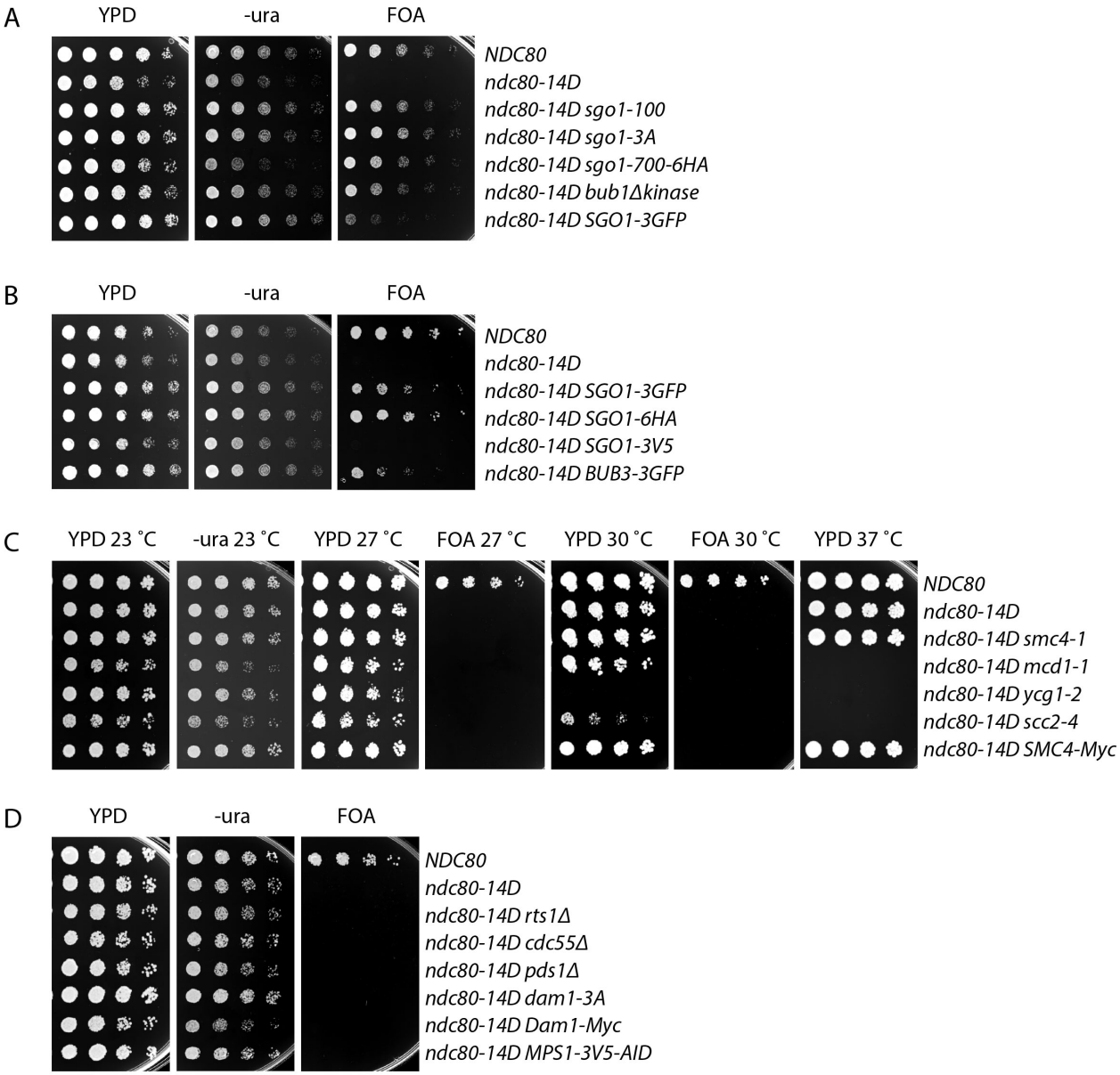

Supplementary Figure 3.3. Plasmid shuffle assay to determine if additional biorientation mutants rescue *ndc80-14D*

(A) Mutations in the Bub1 kinase-Sgo1 biorientation pathway suppress lethality caused by ndc80-14D. 5-fold serial dilutions of the indicated strains were plated on YPD, -ura, and FOA media. Strains used: SBY18446, SBY9453, SBY14429, SBY15524, SBY15526, SBY18187, SBY15033. (B) Tags on Sgo1 and Bub3 suppress ndc80-14D lethality. 5-fold serial dilutions of the indicated strains were plated on YPD, -ura, and FOA media. Strains used: SBY18446, SBY9453, SBY15033, SBY18195, SBY18196,

SBY18186. (C) Condensin and cohesin mutants do not suppress the lethality caused by *ndc80-14D*. 5-fold serial dilutions of the indicated strains were plated on YPD, -ura, and FOA media. Strains used: SBY18446, SBY9453, SBY15221, SBY15420, SBY15421, SBY15384, SBY15395. (D) Various additional biorientation mutants or hypomorphic alleles do not suppress the lethality caused by *ndc80-14D*. 5-fold serial dilutions of the indicated strains were plated on YPD, -ura, and FOA media. Strains used: SBY18446, SBY9453, SBY18188, SBY15148, SBY15061, SBY15134, SBY16554, SBY15129.

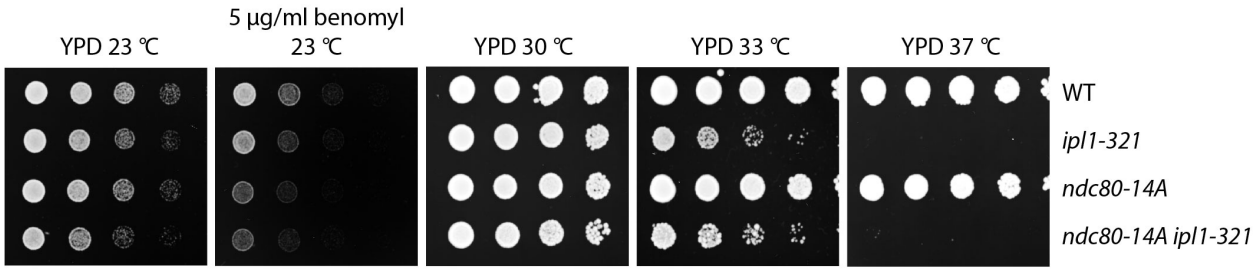

Supplementary Figure 3.4. *ndc80-14A* and *ipl1-321* do not additively compromise growth.

5-fold serial dilutions of the indicated strains were plated to YPD or YPD + 5 ug/ ml benomyl media and grown at the indicated temperatures. Strains used: SBY3, SBY630, SBY14424, SBY17684.

Chapter 4: Conclusions and Perspectives

In this dissertation I present the results of my investigations into the mechanisms that regulate Mps1 localization at the kinetochore. I found that Mps1 association with native kinetochore complexes isolated from budding yeast is not disrupted when kinetochores bind to microtubules in multiple different configurations. Instead, I found that Mps1 autophosphorylation prevents it from binding to kinetochores and I identified several potential phosphorylation sites in the N-terminus of Mps1 that mediate its release from kinetochores in vitro. Mutation of additional potential phosphorylation sites in the N-terminus reduced Mps1 co-immunoprecipitation with kinetochores, suggesting that phosphorylation of certain sites promotes kinetochore association while phosphorylation of others mediates release. In support of this hypothesis, I found that a constitutively catalytically inactive allele of Mps1, Mps1-D580A, consistently had a reduced association with kinetochores compared to wild-type in cells expressing an additional wild-type Mps1. In the future, mutating additional combinations of potential phosphorylation sites in the Mps1 N-terminus and examining the ability of those mutant proteins to associate with kinetochores should identify which sites are important for Mps1 binding versus release from kinetochores. However, it is also possible that mutation of the N-terminus of Mps1 reduces its kinase activity. If so, mutations may indirectly prevent release rather than indicate that the mutated sites are involved in kinetochore association per se. To address this issue, it will be important to measure the kinase activity of specific Mps1 mutants in order to draw more precise conclusions about residues required for Mps1-

kinetochore binding. Recent results suggest that human Mps1 has an auto-inhibitory domain in its N-terminus, consistent with such a possibility (139). Given that co-immunoprecipitations can only give a static depiction of the ability of proteins to remain bound together, the ability of specific Mps1 mutants to associate with purified kinetochores would be better investigated using a more sensitive and potentially dynamic technique such as TIRF microscopy. This would enable a quantitative estimate of the number of mutant Mps1 molecules that can associate with purified kinetochore particles. Additionally, it may be possible to observe binding and release of fluorescently labeled Mps1 to purified kinetochores. This would reveal the kinetics of binding and release and would better characterize the effects of specific point mutations.

In my thesis work, I aimed to identify a mechanism by which Mps1 promotes biorientation independently of the spindle assembly checkpoint. I found that Mps1 phosphorylation of kinetochores weakens kinetochore-microtubule attachments in vitro and that Ndc80 is the relevant substrate for this effect. I also found that Mps1 phosphorylation of Ndc80 is important for proper chromosome segregation in cells because either preventing or mimicking the phosphorylation causes chromosome missegregation. Because preventing Mps1 phosphorylation of Ndc80 with the *ndc80-14A* allele reduced the association of Dam1 complex with kinetochores, it will be important to determine whether Dam1 localization at kinetochores is reduced in *ndc80-14A* cells. This can be visualized by fluorescently tagging Dam1 or through visualizing epitope-tagged Dam1 complex proteins via immunofluorescence. Such a result would help determine whether the chromosome missegregation observed in *ndc80-14A* cells

is primarily due to a Dam1 complex localization defect. If the localization of Dam1 complex appears like wild-type, however, we still could not completely rule out a Dam1 complex defect but it would more strongly suggest that Mps1 phosphorylation influences attachments directly through an effect on Ndc80 function.

Interestingly, I found that mutation of the Bub1-Sgo1-Aurora B^{Ipl1} biorientation pathway rescues the lethality caused by *ndc80-14D*, which mimics constitutive Mps1 phosphorylation of Ndc80. These results suggest that *ndc80-14D* causes an attachment or biorientation defect that is detected by this biorientation pathway. In the future, whether Ndc80-14D directly weakens attachments can be measured by purifying kinetochores from viable double mutants (such as *ndc80-14D ipl1-321*) and measuring their attachment strength using the laser-trapping assay. Chromosome missegregation rates were similar between *ndc80-14D sgo1-100* and *sgo1-100* cells at 150 minutes following G1 release. This latter is consistent with the ability of double mutant cells to grow and suggests that activity of the Bub1-Sgo1-Aurora B^{Ipl1} pathway is primarily responsible for the death of *ndc80-14D* cells, as opposed to an intrinsic attachment defect caused by *ndc80-14D*. Overall, my results suggest that Mps1 and Aurora B^{Ipl1} phosphorylation of Ndc80 both weaken kinetochore-microtubule attachments and that Mps1 phosphorylation of Ndc80 serves as an indirect mechanism to promote error correction by Aurora B^{Ipl1}.

In the future, it will be interesting to compare the effect of Mps1 versus Aurora B^{Ipl1} phosphorylation of specific sites in Ndc80 on kinetochore-microtubule attachments using kinetochore purifications and laser trapping. Based on my observation that *ipl1-321* rescues *ndc80-14D*, I hypothesize that Mps1 and Aurora B^{Ipl1}

phosphorylation will additively weaken attachments and that potentially Aurora B^{Ipl1} phosphorylation weakens attachments more dramatically than Mps1 phosphorylation. Additionally, directly comparing the chromosome missegregation rates of specific phospho-mutants in cells will give a better comparison of the importance of each type of phosphorylation to chromosome segregation. I look forward to further research aimed at addressing these remaining questions on how Mps1 and Aurora B^{Ipl1} influence kinetochore-microtubule attachments.

Tables

Table 1. List of relevant phospho-mutant alleles

Allele	Mutated residues	Source	Plasmid
dsn1-2D	S240D S250D	Akiyoshi et al 2013	pSB1104
mps1-8A	S153A S159A T162A T163A T173A T175A S185A T195A	this study	pSB2642
mps1-16A	S22A, T28A, T47A, S50A, T71A, S129A, T145A, S153A, S159A, T162A, T163A, T173A, T175A, S185, T195A, S203A	this study	pSB2850
ndc80-14A	S4A T5A S6A T21A S22A S37A T38A T43A T74 T79 T82 S205A T248A T252A	Kemmler et al 2009	pSB1848
ndc80-14D	S4D T5D S6D T21D S22D S37D T38D T43D T74D T79D T82D S205D T248D T252D	Kemmler et al 2009	pSB1577
ndc80-7A	T21A S37A T54A T71A T74A S95A S100A	Akiyoshi et al 2009	pSB1336

Table 2: Plasmid List

Plasmid Number	Description	Source
pSB116	*pHIS3-pCUP1-GFP12-LacI12 HIS3 integrating*	Biggins et al 1999
pSB205	*PDS1-18Myc LEU2 integrating*	Shirayama et al 1998
pSB209	*pGAL-12Myc URA3 integrating*	Biggins Lab
pSB563	*pASK1-ASK1-Myc HIS3 integrating*	Ellredge Lab
pSB1104	*DSN1-2D HIS3 integrating*	Akiyoshi et al 2013
pSB1172	*LacO(256) 2kb from CENVIII, near QCR10 integrating*	Ng et al 2009
pSB1302	*pNDC80-NDC80 URA3 CENVI replicating*	Akiyoshi et al 2009
pSB1577 (pSK981)	*pNDC80-ndc80-14D-3HA-KANMX6-Ndc80term integrating*	Kemmler et al 2009
pSB1590	*DSN1-6His-3Flag URA3 integrating*	Akiyoshi et al 2010
pSB1821	*SNAP HPHMX*	Aaron Hoskins, Moore Lab, U Mass Med
pSB1824	*CLIP KANMX*	Aaron Hoskins, Moore Lab, U Mass Med
pSB1848 (pSK1039)	*pNDC80-ndc80-14A-3HA-KANMX6-Ndc80term integrating*	Kemmler et al 2009
pSB1934	*pRS303-pADH1-OsTIR1 HIS3 integrating*	Gottschling Lab, Calico
pSB2046	*3V5-KANMX URA3*	Amon Lab
pSB2067	*pFA6a-3V5-IAA17-KANMX*	Leon Chan, Weis Lab UC Berkeley
pSB2141	*pMPS1-10Myc-MPS1 TRP1 KANMX integrating*	Winey Lab, UC Davis
pSB2188	*pGAL1-12Myc-MPS1-3'UTR URA3 integrating*	this study
pSB2192	*pMPS1-10Myc-mps1-R170S-3'UTR TRP1 KANMX integrating*	this study
pSB2222	*TRP1 single integration*	Leon Chan, Weis Lab, UC Berkeley

pSB2286	*pMPS1-10Myc-mps1Δ2-439-3'UTR TRP1 KANMX integrating*	this study
pSB2378	*pNDC80-NDC80-3V5-IAA7 TRP1 single integration*	Matthew P. Miller, Biggins Lab
pSB2397	*pMPS1-10Myc-MPS1-3'UTR TRP1 single integration*	this study
pSB2439	*DSN1-2D-6His-3Flag URA3 integrating*	Lang et al, under revision
pSB2591	*pGAL1-12Myc-mps1Δ401-765-3'UTR URA3 integrating*	this study
pSB2642	*pMPS1-10Myc-mps1-8A-3'UTR TRP1 single integration*	this study
pSB2643	*pMPS1-MPS1 URA3 CENVI replicating*	this study
pSB2708	*pMPS1-10Myc-mps1-D580A-3'UTR TRP1 single integration*	this study
pSB2850	*pMPS1-10Myc-mps1-16A-3'UTR TRP1 single integration*	this study

Table 3: Strain List

Strain	Genotype	Integrated and [Replicating] plasmids
SBY3	*MAT***a** *ura3-1 leu2,3-112 his3-11 trp1-1 ade2-1 LYS2 can1-100 bar1Δ*	
SBY630	*MAT***a** *ura3-1 leu2,3-112 his3-11 trp1-1 ade2-1 LYS2 can1-100 BAR1 ipl1-321*	
SBY1772	*MAT***a** *ura3-1 leu2,3-112 his3-11::ASK1-Myc:HIS3 trp1-1 ade2-1 LYS2 can1-100 bar1-1*	pSB563
SBY1960	*MAT***a** *ura3-1 leu2,3-112 his3-11 trp1-11 ade2-1 LYS2 can1-100 BAR1 PDS1-Myc:LEU2 DAM1-9Myc:TRP1*	SB205
SBY4880	*MAT***a** *ura3-1 leu2,3-112 his3-11 trp1-1 ade2-1 LYS2 can1-100 bar1-1 PDS1-18Myc:LEU2*	pSB205
SBY8066	*MAT***a** *ura3-1 leu2,3-112 his3-11::dsn1-2D:HIS3 trp1-1 ade2-1 LYS2 can1-100 bar1-1 PDS1-18Myc:LEU2 dsn1Δ::KANMX*	pSB1104, pSB205
SBY8253	*MAT***a** *ura3-1 leu2,3-112 his3-11 trp1-1 ade2-1 LYS2 can1-100 bar1-1 DSN1-6His-3Flag:URA3*	
SBY8366	*MAT***a** *ura3-1 leu2,3-112 his3-11 trp1-1 ade2-1 LYS2 can1-100 bar1-1 ask1-3 DSN1-6His-3Flag:URA3*	
SBY8476	*MAT***α** *ura3-1 leu2,3-112 his3-11 trp1-1 ade2-1 LYS2 can1-100 bar1-1 DSN1-6His-3Flag:URA3*	
SBY8726	*MAT***a** *ura3-1 leu2,3-112 his3-11 trp1-1 ade2-1 LYS2 can1-100 bar1-1 DSN1-6His-3Flag:URA3 mps1-1*	
SBY8938	*MAT***a** *ura3-1 leu2,3-112 his3-11 trp1-1 ade2-1 LYS2 can1-100 bar1-1 DSN1-6His-3Flag:URA3 DAM1-9Myc:TRP1 mps1-1*	
SBY9190	*MAT***a** *ura3-1 leu2,3-112 his3-11 trp1-1 ade2-1 LYS2*	

	can1-100 bar1-1 DSN1-6His-3Flag:URA3 mps1Δ::KANMX:10Myc-MPS1:TRP1	
SBY9453	*MAT***a** *ura3-1 leu2,3-112 his3-11 trp1-1 ade2-1 LYS2 can1-100 bar1-1 ndc80-14D-3HA:KANMX [NDC80 URA3 CEN VI]*	[pSB1302], pSB1577
SBY10274	*MAT***a** *ura3-1 leu2,3-112 his3-11 trp1-1 ade2-1 LYS2 can1-100 bar1-1 DSN1-6His-3Flag:URA3 DAM1-9Myc:TRP1*	
SBY10572	*MAT***α** *ura3-1 leu2,3-112 his3-11 trp1-1 ade2-1 LYS2 can1-100 bar1-1 ndc80-14A-3HA:KANMX DSN1-6His-3Flag:URA3*	pSB1848
SBY11334	*MAT***a** *ura3-1 leu2,3-112 his3-11 trp1-1 ade2-1 LYS2 can1-100 bar1-1 ndc80-14D-3HA:KANMX mad3Δ::HIS3 [NDC80 URA3 CEN VI]*	[pSB1302], pSB1577
SBY11808	*MAT***a** *ura3-1 leu2,3-112 his3-11 trp1-1 ade2-1 LYS2 can1-100 bar1-1 DSN1-6His-3Flag:URA3 NDC80-3HA:KANMX*	
SBY11809	*MAT***α** *ura3-1 leu2,3-112 his3-11 trp1-1 ade2-1 LYS2 can1-100 bar1-1 DSN1-6His-3Flag:URA3 NDC80-3HA:KANMX*	
SBY12039	*MAT***a** *ura3-1 leu2,3-112 his3-11::ASK1-Myc:HIS3 trp1-1 ade2-1 LYS2 can1-100 bar1-1 DSN1-6His-3Flag:URA3 ndc80-14A-3HA:KANMX*	pSB563, pSB1848
SBY12076	*MAT***a** *ura3-1 leu2,3-112 his3-11::ASK1-Myc:HIS3 trp1-1 ade2-1 LYS2 can1-100 bar1-1 DSN1-6His-3Flag:URA3 NDC80-3HA:KANMX*	pSB563
SBY12088	*MAT***a** *ura3-1 leu2,3-112 his3-11::ASK1-Myc:HIS3 trp1-1 ade2-1 LYS2 can1-100 bar1-1 DSN1-6His-3Flag:URA3*	pSB563

SBY12090	*MAT***a** *ura3-1 leu2,3-112 his3-11::ASK1-Myc:HIS3 trp1-1 ade2-1 LYS2 can1-100 bar1-1 DSN1-6His-3Flag:URA3 mps1-1*	pSB563
SBY12352	*MAT***a** *ura3-1 leu2,3-112 his3-11::pADH1-OsTIR1-myc:HIS3 trp1-1 ade2-1 LYS2 can1-100 bar1-1 DSN1-3Flag:KANMX NDC80-3V5-IAA17:KANMX mps1Δ::KANMX:10Myc-MPS1:TRP1*	pSB1934
SBY12374	*MAT***a** *ura3-1::mps1-7 leu2,3-112 his3-11 trp1-1 ade2-1 LYS2 can1-100 BAR1 mps1Δ::KANMX PDS1-Myc:LEU2*	SB205
SBY12412	*MAT***a** *ura3-1 leu2,3-112 his3-11 trp1-1 ade2-1 LYS2 can1-100 bar1-1 MPS1-3V5:KANMX*	
SBY12464	*MAT***a** *ura3-1 leu2,3-112 his3-11 trp1-1 ade2-1 LYS2 can1-100 bar1-1 DAD1-3Flag:TRP1*	
SBY12549	*MAT***a/α** *ura3-1/ura3-1 leu2,3-112/leu2,3-112 his3::pGPD1-OsTIR1-Myc:HIS3/his3-11 trp1-1/trp1-1 ade2-1/ade2-1 LYS2/LYS2 can1-100/can1-100 bar1-1/bar1-1 DSN1-3FLAG:KANMX/DSN1-3FLAG:KANMX mps1Δ::KANMX:pMPS1-10Myc-MPS1:TRP1/mps1Δ::KANMX:pMPS1-10Myc-MPS1:TRP1 NDC80-3HA:KANMX/NDC80-3V5-IAA17:KANMX*	pSB1934
SBY12550	*MAT***a/α** *ura3-1/ura3-1 leu2,3-112/leu2,3-112 his3::pGPD1-OsTIR1-Myc:HIS3/his3-11 trp1-1/trp1-1 ade2-1/ade2-1 LYS2/LYS2 can1-100/can1-100 bar1-1/bar1-1 DSN1-3FLAG:KANMX/DSN1-3FLAG:KANMX mps1Δ::KANMX:pMPS1-10Myc-MPS1:TRP1/mps1Δ::KANMX:pMPS1-10Myc-MPS1:TRP1 ndc80-14A-3HA:KANMX/NDC80-3V5-*	pSB1848, pSB1934

	IAA17:KANMX	
SBY12570	*MAT***a/α** *ura3-1/ura3-1 leu2,3-112/leu2,3-112 his3::pGPD1-OsTIR1-Myc:HIS3/his3-11 trp1-1/trp1-1 ade2-1/ade2-1 LYS2/LYS2 can1-100/can1-100 bar1-1/bar1-1 DSN1-3FLAG:KANMX/DSN1-3FLAG:KANMX mps1Δ::KANMX:pMPS1-10Myc-MPS1:TRP1/mps1Δ::KANMX:pMPS1-10Myc-MPS1:TRP1 ndc80-14D-3HA:KANMX/NDC80-3V5-IAA17:KANMX*	pSB1577, pSB1934
SBY12571	*MAT***a** *ura3-1 leu2,3-112 his3-11 trp1-1 ade2-1 LYS2 can1-100 bar1-1 DSN1-6His-3Flag:URA3 MTW1-CLIP:KANMX MPS1-SNAP:HPH*	
SBY13086	*MAT***a** *ura3-1 leu2,3-112 his3-11 trp1-1 ade2-1 LYS2 can1-100 bar1-1 DSN1-6His-3Flag:URA3 ndc80-14A-3HA:KANMX*	pSB1848
SBY13196	*MAT***a** *ura3-1 leu2,3-112 his3-11 trp1-1 ade2-1 LYS2 can1-100 bar1-1 mps1Δ::KANMX:10Myc-mps1-R170S:TRP1 DSN1-6His-3Flag:URA3*	pSB2192
SBY13704	*MAT***a** *ura3-1 leu2,3-112 his3-11::pADH1-OsTIR1-myc:HIS3 trp1-1::pMPS1-10Myc-mps1Δ2-439:TRP1:KANMX ade2-1 LYS2 can1-100 bar1-1 DSN1-6His-3Flag:URA3 MPS1-3V5-IAA17:KANMX*	pSB1934, pSB1590, pSB2286
SBY14108	*MAT***a** *ura3-1 leu2,3-112 his3-11::pADH1-OsTIR1-myc:HIS3 trp1-1::pMPS1-10Myc-MPS1:TRP1:KANMX ade2-1 LYS2 can1-100 bar1-1 DSN1-6His-3Flag:URA3 MPS1-3V5-IAA17:KANMX*	pSB1934, pSB2397
SBY14424	*MAT***a** *ura3-1 leu2,3-112 his3-11 trp1-1 ade2-1 LYS2 can1-100 bar1-1 ndc80-14A-3HA:KANMX*	pSB1848
SBY14429	*MAT***a** *ura3-1 leu2,3-112 his3-11 trp1-1 ade2-1 LYS2*	[pSB1302],

	can1-100 bar1-1 ndc80-14D-3HA:KANMX sgo1-100:KANMX [NDC80 URA3 CEN VI]	pSB1577
SBY15033	*MAT***a** *ura3-1 leu2,3-112 his3-11 trp1-1 ade2-1 LYS2 can1-100 bar1-1 ndc80-14D-3HA:KANMX SGO1-3GFP:HIS3 [NDC80 URA3 CEN VI]*	[pSB1302], pSB1577
SBY15061	*MAT***a** *ura3-1 leu2,3-112 his3-11 trp1-1 ade2-1 LYS2 can1-100 bar1-1 ndc80-14D-3HA:KANMX pds1Δ::LEU2 [NDC80 URA3 CEN VI]*	[pSB1302], pSB1577
SBY15062	*MAT***a** *ura3-1 leu2,3-112 his3-11 trp1-1 ade2-1 LYS2 can1-100 bar1-1 mad2Δ::HIS3*	
SBY15087	*MAT***a** *ura3-1 leu2,3-112 his3-11 trp1-1 ade2-1 LYS2 can1-100 bar1-1 ndc80-14D-3HA:KANMX mad2Δ::KANMX [NDC80 URA3 CEN VI]*	[pSB1302], pSB1577
SBY15096	*MAT***a** *ura3-1 leu2,3-112 his3-11::pGPD1-OsTIR1:HIS3 trp1-1::pNDC80-NDC80-3V5-IAA7:TRP1 ade2-1 LYS2 can1-100 bar1-1 PDS1-Myc:LEU2*	pSB1934, pSB205, pSB2378
SBY15099	*MAT***a** *ura3-1 leu2,3-112 his3-11::pGPD1-OsTIR1:HIS3 trp1-1 ade2-1 LYS2 can1-100 bar1-1 PDS1-Myc:LEU2*	pSB205
SBY15129	*MAT***a** *ura3-1 leu2,3-112 his3-11 trp1-1 ade2-1 LYS2 can1-100 bar1-1 ndc80-14D-3HA:KANMX MPS1-3V5-IAA17:KANMX [NDC80 URA3 CEN VI]*	[pSB1302], pSB1577
SBY15134	*MAT***a** *ura3-1 leu2,3-112 his3-11 trp1-1 ade2-1 LYS2 can1-100 bar1-1 ndc80-14D-3HA:KANMX dam1-3A (S257A, S265A, S292A):HPH [NDC80 URA3 CEN VI]*	[pSB1302], pSB1577
SBY15139	*MAT***a** *ura3-1 leu2,3-112 his3-11 trp1-1 ade2-1 LYS2 can1-100 bar1-1 ndc80-14D-3HA:KANMX bub1Δ::HPH NDC80:URA3 [NDC80 URA3 CEN VI]*	[pSB1302], pSB1577
SBY15148	*MAT***a** *ura3-1 leu2,3-112 his3-11 trp1-1 ade2-1 LYS2 can1-100 bar1-1 ndc80-14D-3HA:KANMX*	[pSB1302], pSB1577

	cdc55Δ::HPH NDC80:URA3 [NDC80 URA3 CEN VI]	
SBY15149	*MAT***a** *ura3-1 leu2,3-112 his3-11::pGPD1-OsTIR1:HIS3 trp1-1::pNDC80-NDC80-3V5-IAA7:TRP1 ade2-1 LYS2 can1-100 bar1-1 ndc80-14D-3HA:KANMX [NDC80 URA3 CEN VI]*	[pSB1302], pSB1577, pSB2378
SBY15206	*MAT***a** *ura3-1 leu2,3-112 his3-11::pGPD1-OsTIR1:HIS3 trp1-1::pNDC80-NDC80-3V5-IAA7:TRP1 ade2-1 LYS2 can1-100 bar1-1 ndc80-14D-3HA:KANMX PDS1-Myc:LEU2*	pSB2378, pSB1577, pSB205
SBY15221	*MAT***a** *ura3-1 leu2,3-112 his3-11 trp1-1 ade2-1 LYS2 can1-100 bar1-1 ndc80-14D-3HA:KANMX smc4-1 [NDC80 URA3 CEN VI]*	[pSB1302], pSB1577
SBY15285	*MAT***a** *ura3-1 leu2,3-112 his3-11 trp1-1 ade2-1 LYS2 can1-100 bar1-1 dsn1-2D-6His-3Flag:URA3 MTW1-CLIP:KANMX MPS1-SNAP:HPH*	
SBY15384	*MAT***a** *ura3-1 leu2,3-112 his3-11 trp1-1 ade2-1 LYS2 can1-100 bar1-1 ndc80-14D-3HA:KANMX scc2-4 [NDC80 URA3 CEN VI]*	[pSB1302], pSB1577
SBY15395	*MAT***a** *ura3-1 leu2,3-112 his3-11 trp1-1 ade2-1 LYS2 can1-100 bar1-1 ndc80-14D-3HA:KANMX SMC4-Myc:TRP1 [NDC80 URA3 CEN VI]*	[pSB1302], pSB1577
SBY15420	*MAT***a** *ura3-1 leu2,3-112 his3-11 trp1-1 ade2-1 LYS2 can1-100 bar1-1 ndc80-14D-3HA:KANMX mcd1-1 [NDC80 URA3 CEN VI]*	[pSB1302], pSB1577
SBY15421	*MAT***a** *ura3-1 leu2,3-112 his3-11 trp1-1 ade2-1 LYS2 can1-100 bar1-1 ndc80-14D-3HA:KANMX ycg1-2 [NDC80 URA3 CEN VI]*	[pSB1302], pSB1577
SBY15524	*MAT***a** *ura3-1 leu2,3-112 his3-11 trp1-1 ade2-1 LYS2 can1-100 bar1-1 ndc80-14D-3HA:KANMX sgo1-3A*	[pSB1302], pSB1577

	(Y47A, Q50A, S52A):HPH [NDC80 URA3 CEN VI]	
SBY15526	*MAT***a** *ura3-1 leu2,3-112 his3-11 trp1-1 ade2-1 LYS2 can1-100 bar1-1 ndc80-14D-3HA:KANMX sgo1-700-63HA:TRP1 [NDC80 URA3 CEN VI]*	[pSB1302], pSB1577
SBY15829	*MAT***a** *ura3-1 leu2,3-112::pGPD1-OsTIR1:LEU2 his3-11::pCUP1-GFP12-LacI12:HIS3 trp1-1::pNDC80-NDC80-3V5-IAA7:TRP1 ade2-1 LYS2 can1-100 bar1-1 CENVIII-LacOs:TRP1 mad2Δ::KANMX*	pSB116, pSB1577, pSB2378, pSB1172
SBY15830	*MAT***a** *ura3-1 leu2,3-112::pGPD1-OsTIR1:LEU2 his3-11::pCUP1-GFP12-LacI12:HIS3 trp1-1::pNDC80-NDC80-3V5-IAA7:TRP1 ade2-1 LYS2 can1-100 bar1-1 ndc80-14D-3HA:KANMX CENVIII-LacOs:TRP1 mad2Δ::KANMX*	pSB116, pSB1577, pSB2378, pSB1172
SBY16381	*MAT***a** *ura3-1, leu2,3-112 his3-11 trp1-1 ade2-1 LYS2 can1-100 bar1-1 DSN1-6His-3Flag:URA3 MTW1-CLIP:KANMX MPS1-SNAP:HPH PDS1-18myc:LEU2*	pSB205
SBY16417	*MAT***a** *ura3-1 leu2,3-112 his3-11 trp1-1 ade2-1 LYS2 can1-100 bar1-1 dsn1-2D-6His-3Flag:URA3 MTW1-CLIP:KANMX MPS1-SNAP:HPH PDS1-18myc:LEU2*	pSB205
SBY16554	*MAT***a** *ura3-1 leu2,3-112 his3-11 trp1-1 ade2-1 LYS2 can1-100 bar1-1 ndc80-14D-3HA:KANMX DAM1-9Myc:TRP1 [NDC80 URA3 CEN VI]*	[pSB1302], pSB1577
SBY16862	*MAT***a** *ura3-1::pGAL-12Myc-mps1Δ401-765:URA3 leu2,3-112 his3-11 trp1-1 ade2-1 LYS2 can1-100 bar1-1 DSN1-6His-3Flag:URA3 MPS1-3V5:KANMX*	pSB2591
SBY17018	*MAT***a** *ura3-1::pGAL-12Myc-MPS1:URA3 leu2,3-112 his3-11 trp1-1 ade2-1 LYS2 can1-100 bar1-1 DSN1-6His-3Flag:URA3 MPS1-3V5:KANMX*	pSB2188
SBY17182	*MAT***a** *ura3-1 leu2,3-112 his3-11 trp1-1::pMPS1-*	pSB2397

	10Myc-MPS1:TRP1 ade2-1 LYS2 can1-100 bar1-1 MPS1-3V5:KANMX	
SBY17183	*MAT***a** *ura3-1 leu2,3-112 his3-11 trp1-1::pMPS1-10Myc-mps1-D580A:TRP1 ade2-1 LYS2 can1-100 bar1-1 MPS1-3V5:KANMX*	pSB2708
SBY17184	*MAT***a** *ura3-1 leu2,3-112 his3-11 trp1-1::pMPS1-10Myc-mps1-8A:TRP1 ade2-1 LYS2 can1-100 bar1-1 mps1Δ::KANMX*	pSB2642
SBY17274	*MAT***a** *ura3-1 leu2,3-112 his3-11 trp1-1::pMPS1-10Myc-mps1-8A:TRP1 ade2-1 LYS2 can1-100 bar1-1 DSN1-6His-3Flag:URA3 mps1Δ::KANMX*	pSB2642
SBY17366	*MAT***a** *ura3-1 leu2,3-112 his3-11 trp1-1::pMPS1-10Myc-MPS1:TRP1 ade2-1 LYS2 can1-100 bar1-1 mps1Δ::KANMX*	pSB2397
SBY17383	*MAT***a** *ura3-1 leu2,3-112 his3-11 trp1-1::pMPS1-10Myc-MPS1:TRP1 ade2-1 LYS2 can1-100 bar1-1 DSN1-6His-3Flag:URA3 MPS1-3V5:KANMX*	pSB2397
SBY17475	*MAT***a** *ura3-1 leu2,3-112 his3-11 trp1-1::pMPS1-10Myc-MPS1:TRP1 ade2-1 LYS2 can1-100 bar1-1 mps1Δ::KANMX [MPS1 URA3 CEN VI]*	pSB2397, [pSB2643]
SBY17564	*MAT***a** *ura3-1 leu2,3-112 his3-11::pCUP1-GFP12-LacI12:HIS3 trp1-1 ade2-1 LYS2 can1-100 bar1-1 ndc80-14A-3HA:KANMX CENVIII-LacOs:TRP1*	pSB116, pSB1848, pSB1172
SBY17565	*MAT***a** *ura3-1 leu2,3-112 his3-11::pCUP1-GFP12-LacI12:HIS3 trp1-1 ade2-1 LYS2 can1-100 bar1-1 NDC80-3HA:KANMX CENVIII-LacOs:TRP1*	pSB116, pSB1172
SBY17571	*MAT***a** *ura3-1 leu2,3-112 his3-11 trp1-1::pMPS1-10Myc-mps1-16A:TRP1 ade2-1 LYS2 can1-100 bar1-1 mps1Δ::KAN [MPS1 URA3 CEN VI]*	pSB2850, [pSB2643]

SBY17624	*MAT***a** *ura3-1 leu2,3-112 his3-11 trp1-1 ade2-1 LYS2 can1-100 bar1-1 NDC80-3HA:KANMX mad2Δ::HIS3 PDS1-Myc:LEU2*	pSB205
SBY17628	*MAT***a** *ura3-1 leu2,3-112 his3-11 trp1-1::pMPS1-10Myc-mps1-D580A:TRP1 ade2-1 LYS2 can1-100 bar1-1 MPS1-3V5:KANMX DSN1-6His-3Flag:URA3*	pSB2708
SBY17629	*MAT***a** *ura3-1 leu2,3-112 his3-11 trp1-1::pMPS1-10Myc-mps1-16A:TRP1 ade2-1 LYS2 can1-100 bar1-1 MPS1-3V5:KANMX DSN1-6His-3Flag:URA3*	pSB2850
SBY17648	*MAT***a** *ura3-1 leu2,3-112 his3-11 trp1-1 ade2-1 LYS2 can1-100 bar1-1 NDC80-3HA:KANMX PDS1-Myc:LEU2*	pSB205
SBY17684	*MAT***a** *ura3-1 leu2,3-112 his3-11 trp1-1 ade2-1 LYS2 can1-100 bar1-1 ndc80-14A-3HA:KANMX ipl1-321*	pSB1848
SBY17807	*MAT***a** *ura3-1 leu2,3-112 his3-11 trp1-1 ade2-1 LYS2 can1-100 bar1-1 ndc80-14A-3HA:KANMX PDS1-Myc:LEU2*	pSB1848, pSB205
SBY17895	*MAT***a** *ura3-1 leu2,3-112 his3-11 trp1-1 ade2-1 LYS2 can1-100 bar1-1 ndc80-14A-3HA:KANMX mad2Δ::HIS3 PDS1-Myc:LEU2*	pSB1848, pSB205
SBY17898	*MAT***a** *ura3-1 leu2,3-112 his3-11::pCUP1-GFP12-LacI12:HIS3 trp1-1 ade2-1 LYS2 can1-100 bar1-1 ndc80-14A-3HA:KANMX CENVIII-LacOs:TRP1 spc110Δ::SPC110-mCherry:HIS3*	pSB116, pSB1172, pSB1848
SBY17901	*MAT***a** *ura3-1 leu2,3-112 his3-11::pCUP1-GFP12-LacI12:HIS3 trp1-1 ade2-1 LYS2 can1-100 bar1-1 NDC80-3HA:KANMX CENVIII-LacOs:TRP1 spc110Δ::SPC110-mCherry:HIS3*	pSB116, pSB1172
SBY17906	*MAT***a** *ura3-1 leu2,3-112 his3-11 trp1-1::pMPS1-*	pSB2397, pSB205

	10Myc-MPS1:TRP1 ade2-1 LYS2 can1-100 bar1-1 DSN1-3Flag:KANMX mps1Δ::KAN PDS1-18Myc:LEU2	
SBY17909	*MAT***a** *ura3-1 leu2,3-112 his3-11 trp1-1::pMPS1-10Myc-mps1-8A:TRP1 ade2-1 LYS2 can1-100 bar1-1 DSN1-3Flag:KANMX mps1Δ::KAN PDS1-18Myc:LEU2*	pSB205, pSB2642
SBY17931	*MAT***a** *ura3-1 leu2,3-112 his3-11 trp1-1::pMPS1-10Myc-MPS1:TRP1 ade2-1 LYS2 can1-100 bar1-1 DSN1-6His-3Flag:URA3 mps1Δ::KANMX*	pSB2397
SBY17991	*MAT***a** *ura3-1 leu2,3-112 his3-11 trp1-1 ade2-1 LYS2 can1-100 bar1-1 ndc80-14D-3HA:KANMX bub3Δ::HPH [NDC80 URA3 CEN VI]*	[pSB1302], pSB1577
SBY17993	*MAT***a** *ura3-1 leu2,3-112 his3-11 trp1-1 ade2-1 LYS2 can1-100 bar1-1 ndc80-14D-3HA:KANMX mad1Δ::HIS3 [NDC80 URA3 CEN VI]*	[pSB1302], pSB1577
SBY18141	*MAT***a** *ura3-1 leu2,3-112 his3-11::pCUP1-GFP12-LacI12:HIS3 trp1-1 ade2-1 LYS2 can1-100 bar1-1 NDC80-3HA:KANMX mad2Δ::HIS3 CENVIII-LacOs:TRP1 spc110Δ::SPC110-mCherry:HIS3*	pSB116, pSB1172
SBY18186	*MAT***a** *ura3-1 leu2,3-112 his3-11 trp1-1 ade2-1 LYS2 can1-100 bar1-1 ndc80-14D-3HA:KANMX BUB3-3GFP:HIS3 [NDC80 URA3 CEN VI]*	[pSB1302], pSB1577
SBY18187	*MAT***a** *ura3-1 leu2,3-112 his3-11 trp1-1 ade2-1 LYS2 can1-100 bar1-1 ndc80-14D-3HA:KANMX bub1Δkinase:HPH [NDC80 URA3 CEN VI]*	[pSB1302], pSB1577
SBY18188	*MAT***a** *ura3-1 leu2,3-112 his3-11 trp1-1 ade2-1 LYS2 can1-100 bar1-1 ndc80-14D-3HA:KANMX rts1Δ::HPH [NDC80 URA3 CEN VI]*	[pSB1302], pSB1577
SBY18195	*MAT***a** *ura3-1 leu2,3-112 his3-11 trp1-1 ade2-1 LYS2 can1-100 bar1-1 ndc80-14D-3HA:KANMX SGO1-*	[pSB1302], pSB1577

	63HA:TRP1 [NDC80 URA3 CEN VI]	
SBY18196	*MAT***a** *ura3-1 leu2,3-112 his3-11 trp1-1 ade2-1 LYS2 can1-100 bar1-1 ndc80-14D-3HA:KANMX SGO1-3V5:HIS3 [NDC80 URA3 CEN VI]*	[pSB1302], pSB1577
SBY18208	*MAT***a** *ura3-1 leu2,3-112 his3-11::pCUP1-GFP12-LacI12:HIS3 trp1-1 ade2-1 LYS2 can1-100 bar1-1 ndc80-14A-3HA:KANMX mad2Δ::HIS3 CENVIII-LacOs:TRP1 spc110Δ::SPC110-mCherry:HIS3*	pSB116,pSB1172, pSB1848
SBY18307	*MAT***a** *ura3-1 leu2,3-112 his3-11 trp1-1::pMPS1-10Myc-MPS1:TRP1 ade2-1 LYS2 can1-100 bar1-1 mps1Δ::KANMX*	pSB2397
SBY18308	*MAT***a** *ura3-1 leu2,3-112 his3-11 trp1-1::pMPS1-10Myc-mps1-16A:TRP1 ade2-1 LYS2 can1-100 bar1-1 mps1Δ::KANMX*	pSB2850
SBY18316	*MAT***a** *ura3-1 leu2,3-112 his3-11 trp1-1::pMPS1-10Myc-MPS1:TRP1 ade2-1 LYS2 can1-100 bar1-1 MPS1-3V5:KANMX DSN1-6His-3Flag:URA3 PDS1-Myc:LEU2*	pSB2397, pSB205
SBY18317	*MAT***a** *ura3-1 leu2,3-112 his3-11 trp1-1::pMPS1-10Myc-mps1-D580A:TRP1 ade2-1 LYS2 can1-100 bar1-1 MPS1-3V5:KANMX DSN1-6His-3Flag:URA3 PDS1-Myc:LEU2*	pSB205, pSB2708
SBY18318	*MAT***a** *ura3-1 leu2,3-112 his3-11 trp1-1::pMPS1-10Myc-mps1-16A:TRP1 ade2-1 LYS2 can1-100 bar1-1 MPS1-3V5:KANMX DSN1-6His-3Flag:URA3 PDS1-Myc:LEU2*	pSB205, pSB2850
SBY18319	*MAT***a** *ura3-1 leu2,3-112 his3-11 trp1-1::pMPS1-10Myc-MPS1:TRP1 ade2-1 LYS2 can1-100 bar1-1 mps1Δ::KANMX PDS1-Myc:LEU2*	pSB205, pSB2397

SBY18320	*MAT***a** *ura3-1 leu2,3-112 his3-11 trp1-1::pMPS1-10Myc-mps1-16A:TRP1 ade2-1 LYS2 can1-100 bar1-1 mps1Δ::KANMX PDS1-Myc:LEU2*	pSB205, pSB2850
SBY18446	*MAT***a** *ura3-1 leu2,3-112 his3-11 trp1-1 ade2-1 LYS2 can1-100 bar1-1 NDC80-3HA:KANMX [NDC80 URA3 CEN VI]*	[pSB1302], pSB1577
SBY18561	*MAT***a** *ura3-1 leu2,3-112 his3-11 trp1-1 ade2-1 LYS2 can1-100 bar1-1 ndc80-14D-3HA:KANMX ipl1-321 [NDC80 URA3 CEN VI]*	[pSB1302], pSB1577

References

1. Mitchison T, Kirschner M (1984) Dynamic instability of microtubule growth. *Nature* 312(5991):237–242.

2. Biggins S (2013) The Composition, Functions, and Regulation of the Budding Yeast Kinetochore. *Genetics* 194(4):817–846.

3. Walczak CE, Cai S, Khodjakov A (2010) Mechanisms of chromosome behaviour during mitosis. *Nat Rev Mol Cell Biol* 11(2):91–102.

4. Winey M, et al. (1995) Three-dimensional ultrastructural analysis of the Saccharomyces cerevisiae mitotic spindle. *J Cell Biol* 129(6):1601–1615.

5. Joglekar AP, Salmon ED, Bloom KS (2008) Counting Kinetochore Protein Numbers in Budding Yeast Using Genetically Encoded Fluorescent Proteins. *Methods Cell Biol* 85:127–151.

6. Varma D, Salmon ED (2012) The KMN protein network – chief conductors of the kinetochore orchestra. *J Cell Sci* 125(24):5927–5936.

7. Tooley J, Stukenberg PT (2011) The Ndc80 complex: integrating the kinetochore's many movements. *Chromosome Res Int J Mol Supramol Evol Asp Chromosome Biol* 19(3):377–391.

8. Wei RR, Sorger PK, Harrison SC (2005) Molecular organization of the Ndc80 complex, an essential kinetochore component. *Proc Natl Acad Sci U S A* 102(15):5363–5367.

9. Ciferri C, et al. (2005) Architecture of the human ndc80-hec1 complex, a critical constituent of the outer kinetochore. *J Biol Chem* 280(32):29088–29095.

10. Tien JF, et al. (2013) Coupling Unbiased Mutagenesis to High-throughput DNA Sequencing Uncovers Functional Domains in the Ndc80 Kinetochore Protein of Saccharomyces cerevisiae. *Genetics* 195(1):159–170.

11. Demirel PB, Keyes BE, Chaterjee M, Remington CE, Burke DJ (2012) A redundant function for the N-terminal tail of Ndc80 in kinetochore-microtubule interaction in Saccharomyces cerevisiae. *Genetics* 192(2):753–756.

12. Guimaraes GJ, Dong Y, McEwen BF, Deluca JG (2008) Kinetochore-microtubule attachment relies on the disordered N-terminal tail domain of Hec1. *Curr Biol CB* 18(22):1778–1784.

13. Lampert F, Mieck C, Alushin GM, Nogales E, Westermann S (2013) Molecular requirements for the formation of a kinetochore-microtubule interface by Dam1 and Ndc80 complexes. *J Cell Biol* 200(1):21–30.

14. Suzuki A, et al. (2016) How the kinetochore couples microtubule force and centromere stretch to move chromosomes. *Nat Cell Biol* 18(4):382–392.

15. Hanisch A, Silljé HHW, Nigg EA (2006) Timely anaphase onset requires a novel spindle and kinetochore complex comprising Ska1 and Ska2. *EMBO J* 25(23):5504–5515.

16. Welburn JPI, et al. (2009) The human kinetochore Ska1 complex facilitates microtubule depolymerization-coupled motility. *Dev Cell* 16(3):374–385.

17. Gaitanos TN, et al. (2009) Stable kinetochore-microtubule interactions depend on the Ska complex and its new component Ska3/C13Orf3. *EMBO J* 28(10):1442–1452.

18. Theis M, et al. (2009) Comparative profiling identifies C13orf3 as a component of the Ska complex required for mammalian cell division. *EMBO J* 28(10):1453–1465.

19. Cheeseman IM, et al. (2001) Implication of a novel multiprotein Dam1p complex in outer kinetochore function. *J Cell Biol* 155(7):1137–1146.

20. Janke C, Ortíz J, Tanaka TU, Lechner J, Schiebel E (2002) Four new subunits of the Dam1–Duo1 complex reveal novel functions in sister kinetochore biorientation. *EMBO J* 21(1–2):181–193.

21. Li Y, et al. (2002) The mitotic spindle is required for loading of the DASH complex onto the kinetochore. *Genes Dev* 16(2):183–197.

22. Zelter A, et al. (2015) The molecular architecture of the Dam1 kinetochore complex is defined by cross-linking based structural modelling. *Nat Commun* 6. doi:10.1038/ncomms9673.

23. Jenni S, Harrison SC (2018) Structure of the DASH/Dam1 complex shows its role at the yeast kinetochore-microtubule interface. *Science* 360(6388):552–558.

24. Westermann S, et al. (2005) Formation of a dynamic kinetochore- microtubule interface through assembly of the Dam1 ring complex. *Mol Cell* 17(2):277–290.

25. Miranda JJL, De Wulf P, Sorger PK, Harrison SC (2005) The yeast DASH complex forms closed rings on microtubules. *Nat Struct Mol Biol* 12(2):138–143.

26. Gestaut DR, et al. (2008) Phosphoregulation and depolymerization-driven movement of the Dam1 complex do not require ring formation. *Nat Cell Biol* 10(4):407–414.

27. Hayden JH, Bowser SS, Rieder CL (1990) Kinetochores capture astral microtubules during chromosome attachment to the mitotic spindle: direct visualization in live newt lung cells. *J Cell Biol* 111(3):1039–1045.

28. Merdes A, De JM (1990) The mechanism of kinetochore-spindle attachment and polewards movement analyzed in PtK2 cells at the prophase-prometaphase transition. *Eur J Cell Biol* 53(2):313–325.

29. Rieder CL (1990) Formation of the astral mitotic spindle: Ultrastructural basis for the centrosome-kinetochore interaction. *Electron Microsc Rev* 3(2):269–300.

30. Tanaka TU (2010) Kinetochore-microtubule interactions: steps towards bi-orientation. *EMBO J* 29(24):4070–4082.

31. Gregan J, Polakova S, Zhang L, Tolić-Nørrelykke IM, Cimini D (2011) Merotelic kinetochore attachment: causes and effects. *Trends Cell Biol* 21(6):374–381.

32. Cimini D, Moree B, Canman JC, Salmon ED (2003) Merotelic kinetochore orientation occurs frequently during early mitosis in mammalian tissue cells and error correction is achieved by two different mechanisms. *J Cell Sci* 116(20):4213–4225.

33. Verzijlbergen KF, et al. (2014) Shugoshin biases chromosomes for biorientation through condensin recruitment to the pericentromere. *eLife* 3:e01374.

34. Hauf S, Watanabe Y (2004) Kinetochore Orientation in Mitosis and Meiosis. *Cell* 119(3):317–327.

35. Indjeian VB, Murray AW (2007) Budding Yeast Mitotic Chromosomes Have an Intrinsic Bias to Biorient on the Spindle. *Curr Biol* 17(21):1837–1846.

36. Biggins S, et al. (1999) The conserved protein kinase Ipl1 regulates microtubule binding to kinetochores in budding yeast. *Genes Dev* 13(5):532–544.

37. Biggins S, Murray AW (2001) The budding yeast protein kinase Ipl1/Aurora allows the absence of tension to activate the spindle checkpoint. *Genes Dev* 15(23):3118–3129.

38. Tanaka TU, et al. (2002) Evidence that the Ipl1-Sli15 (Aurora kinase-INCENP) complex promotes chromosome bi-orientation by altering kinetochore-spindle pole connections. *Cell* 108(3):317–329.

39. Cheeseman IM, et al. (2002) Phospho-regulation of kinetochore-microtubule attachments by the Aurora kinase Ipl1p. *Cell* 111(2):163–172.

40. Pinsky BA, Kung C, Shokat KM, Biggins S (2006) The Ipl1-Aurora protein kinase activates the spindle checkpoint by creating unattached kinetochores. *Nat Cell Biol* 8(1):78–83.

41. Cheeseman IM, Chappie JS, Wilson-Kubalek EM, Desai A (2006) The conserved KMN network constitutes the core microtubule-binding site of the kinetochore. *Cell* 127(5):983–997.

42. DeLuca JG, et al. (2006) Kinetochore microtubule dynamics and attachment stability are regulated by Hec1. *Cell* 127(5):969–982.

43. Akiyoshi B, Nelson CR, Ranish JA, Biggins S (2009) Analysis of Ipl1-mediated phosphorylation of the Ndc80 kinetochore protein in Saccharomyces cerevisiae. *Genetics* 183(4):1591–1595.

44. Ciferri C, et al. (2008) Implications for Kinetochore-Microtubule Attachment from the Structure of an Engineered Ndc80 Complex. *Cell* 133(3):427–439.

45. Welburn JPI, et al. (2010) Aurora B phosphorylates spatially distinct targets to differentially regulate the kinetochore-microtubule interface. *Mol Cell* 38(3):383–392.

46. Tien JF, et al. (2010) Cooperation of the Dam1 and Ndc80 kinetochore complexes enhances microtubule coupling and is regulated by aurora B. *J Cell Biol* 189(4):713–723.

47. Shang C, et al. (2003) Kinetochore Protein Interactions and their Regulation by the Aurora Kinase Ipl1p. *Mol Biol Cell* 14(8):3342–3355.

48. Wang H-W, et al. (2007) Architecture of the Dam1 kinetochore ring complex and implications for microtubule-driven assembly and force-coupling mechanisms. *Nat Struct Mol Biol* 14(8):721–726.

49. Zaytsev AV, et al. (2015) Multisite phosphorylation of the NDC80 complex gradually tunes its microtubule-binding affinity. *Mol Biol Cell* 26(10):1829–1844.

50. Sarangapani KK, Akiyoshi B, Duggan NM, Biggins S, Asbury CL (2013) Phosphoregulation promotes release of kinetochores from dynamic microtubules via multiple mechanisms. *Proc Natl Acad Sci U S A* 110(18):7282–7287.

51. Umbreit NT, et al. (2012) The Ndc80 kinetochore complex directly modulates microtubule dynamics. *Proc Natl Acad Sci* 109(40):16113–16118.

52. Liu D, Vader G, Vromans MJM, Lampson MA, Lens SMA (2009) Sensing Chromosome Bi-Orientation by Spatial Separation of Aurora B Kinase from Kinetochore Substrates. *Science* 323(5919):1350–1353.

53. Campbell CS, Desai A (2013) Tension sensing by Aurora B kinase is independent of survivin-based centromere localization. *Nature* 497(7447):118–121.

54. Hindriksen S, Lens SMA, Hadders MA (2017) The Ins and Outs of Aurora B Inner Centromere Localization. *Front Cell Dev Biol* 5. doi:10.3389/fcell.2017.00112.

55. Liu X, Winey M (2012) The MPS1 Family of Protein Kinases. *Annu Rev Biochem* 81:561–585.

56. Winey M, Goetsch L, Baum P, Byers B (1991) MPS1 and MPS2: novel yeast genes defining distinct steps of spindle pole body duplication. *J Cell Biol* 114(4):745–754.

57. Pike AN, Fisk HA (2011) Centriole assembly and the role of Mps1: defensible or dispensable? *Cell Div* 6:9.

58. Weiss E, Winey M (1996) The Saccharomyces cerevisiae spindle pole body duplication gene MPS1 is part of a mitotic checkpoint. *J Cell Biol* 132(1–2):111–123.

59. London N, Biggins S (2014) Signalling dynamics in the spindle checkpoint response. *Nat Rev Mol Cell Biol* 15(11):736–747.

60. Maure J-F, Kitamura E, Tanaka TU (2007) Mps1 kinase promotes sister-kinetochore bi-orientation by a tension-dependent mechanism. *Curr Biol CB* 17(24):2175–2182.

61. Jones MH, et al. (2005) Chemical genetics reveals a role for Mps1 kinase in kinetochore attachment during mitosis. *Curr Biol CB* 15(2):160–165.

62. Meyer RE, et al. (2013) Mps1 and Ipl1/Aurora B act sequentially to correctly orient chromosomes on the meiotic spindle of budding yeast. *Science* 339(6123):1071–1074.

63. Meyer RE, Brown J, Beck L, Dawson DS (2017) Mps1 promotes chromosome meiotic chromosome biorientation through Dam1. *Mol Biol Cell* 29(4):479–489.

64. Shimogawa MM, et al. (2006) Mps1 Phosphorylation of Dam1 Couples Kinetochores to Microtubule Plus Ends at Metaphase. *Curr Biol CB* 16(15):1489–1501.

65. van der Waal MS, et al. (2012) Mps1 promotes rapid centromere accumulation of Aurora B. *EMBO Rep* 13(9):847–854.

66. Nijenhuis W, et al. (2013) A TPR domain–containing N-terminal module of MPS1 is required for its kinetochore localization by Aurora B. *J Cell Biol* 201(2):217.

67. Saurin AT, van der Waal MS, Medema RH, Lens SMA, Kops GJPL (2011) Aurora B potentiates Mps1 activation to ensure rapid checkpoint establishment at the onset of mitosis. *Nat Commun* 2:316.

68. Santaguida S, Tighe A, D'Alise AM, Taylor SS, Musacchio A (2010) Dissecting the role of MPS1 in chromosome biorientation and the spindle checkpoint through the small molecule inhibitor reversine. *J Cell Biol* 190(1):73–87.

69. Maciejowski J, et al. (2010) Mps1 directs the assembly of Cdc20 inhibitory complexes during interphase and mitosis to control M phase timing and spindle checkpoint signaling. *J Cell Biol* 190(1):89–100.

70. Maciejowski J, et al. (2017) Mps1 Regulates Kinetochore-Microtubule Attachment Stability via the Ska Complex to Ensure Error-Free Chromosome Segregation. *Dev Cell* 41(2):143-156.e6.

71. Primorac I, Musacchio A (2013) Panta rhei: the APC/C at steady state. *J Cell Biol* 201(2):177–189.

72. Hoyt MA, Totis L, Roberts BT (1991) S. cerevisiae genes required for cell cycle arrest in response to loss of microtubule function. *Cell* 66(3):507–517.

73. Li R, Murray AW (1991) Feedback control of mitosis in budding yeast. *Cell* 66(3):519–531.

74. Gillett ES, Espelin CW, Sorger PK (2004) Spindle checkpoint proteins and chromosome-microtubule attachment in budding yeast. *J Cell Biol* 164(4):535–546.

75. Howell BJ, et al. (2004) Spindle checkpoint protein dynamics at kinetochores in living cells. *Curr Biol CB* 14(11):953–964.

76. Shah JV, et al. (2004) Dynamics of Centromere and Kinetochore Proteins: Implications for Checkpoint Signaling and Silencing. *Curr Biol* 14(11):942–952.

77. Mapelli M, Massimiliano L, Santaguida S, Musacchio A (2007) The Mad2 Conformational Dimer: Structure and Implications for the Spindle Assembly Checkpoint. *Cell* 131(4):730–743.

78. Luo X, Yu H (2008) Protein Metamorphosis: The Two-State Behavior of Mad2. *Structure* 16(11):1616–1625.

79. Hardwick KG, Weiss E, Luca FC, Winey M, Murray AW (1996) Activation of the budding yeast spindle assembly checkpoint without mitotic spindle disruption. *Science* 273(5277):953–956.

80. London N, Ceto S, Ranish JA, Biggins S (2012) Phosphoregulation of Spc105 by Mps1 and PP1 regulates Bub1 localization to kinetochores. *Curr Biol CB* 22(10):900–906.

81. Shepperd LA, et al. (2012) Phosphodependent recruitment of Bub1 and Bub3 to Spc7/KNL1 by Mph1 kinase maintains the spindle checkpoint. *Curr Biol CB* 22(10):891–899.

82. Yamagishi Y, Yang C-H, Tanno Y, Watanabe Y (2012) MPS1/Mph1 phosphorylates the kinetochore protein KNL1/Spc7 to recruit SAC components. *Nat Cell Biol* 14(7):746–752.

83. Primorac I, et al. (2013) Bub3 reads phosphorylated MELT repeats to promote spindle assembly checkpoint signaling. *eLife* 2:e01030.

84. Kiyomitsu T, Obuse C, Yanagida M (2007) Human Blinkin/AF15q14 is required for chromosome alignment and the mitotic checkpoint through direct interaction with Bub1 and BubR1. *Dev Cell* 13(5):663–676.

85. London N, Biggins S (2014) Mad1 kinetochore recruitment by Mps1-mediated phosphorylation of Bub1 signals the spindle checkpoint. *Genes Dev* 28(2):140–152.

86. Ji Z, Gao H, Jia L, Li B, Yu H (2017) A sequential multi-target Mps1 phosphorylation cascade promotes spindle checkpoint signaling. *eLife* 6. doi:10.7554/eLife.22513.

87. Krenn V, Overlack K, Primorac I, van Gerwen S, Musacchio A (2014) KI motifs of human Knl1 enhance assembly of comprehensive spindle checkpoint complexes around MELT repeats. *Curr Biol CB* 24(1):29–39.

88. Vleugel M, et al. (2015) Sequential multisite phospho-regulation of KNL1-BUB3 interfaces at mitotic kinetochores. *Mol Cell* 57(5):824–835.

89. Kawashima SA, Yamagishi Y, Honda T, Ishiguro K, Watanabe Y (2010) Phosphorylation of H2A by Bub1 prevents chromosomal instability through localizing shugoshin. *Science* 327(5962):172–177.

90. Kitajima TS, Kawashima SA, Watanabe Y (2004) The conserved kinetochore protein shugoshin protects centromeric cohesion during meiosis. *Nature* 427(6974):510–517.

91. Marston AL, Tham W-H, Shah H, Amon A (2004) A genome-wide screen identifies genes required for centromeric cohesion. *Science* 303(5662):1367–1370.

92. Peplowska K, Wallek AU, Storchova Z (2014) Sgo1 Regulates Both Condensin and Ipl1/Aurora B to Promote Chromosome Biorientation. *PLoS Genet* 10(6). doi:10.1371/journal.pgen.1004411.

93. Indjeian VB, Stern BM, Murray AW (2005) The centromeric protein Sgo1 is required to sense lack of tension on mitotic chromosomes. *Science* 307(5706):130–133.

94. Nerusheva OO, Galander S, Fernius J, Kelly D, Marston AL (2014) Tension-dependent removal of pericentromeric shugoshin is an indicator of sister chromosome biorientation. *Genes Dev* 28(12):1291–1309.

95. Marston AL (2015) Shugoshins: Tension-Sensitive Pericentromeric Adaptors Safeguarding Chromosome Segregation. *Mol Cell Biol* 35(4):634–648.

96. Pinsky BA, Nelson CR, Biggins S (2009) Protein phosphatase 1 regulates exit from the spindle checkpoint in budding yeast. *Curr Biol CB* 19(14):1182–1187.

97. Nijenhuis W, Vallardi G, Teixeira A, Kops GJPL, Saurin AT (2014) Negative feedback at kinetochores underlies a responsive spindle checkpoint signal. *Nat Cell Biol* 16(12):1257–1264.

98. Faesen AC, et al. (2017) Basis of catalytic assembly of the mitotic checkpoint complex. *Nature* 542(7642):498–502.

99. Palframan WJ, Meehl JB, Jaspersen SL, Winey M, Murray AW (2006) Anaphase inactivation of the spindle checkpoint. *Science* 313(5787):680–684.

100. Jelluma N, Dansen TB, Sliedrecht T, Kwiatkowski NP, Kops GJPL (2010) Release of Mps1 from kinetochores is crucial for timely anaphase onset. *J Cell Biol* 191(2):281–290.

101. Aravamudhan P, Goldfarb AA, Joglekar AP (2015) The kinetochore encodes a mechanical switch to disrupt spindle assembly checkpoint signalling. *Nat Cell Biol* 17(7):868–879.

102. Hiruma Y, et al. (2015) CELL DIVISION CYCLE. Competition between MPS1 and microtubules at kinetochores regulates spindle checkpoint signaling. *Science* 348(6240):1264–1267.

103. Dou Z, et al. (2015) Dynamic localization of Mps1 kinase to kinetochores is essential for accurate spindle microtubule attachment. *Proc Natl Acad Sci U S A* 112(33):E4546-4555.

104. Kang J, Chen Y, Zhao Y, Yu H (2007) Autophosphorylation-dependent activation of human Mps1 is required for the spindle checkpoint. *Proc Natl Acad Sci U S A* 104(51):20232–20237.

105. Mattison CP, et al. (2007) Mps1 activation loop autophosphorylation enhances kinase activity. *J Biol Chem* 282(42):30553–30561.

106. Ji Z, Gao H, Yu H (2015) CELL DIVISION CYCLE. Kinetochore attachment sensed by competitive Mps1 and microtubule binding to Ndc80C. *Science* 348(6240):1260–1264.

107. Liu S-T, et al. (2003) Human MPS1 Kinase Is Required for Mitotic Arrest Induced by the Loss of CENP-E from Kinetochores. *Mol Biol Cell* 14(4):1638–1651.

108. Wang X, et al. (2014) Dynamic autophosphorylation of mps1 kinase is required for faithful mitotic progression. *PloS One* 9(9):e104723.

109. Xu Q, et al. (2009) Regulation of Kinetochore Recruitment of Two Essential Mitotic Spindle Checkpoint Proteins by Mps1 Phosphorylation. *Mol Biol Cell* 20(1):10–20.

110. Stucke VM, Baumann C, Nigg EA (2004) Kinetochore localization and microtubule interaction of the human spindle checkpoint kinase Mps1. *Chromosoma* 113(1):1–15.

111. Kemmler S, et al. (2009) Mimicking Ndc80 phosphorylation triggers spindle assembly checkpoint signalling. *EMBO J* 28(8):1099–1110.

112. Akiyoshi B, et al. (2010) Tension directly stabilizes reconstituted kinetochore-microtubule attachments. *Nature* 468(7323):576–579.

113. Gupta A, Evans RK, Koch LB, Littleton AJ, Biggins S (2018) Purification of kinetochores from the budding yeast Saccharomyces cerevisiae. *Methods Cell Biol* 144:349–370.

114. Gordon DJ, Resio B, Pellman D (2012) Causes and consequences of aneuploidy in cancer. *Nat Rev Genet* 13(3):189–203.

115. Musacchio A (2015) The Molecular Biology of Spindle Assembly Checkpoint Signaling Dynamics. *Curr Biol* 25(20):R1002–R1018.

116. Rieder CL, Maiato H (2004) Stuck in Division or Passing through: What Happens When Cells Cannot Satisfy the Spindle Assembly Checkpoint. *Dev Cell* 7(5):637–651.

117. Kops GJPL, Weaver BAA, Cleveland DW (2005) On the road to cancer: aneuploidy and the mitotic checkpoint. *Nat Rev Cancer* 5(10):773–785.

118. Martin-Lluesma S, Stucke VM, Nigg EA (2002) Role of Hec1 in spindle checkpoint signaling and kinetochore recruitment of Mad1/Mad2. *Science* 297(5590):2267–2270.

119. Dou Z, et al. (2003) Dynamic distribution of TTK in HeLa cells: insights from an ultrastructural study. *Cell Res* 13(6):443–449.

120. Moura M, et al. (2017) Protein Phosphatase 1 inactivates Mps1 to ensure efficient Spindle Assembly Checkpoint silencing. *eLife* 6. doi:10.7554/eLife.25366.

121. Hewitt L, et al. (2010) Sustained Mps1 activity is required in mitosis to recruit O-Mad2 to the Mad1-C-Mad2 core complex. *J Cell Biol* 190(1):25–34.

122. Kwiatkowski N, et al. (2010) Small-molecule kinase inhibitors provide insight into Mps1 cell cycle function. *Nat Chem Biol* 6(5):359–368.

123. Sliedrecht T, Zhang C, Shokat KM, Kops GJPL (2010) Chemical genetic inhibition of Mps1 in stable human cell lines reveals novel aspects of Mps1 function in mitosis. *PloS One* 5(4):e10251.

124. Colombo R, et al. (2010) Targeting the mitotic checkpoint for cancer therapy with NMS-P715, an inhibitor of MPS1 kinase. *Cancer Res* 70(24):10255–10264.

125. Johnston K, et al. (2010) Vertebrate kinetochore protein architecture: protein copy number. *J Cell Biol* 189(6):937–943.

126. Hoskins AA, et al. (2011) Ordered and dynamic assembly of single spliceosomes. *Science* 331(6022):1289–1295.

127. Sarangapani KK, et al. (2014) Sister kinetochores are mechanically fused during meiosis I in yeast. *Science* 346(6206):248–251.

128. Akiyoshi B, Nelson CR, Biggins S (2013) The Aurora B Kinase Promotes Inner and Outer Kinetochore Interactions in Budding Yeast. *Genetics* 194(3):785–789.

129. Dimitrova YN, Jenni S, Valverde R, Khin Y, Harrison SC (2016) Structure of the MIND Complex Defines a Regulatory Focus for Yeast Kinetochore Assembly. *Cell* 167(4):1014-1027.e12.

130. Kuhn J, Dumont S (2017) Spindle assembly checkpoint satisfaction occurs via end-on but not lateral attachments under tension. *J Cell Biol* 216(6):1533–1542.

131. Koshland DE, Mitchison TJ, Kirschner MW (1988) Polewards chromosome movement driven by microtubule depolymerization in vitro. *Nature* 331(6156):499–504.

132. Inoué S, Salmon ED (1995) Force generation by microtubule assembly/disassembly in mitosis and related movements. *Mol Biol Cell* 6(12):1619–1640.

133. Araki Y, et al. (2010) N-terminal regions of Mps1 kinase determine functional bifurcation. *J Cell Biol* 189(1):41–56.

134. Breitkreutz A, et al. (2010) A global protein kinase and phosphatase interaction network in yeast. *Science* 328(5981):1043–1046.

135. Hennrich ML, et al. (2013) Universal quantitative kinase assay based on diagonal SCX chromatography and stable isotope dimethyl labeling provides high-definition kinase consensus motifs for PKA and human Mps1. *J Proteome Res* 12(5):2214–2224.

136. Boeke JD, Trueheart J, Natsoulis G, Fink GR (1987) 5-Fluoroorotic acid as a selective agent in yeast molecular genetics. *Methods Enzymol* 154:164–175.

137. Lauzé E, et al. (1995) Yeast spindle pole body duplication gene MPS1 encodes an essential dual specificity protein kinase. *EMBO J* 14(8):1655–1663.

138. Castillo AR (2000) Analysis of MPS1 Separation of Function Alleles Reveals a Novel Interaction at the Spindle Pole Bodies of Budding Yeast.

139. Combes G, et al. (2018) Mps1 Phosphorylates Its N-Terminal Extension to Relieve Autoinhibition and Activate the Spindle Assembly Checkpoint. *Curr Biol* 28(6):872-883.e5.

140. Morin V, et al. (2012) CDK-dependent potentiation of MPS1 kinase activity is essential to the mitotic checkpoint. *Curr Biol CB* 22(4):289–295.

141. Sherman F, Fink, G, Lawrence C (1974) *Methods in Yeast Genetics* (Cold Spring Harbor Laboratory Press, Cold Spring Harbor, New York).

142. Miller MP, Asbury CL, Biggins S (2016) A TOG Protein Confers Tension Sensitivity to Kinetochore-Microtubule Attachments. *Cell* 165(6):1428–1439.

143. Deng Y, Asbury CL (2017) Simultaneous Manipulation and Super-Resolution Fluorescence Imaging of Individual Kinetochores Coupled to Microtubule Tips. *Methods Mol Biol Clifton NJ* 1486:437–467.

144. Cheerambathur DK, et al. (2017) Dephosphorylation of the Ndc80 Tail Stabilizes Kinetochore-Microtubule Attachments via the Ska Complex. *Dev Cell* 41(4):424-437.e4.

145. Chan YW, Jeyaprakash AA, Nigg EA, Santamaria A (2012) Aurora B controls kinetochore–microtubule attachments by inhibiting Ska complex–KMN network interaction. *J Cell Biol* 196(5):563–571.

146. Jelluma N, et al. (2008) Mps1 phosphorylates Borealin to control Aurora B activity and chromosome alignment. *Cell* 132(2):233–246.

147. Espeut J, et al. (2008) Phosphorylation relieves autoinhibition of the kinetochore motor Cenp-E. *Mol Cell* 29(5):637–643.

148. Nishimura K, Fukagawa T, Takisawa H, Kakimoto T, Kanemaki M (2009) An auxin-based degron system for the rapid depletion of proteins in nonplant cells. *Nat Methods* 6(12):917–922.

149. Straight AF, Belmont AS, Robinett CC, Murray AW (1996) GFP tagging of budding yeast chromosomes reveals that protein-protein interactions can mediate sister chromatid cohesion. *Curr Biol CB* 6(12):1599–1608.

150. Xu Z, et al. (2009) Structure and function of the PP2A-shugoshin interaction. *Mol Cell* 35(4):426–441.

151. Eshleman HD, Morgan DO (2014) Sgo1 recruits PP2A to chromosomes to ensure sister chromatid bi-orientation during mitosis. *J Cell Sci* 127(22):4974–4983.

152. Rosenberg JS, Cross FR, Funabiki H (2011) KNL1/Spc105 Recruits PP1 to Silence the Spindle Assembly Checkpoint. *Curr Biol CB* 21(11):942–947.

153. Caldas GV, DeLuca KF, DeLuca JG (2013) KNL1 facilitates phosphorylation of outer kinetochore proteins by promoting Aurora B kinase activity. *J Cell Biol* 203(6):957–969.

154. Storchová Z, Becker JS, Talarek N, Kögelsberger S, Pellman D (2011) Bub1, Sgo1, and Mps1 mediate a distinct pathway for chromosome biorientation in budding yeast. *Mol Biol Cell* 22(9):1473–1485.

155. Duro E, Marston AL (2015) From equator to pole: splitting chromosomes in mitosis and meiosis. *Genes Dev* 29(2):109–122.

156. Marston AL, Wassmann K (2017) Multiple Duties for Spindle Assembly Checkpoint Kinases in Meiosis. *Front Cell Dev Biol* 5. doi:10.3389/fcell.2017.00109.

157. DeLuca KF, Lens SMA, DeLuca JG (2011) Temporal changes in Hec1 phosphorylation control kinetochore–microtubule attachment stability during mitosis. *J Cell Sci* 124(4):622–634.

158. DeLuca KF, et al. (2017) Aurora A kinase phosphorylates Hec1 to regulate metaphase kinetochore–microtubule dynamics. *J Cell Biol*:jcb.201707160.